Dynamical Climatology

Simulations of linear and nonlinear disturbances in the stratosphere.

by

A. O'Neill and V.D. Pope

DCTN 53

April 1987

Meteorological Office (Met. O. 20)
London Road
Bracknell
Berkshire RG12 2SZ

DYNAMICAL CLIMATOLOGY TECHNICAL NOTE NO. 53

SIMULATIONS OF LINEAR AND NONLINEAR DISTURBANCES IN THE STRATOSPHERE

by

A O'Neill and V D Pope

This paper has been submitted to the Quarterly Journal of the Royal Meteorological Society.

Met O 20 (Dynamical Climatology Branch)
Meteorological Office
London Road
Bracknell
Berkshire RG12 2SZ U.K.

April 1987

Note: This paper has not been published. Permission to quote from it should be obtained from the Assistant Director of the above Meteorological Office Branch.

LF/M020

SIMULATIONS OF LINEAR AND NONLINEAR DISTURBANCES IN THE STRATOSPHERE

A O'Neill and V D Pope

Meteorological Office,
London Road, Bracknell,
Berks, RG12 2SZ

MARCH 1987

SUMMARY

The aim is to study and contrast the dynamics of linear and nonlinear, large-scale disturbances generated in the stratosphere by a localised perturbation in the troposphere. The perturbation is applied at the lower boundary of a primitive equation model of the stratosphere and mesosphere. The experiments are diagnosed using a range of dynamical quantities; in particular isentropic maps of Ertel's potential vorticity reveal where and how the stratospheric disturbance becomes nonlinear.

The simulations are contrasted with an idealised theoretical model of a nonlinear critical layer, and the relevance for our experiments of 'wave breaking' and irreversible mixing of potential vorticity is discussed. Apparent polar focusing of Eliassen-Palm fluxes is related to localised changes in a widening 'buckling zone'. Wave amplitudes are far too large to apply simple ideas of wave propagation.

The notion of pre-conditioning as it has been applied to the stratosphere is challenged; there are occasions when it is an over-simplification to regard the troposphere as a wavemaker forcing changes in the stratosphere according to the tenets of wave, mean-flow theory. Preceding a major warming, the flow is asymmetric about any axis (even in the much-studied case of February 1979), and strong warmings develop through the nonlinear interaction of large, deep vortices associated with a tropospheric asymmetry. The nonlinearity of the flow is also manifested in an anticorrelation in time between zonal harmonics one and two over a deep layer, and by a phase shift of harmonics as amplitudes change.

Associated changes in zonal mean winds give the appearance of distinct minor and major warmings, though a synoptic view allows systematic changes to be seen which caution against dividing the evolution into separate events.

1. INTRODUCTION

Our aim in this paper is to compare, contrast and account for differences in the ways that the stratosphere responds to weak and strong disturbances in the troposphere. We show how and why linear theory breaks down, The results lead us to challenge some of the assumptions that underlie currently accepted dynamical thinking about the stratosphere and how it is coupled to the troposphere. We do this by using a numerical model of the stratosphere and mesosphere, based on the primitive equations, whose lower boundary near the tropopause is prescribed to be axially symmetric save for a localised disturbance in geopotential height.

Since the analytical study of Charney and Drazin (1961), which was based on linear theory, the traditional view of troposphere-stratosphere coupling is that planetary waves grow in the troposphere and propagate upwards into the stratosphere according to the zonal wind distribution aloft. Stratospheric sudden warmings involve changes in the zonal-mean wind, and in the theory of wave, mean-flow interaction (developed notably by Andrews and McIntyre, 1976, 1978) these changes, which may be irreversible, are attributed to the effects of transient or dissipating

planetary waves. Much of our current understanding of warmings makes use of this theory, beginning with the seminal modelling work of Matsuno (1971).

This theory has strongly influenced the way observational data have been interpreted. Usually, a causal chain of reasoning is presented: waves are regarded as propagating on some 'basic state' (typically, the current zonal-mean state), and then thought of as 'forcing' or 'driving' zonal wind deceleration where wave activity converges.

Some warmings are 'major', others are not. A popular explanation is that, prior to major warmings, the stratosphere is 'pre-conditioned' for disruption; it is held (e.g. Kanzawa, 1980) that an anomalous basic state is produced by an earlier minor warming. It is tacitly assumed that this basic state varies slowly enough in time for wave, mean-flow theory to be applicable.

Our idealised experiments point out some of the inadequacies of the above line of thinking. We begin by studying the dynamics of a linear Rossby wavetrain emanating from a weak localised tropospheric disturbance. Even though this wavetrain is far too weak in the stratosphere to be a model for observed conditions, we discuss the dynamics of its formation in some detail. We do so to make a clear distinction with the dynamics of nonlinear perturbations generated by strong localised disturbances. One of the principal findings from the latter experiments is that when the simulated stratosphere is as strongly disturbed as the real one is in northern winter, it is more meaningful to talk of deep vortices interacting

with each other than of propagating waves interacting with the zonal mean flow, though the theory of vortex interactions (developed, for example, by Saffman and Baker, 1979, and by Dritschel, 1986) is still rudimentary for stratospheric applications.

Our choice of local forcing rather than forcing by a single zonal harmonic (as was used, by Matsuno, 1971, Holton, 1976, Dunkerton et al., 1981, and by Butchart et al., 1982) is motivated by a desire to adopt a local view of the dynamics. In this, we follow the example set by McIntyre and Palmer (1983, 1984, 1985). We do not claim that the boundary condition used in our model is any less of an idealisation of troposphere-stratosphere coupling than that comprising a single harmonic on a zonal mean flow. We know, however, of no mechanism that selectively favours the growth over a week or so of wave 1 or wave 2 in the troposphere. It turns out (in experiments we have done, not reported here) that constructive superposition of harmonics in a localised disturbance can significantly influence the way the stratosphere responds. For example, the stratospheric signal in wave 1 from localised forcing may be very much stronger than it is when only the wave-1 component of the forcing is applied.

Studies of stratospheric dynamics are usually pursued by taking simplified conceptual, analytical or mechanistic models and then looking for points of similarity between the idealised and real worlds. We take the equally constructive but opposite standpoint of critically assessing

simple models to determine where underlying approximations break down and what the consequences then are. In the absence of an adequate theory of nonlinear flows in the atmsophere, this gives an understanding of sorts.

The plan of the paper is as follows. In section 2 we describe our numerical model and give details of the forcing that we use. Section 3 lists the diagnostics used to study the experiments, and contains some background theory. In section 4 we discuss the linear dynamics of a wavetrain propagating upwards and downstream from weak forcing, and in section 5 we consider the contrasting response to strong forcing. Section 6 includes a detailed comparison of our simulated fields with a weakly nonlinear analytical solution for waves impinging on a zero-wind (critical) line. For comparison with results and interpretations of other studies we describe, in section 7, the evolution of quantities based on zonal averaging and departures therefrom. This is not a retreat from our emphasis on local dynamics; we interpret changes in such quantities in terms of localised changes on synoptic maps. Section 8 demonstrates that strong nonlinearities are not confined to the edge of a westerly vortex where winds are weak; they can arise high in the atmosphere in the jet core where winds are strongest.

2. GENERAL DESCRIPTION OF MODEL AND EXPERIMENTS

(a) The model

We use a global model of the stratosphere and mesosphere based on the primitive equations. The height of its lowest isobaric surface, 300 mb, can be prescribed and this allows departures from axially symmetric motion in the upper atmosphere to be forced from below. A full description of the model has been given by Butchart et al. (1982), although our version uses finite differencing accurate to fourth order rather than to second order. Summarising its main features, it has a regular grid in spherical co-ordinates with 16 points along a latitude circle, 36 points along a meridian from pole to pole and 33 levels at equal intervals of log (pressure), giving a vertical spacing of about 2.6 km. Radiative damping is represented by a simple Newtonian scheme in which temperature is relaxed to its initial value with a time scale of about 20 days in the lower and middle stratosphere and about 5 days in the upper stratosphere and mesosphere. The Rayleigh friction used by Holton (1976) is included in the mesosphere as a parametrization of the drag due to the dissipation of gravity waves. The drag has only a small effect in the stratosphere which is the region of interest.

We chose two zonally averaged states of the stratosphere as initial fields for our experiments. The first state is during a northern winter, and the second is during a southern winter. The states were chosen to illustrate a range of dynamical behaviour, and to study the influence of the initial fields on the response of the stratosphere to tropospheric forcing.

The two states were obtained using observational analyses of geopotential heights and gradient winds. In the stratosphere, thicknesses between various isobaric levels are derived principally from radiance measurements by a stratospheric sounding unit (SSU) on the satellite NOAA-6. These thicknesses are tied to an analysis of the 100 mb surface which is made, using conventional data, by the National Meteorological Center, Washington. The observational data extend up to 1 mb, near the stratopause. The numerical experiments were conducted without access to data for the mesosphere, whose circulation was crudely represented by extending the observed data upwards using a vertical profile of static stability derived from climatology. The mesospheric levels are included in the model only as a device for keeping the model's 'rigid lid' away from the domain of interest. The influence of the rigid lid on lower levels should be limited by the strong radiative and Rayleigh damping of disturbances impinging on it.

(b) Applied forcing at the lower boundary

The experiments that we report here have been conducted using as initial flows two zonally averaged states of the upper troposphere and stratosphere. For each of these states, the field at the lower boundary (300 mb) was the appropriate zonally averaged field of geopotential height taken from observations. To this was added an idealised, growing perturbation in geopotential height, ϕ'_B, of the form

$$\phi'_B = B\, f(t) \exp(-\theta^2/\alpha^2) \qquad (1)$$

where θ is the co-latitude from a co-ordinate pole placed at 180°E and 45° latitude. When this circular 'high' or 'low' is added to a zonally averaged field a ridge or trough is obtained. The constant α has a value of 15°. This value is chosen so that the perturbation has a horizontal scale comparable with persistent troughs and blocking ridges in the troposphere.

The function f(t) has the form

$$f(t) = 1 - \exp(-t/\tau) \qquad (2)$$

where τ has a value of 5 days. The perturbation almost reaches full amplitude after 10 days and remains nearly steady thereafter.

Experiments were conducted with cyclonic and anticyclonic perturbations of small and large amplitude,

$$B = \begin{matrix} \pm 100 \text{ gpm} \\ \\ \pm 600 \text{ gpm} \end{matrix} \qquad (3)$$

The amplitude with largest modulus is roughly the maximum deviation in geopotential height from its zonal mean value found in observations at 300 mb, occurring in the centre of intense blocking anticyclones or persistent troughs like the trough over SE Asia. For $|B|$ of 600 gpm, zonal

wavenumbers 1, 2 and 3 reach amplitudes 121, 109 and 92 gpm respectively. Similar values for these amplitudes are found on average in the upper troposphere of the real atmosphere (Geller et al., 1983).

In emphasising a local view of the dynamics, we avoid defining the perturbation response as a departure from the current zonal mean. Instead, a perturbation field ϕ' is measured as an anomaly,

$$\phi' = \phi - \phi_c \qquad (4)$$

where ϕ is the value in the perturbation experiment and ϕ_c is the corresponding value in a control run without the disturbance ϕ'_B at the lower boundary. All fields ϕ_c are independent of longitude, but change slowly with time in the stratosphere because of the parametrized frictional drag and radiative relaxation included in the model.

The purpose of the experiments with weak forcing is to demonstrate the structure and propagation of disturbances for which linear theory should be closely applicable over most of the atmospheric domain. We test for linearity by changing the sign of B and noting whether ϕ' also changes sign. Even for small $|B|$ it is necessary to test the experiments for linearity because we employ a fully nonlinear model. We find that the linear approximation for small $|B|$ is good except in the vicinity of a zero-wind line, or critical line. This nonlinear region remains narrow latitudinally for the duration of the experiments. For comparison with the experiments with strong forcing, we display ϕ' multiplied by 6. Except

near a critical line, these scaled fields are then approximately the response that would be obtained in a linear model forced with B = $\pm$ 600 gpm.

The purpose of the experiments with strong forcing is to show how nonlinear processes occurring locally affect the flow when perturbations are as strong as those typically found in the real atmosphere during winter. We do this in two ways. First, we compare fields of ϕ' with scaled fields from the experiments with weak forcing. Second, we study the isentropic advection of potential vorticity, and compare linear and nonlinear terms in the governing equation. We define nonlinearity to mean that products of perturbations from the control state cannot be neglected. It seems reasonable, on physical grounds, to define linearity and nonlinearity in terms of the state that would exist if the perturbation were not there.

3. DIAGNOSTICS

Various diagnostics are used to analyse our perturbation experiments. In this section we explain why we used them, and give some background theory. Details of notation are contained in the Appendix.

(a) Maps of ϕ' and Q

It is convenient to use the perturbation in geopotential height, ϕ', when comparing the results of experiments with small and large amplitude disturbances, as ϕ' does not involve products of perturbation quantities. We use it to check for linearity, and then to infer the structure and propagation of linear Rossby waves.

For the experiments with strong forcing, we also study the behaviour of potential vorticity, Q, a quantity which is conserved along an air parcel's trajectory for frictionless adiabatic motion. The dynamical importance of this quantity has been discussed by McIntyre and Palmer (1984) and by Hoskins et al. (1985). Over periods of a week or so, we take the movement of contours of constant Q on isentropic surfaces as being approximately that of material lines. In the model, radiative effects can reasonably be neglected over such periods in the middle stratosphere. The limited resolution in the present version of the model is perhaps more restrictive to the interpretation of isentropic maps of Q, owing to the loss of small scales by truncation in the model.

(b) Fluxes of wave activity

The Eliassen-Palm flux, $\underline{F}$, has frequently been taken as a measure of the net meridional propagation of linear waves on a zonally symmetric basic state (e.g. Edmon et al., 1980). For linear, undamped planetary waves, the following equation holds under quasi-geostrophic assumptions

$$\partial A/\partial t + \nabla.\underline{F} = 0 \qquad (5)$$

where A is the Eliassen-Palm wave activity given by

$$A = \rho_o \overline{q'^2} / 2 \bar{q}_y \qquad (6),$$

and q is quasi-geostrophic potential vorticity.

We take an increase in the positive quantity $\overline{q'^2}$ to indicate that the disturbance is growing. Eq. (5) shows that this will be connected with convergence or divergence of $\underline{F}$ according to whether $\bar{q}_y$ is positive or negative. On cross-sections of $\underline{F}$, we also plot the quantity denoted D_F by Dunkerton et al. (1981). D_F is $\nabla.\underline{F}$ normalized to give the zonal force per unit mass; it enters the expression for the time rate of change of zonal mean wind in the transformed Eulerian zonal-mean formalism introduced by Andrews and McIntyre (1976).

To calculate $\underline{F}$ and D_F, we define perturbation fields as departures not from a control state but from the current zonal mean state. We do this to compare the results of our experiments with observational studies. The two definitions of perturbation fields are nearly equivalent when perturbations are weak, but not when they are strong. We use the full expressions for $\underline{F}$ and D_F given by Dunkerton et al. (their Eqs. A1 and 4.3). Ageostrophic terms are included as these can be large when perturbations are strong.

For a single, locally sinusoidal wavetrain in a slowly varying basic state (the WKB approximation),

$$\underline{F} = A\,(C_{gy},\ C_{gz}) \qquad (7)$$

where the vector on the right is the meridional group velocity showing the propagation of wave activity, A (Edmon et al., 1980).

Plumb (1985) extended Eq. (5) to three dimensions by introducing a flux, $\underline{P}$, having three components. The general expression for $\underline{P}$ simplifies to Plumb's Eq. (7.1) when waves are stationary. Although the wavetrains that we study are not strictly stationary, scale analysis proves this equation to be an acceptable approximation (Marks, 1986). $\underline{P}$ is again parallel to the group velocity for a single wavetrain in the WKB approximation.

(c) Displacement fields

We calculate the meridional displacement on an isentropic surface of contours of Q from their location in the control (zonally symmetric) experiment. In so far as Q is conserved, we obtain the meridional displacement of a chain of air parcels initially aligned along a latitude circle. This displacement is, to leading order in wave amplitude, the particle displacement, η', that enters the linear version of the generalised Lagrangian-mean (GLM) equations (Andrews and McIntyre, 1978) Strictly, this approximation holds for the equations in isentropic co-ordinates.

The displacement, η', is more closely connected with wave activity A than is ϕ'. In the quasi-geostrophic formulation, η' satisfies

$$\eta' = -q'/\bar{q}_y \qquad (8)$$

By Eq. (6) it is related to wave activity by

$$A = \rho_o \overline{\eta'^2}\, \bar{q}_y/2 \qquad (9)$$

The reason we display the perturbation response mainly by fields of ϕ' rather than those of displacement is that the algorithm we use to calculate displacement works only when Q varies monotonically with latitude. In one of our control states, the horizontal gradient of Q changes sign, so a chain of air parcels may not be labelled uniquely by a value of Q. Also, extreme buckling of Q contours in experiments with strong forcing eventually reverses the gradient of Q locally.

4. EXPERIMENTS WITH WEAK FORCING

In this section, we present results of experiments in which a zonally symmetric flow is subjected to localised disturbances of small amplitude (B = $\pm$ 100 gpm in Eq. (1)).

(a) The initial state

The initial state is the zonally averaged flow on 19 January 1982, about a week before a strong stratospheric warming. Fig. 1(a) shows the zonal mean (gradient) winds for the northern hemisphere. The core of a tight westerly jet is located at high latitudes in the upper stratosphere, and easterlies extend to middle latitudes in the mid stratosphere. Fig. 1(b) shows the associated distribution of Ertel's potential vorticity, Q, on the 850 K isentropic surface (near 10 mb, about 30 km) along with wind vectors on the same surface. The gradient of Q is positive (Q increasing polewards) except for a narrow region in the mid stratosphere (stippled in Fig. 1(b)) where it is weakly negative. This change in gradient is associated with strong lateral wind shear, and it arises because we have taken a zonal mean of an asymmetric flow. The zero wind contour (marked by the dashed line in Fig. 1(b) is embedded in the region of negative gradient. Above 50 km at high latitudes is another region where the gradient of Q is negative (not shown). It is connected with a decrease in wind speed with height.

Linear WKB theory predicts that stationary Rossby waves can propagate only where the refractive index defined by Matsuno (1970) is positive. (Strictly, the theory refers to the quasi-geostrophic approximation to Q, but for our fields the full and approximate forms have similar structure.) Linear theory predicts that the two regions where the gradient of Q is negative and winds are westerly act as barriers. The waveguide thus formed confines weak waves to high latitudes and traps them in the vertical.

(b) Results

The (scaled) perturbation response to a localised 'low' of amplitude 100 gpm is shown as a longitude height section of ϕ' in Fig. 2. It is taken at a latitude where ϕ' and the stratospheric winds are largest. After 11 days when the applied forcing has almost reached maximum amplitude, a stationary Rossby wavetrain of 'highs' and 'lows' extends upwards and downstream from the forcing centred at 180°E, 45°N. The separation of the highs and lows is about 100°, roughly that of zonal wavenumber 2. The wavetrain has almost wrapped around the latitude circle and a high is building near 60°W. Fig. 3(a) shows ϕ' at a level in the middle of the stratosphere on day 16. The downstream signal has intensified and interference effects occur as it wraps around the globe. It seems that the forcing has excited a wavetrain which has propagated predominantly downstream in a channel north of the reversed gradient of Q, as we anticipated and confirm below.

The wavetrain in ϕ' lies along a line of latitude near 60°N. This in itself is not evidence for confinement since we find for our other initial state that maxima in ϕ' lie near the jet core even though wave activity propagates meridionally (an explanation for this behaviour has been offered by Simmons, 1974). The latitudinal trapping is confirmed by fields of $\underline{F}$.

We investigate whether the response is linear by changing the sign of the applied forcing. Fig. 3(b) shows the field ϕ' induced by forcing with a localised high. Comparing Figs. 3(a) and (b), we see that the fields are in good agreement at middle and high latitudes, except for a change of sign.

Nonlinearity is expected to be important where waves strike regions where winds are weak, in this case, at mid latitudes. Using an idealised model, Stewartson (1978), and Warn and Warn (1978) showed that the nonlinearity is manifested by extreme and irreversible buckling of Q contours in a "critical layer". This buckling zone remains narrow in the present experiments because the perturbations are weak and damped. Of the Q contours plotted in Fig. 1(b), only the one labelled 2.4 buckles during the 30 days of integration. This behaviour contrasts markedly with the evolution when the perturbations are strong, the buckling zone being then much wider.

The growth of the forcing excites travelling waves, which are free modes of the model. For our basic state, wave 1 is dominated by the stationary component. Travelling waves with wavenumber 2 or greater move eastwards and have amplitudes comparable to their stationary counterparts. These travelling waves are radiatively damped but have significant amplitude long after the applied forcing becomes steady because they are confined in a waveguide. They can be thought of as arising from the downstream propagation of the wave front at the group velocity.

Figure 4 shows the cross section of ϕ' on day 29. The perturbation in the stratosphere comprises a single high and low around a latitude circle. The dominance of zonal wave 1 is temporary; it arises as the wavetrain wraps right around a latitude circle (a process which may be viewed alternatively as destructive interference mainly between travelling and stationary waves of wavenumber 2). There is only weak westward tilt with height at high latitudes, suggesting that the disturbance is partially trapped in the vertical, as other diagnostics confirm.

As we noted in section 4(a), our basic state contains a waveguide for linear waves. The latitudinal confinement of the perturbation is demonstrated by the pattern of $\underline{F}$. Fig. 5 shows on day 11 normalised arrows giving the direction of $\underline{F}$, and also contours of D_F indicating where $\underline{F}$ converges or diverges. Poleward of 45°N, arrows point mostly upward or poleward; except in the upper stratosphere there is little equatorward propagation. Eq. (5) and the convergence shown in Fig. 5 imply that wave activity is being focused into high latitudes. The convergence is related firstly to transience as wave activity builds and secondly to dissipation. After the applied forcing reaches steady amplitude, the transient contribution slowly diminishes as wave activity leaks out of the waveguide, but the convergence due to dissipation remains.

Fig. 5 also shows a region of divergence near 45°N out of which $\underline{F}$ points polewards and equatorwards. This divergence is consistent with Eqs. (5) and (6) for a growing perturbation in a region where the gradient of Q is negative. (At this early stage, nonlinearities are small even near the zero-wind line.) The poleward direction of $\underline{F}$ shows that the reversed

gradient of Q not only impedes the equatorward escape of wave activity but also over-reflects it back into high latitudes. That is, more wave activity returns than leaves high latitudes in the mid stratosphere.

To account for the poleward pointing fluxes, we again resort to linear theory. $\underline{F}$ is small to the south of the reversed Q gradient because winds are easterly, and stationary waves cannot propagate. Given that $\underline{F}$ diverges and the vertical derivative of $\underline{F}$ gives convergence (because of transience and dissipation), $\underline{F}$ must point polewards on the northern side of the negative Q gradient where fluxes are large. On the basis of this argument, we would expect pronounced over-reflection of stationary waves when the zero-wind line is embedded in a band where the gradient of Q is negative, as it is in our basic state. This suggestion is supported by results obtained by Lindzen and Tung (1978) who used a linear, steady-state, analytical model.

Robinson (1987) obtained similar patterns for $\underline{F}$ and D_F to those shown in Fig. 5. He used a linear, time dependent model of planetary waves with an initial state similar to ours; in particular, there was an over-reflecting barrier at mid latitudes. He argued that such a state could be considered as pre-conditioned for a strong stratospheric warming. We find, as does Marks (1986), that linear wave structure is sensitive even to narrow regions where the gradient of Q is reversed. When disturbances are strong, over-reflection may only be transitory, as we note in section 6(b), so ideas about pre-conditioning based exclusively on linear theory may be unsound.

The propagation of wave activity in three dimensions is shown at 8 mb by Fig. 6 for day 16. Arrows represent the horizontal projection of Plumb's flux, $\underline{P}$, and the contours give its vertical component. The arrows confirm that wave activity is confined to high latitudes and propagates mainly downstream at this level. The contours show that $\underline{P}$ first points upwards between about 180°E and 0°E and then downwards as the wave propagates downstream. As expected, wave activity is reflected downwards from the upper stratosphere. Our basic state acts as an efficient waveguide both in the vertical and in the horizontal.

A similar picture of wave propagation emerges from the calculation of ray paths and associated group velocities for our basic state by Marks (1986). These are derived from the wave dispersion relation which is based on the WKB approximation. Marks shows that the disturbance propagates quickly upwards with a typical group velocity of about 10 km day^{-1}, and radiates downstream at about 60° of longitude per day.

Figs. 3(a) and 6 show that the vertical component of $\underline{P}$ has a noticeable variation with twice the zonal wavenumber of the geopotential wave. As Plumb (1985) notes, this high wavenumber ripple would be small if the WKB approximation and hence group velocity concepts worked well. In our case, $\underline{P}$ has limited usefulness, and Fig. 6 should only be taken to give a rough, qualitative picture of wave propagation. Marks demonstrates that the WKB approximation is poor because the waves are not well dispersed in the waveguide.

5. EXPERIMENTS WITH STRONG FORCING

This section begins with a synoptic description of the differences between linear and nonlinear disturbances excited by localised forcing. Next, we turn to isentropic maps of Q to describe how these differences arise. We extend our description of the experiment with strong forcing to cover a simulated major warming, and then discuss another experiment in which a (idealised) blocking anticyclone in the upper troposphere extends upwards.

(a) Synoptic description

Early on, the wavetrains excited by strong and weak forcing are similar. Nonlinear effects become apparent in ϕ' after about day 11. By day 16, the response at 8 mb is as shown in Fig. 7 which may be compared with Fig. 3(a). Downstream from the forcing at 180°E, the first high (140°W) becomes stronger and the first low (40°W) weaker than their scaled linear counterparts. Zonal winds decrease as geopotential heights rise at high latitudes. In Fig. 7, the two highs shown separated in Fig. 3(a) merge as the high near 90°E moves eastwards.

A feature which only becomes significant when the forcing is strong is the high that forms at low latitudes near 0°E in Fig. 7. It moves north eastwards into middle latitudes as it intensifies, so by day 29 a cross-section of ϕ', Fig. 8, shows that the perturbation extends right round the latitude circle. The migrating anticyclone, centred at 40°E, becomes the dominant feature in the perturbation field in the upper

stratosphere. As it intensifies wave 2 increases in the mid stratosphere while wave 1 decreases. The highs in Fig. 8 are associated with two deep, closed anticyclonic circulations in the total field (control plus perturbation). The one at 240°E extends from about 100 mb to 1 mb, and the other reaches from the mid stratosphere into the mesosphere. The linear response on the same day is mainly in wave 1 (Fig. 4). The disturbance generated by strong forcing must therefore involve nonlinear dynamics.

Through the invertibility principle discussed by Hoskins et al. (1985), adiabatic changes in meteorological fields can be connected with advection of Q on isentropic surfaces. We now turn to isentropic maps of Q to try to understand the differences between experiments with weak and strong forcing. Nonlinear advection of Q proves to be much more important in the latter experiments (i.e. advection of perturbation potential vorticity by the perturbation velocity), particularly at latitudes where Q contours buckle irreversibly.

On the 850 K isentropic surface (near 10 mb), the narrow ring of locally high Q at mid latitudes (Fig. 1(b)) breaks up soon after the tropospheric perturbation is applied. This presumably happens because the model has limited resolution and because the zonal flow may be unstable where the poleward gradient of Q is negative (the necessary criterion for instability derived by Charney and Stern, 1962). At this level, closed anticyclonic circulations form where winds are weak at the edge of the main westerly vortex. Remnants of the ring of high Q are advected by these circulations and merge with the main body of high Q in the westerly vortex. On the equatorward flank of lows in the perturbation height field, material

lines move closer together and the ring vanishes through lack of resolution. So at an early stage of the experiment with strong forcing, the ring of high Q, which acts as an over-reflecting barrier to linear waves, mostly disappears.

The distribution of Q on day 16 is shown in Fig. 9(a). In the top left quadrant, a tongue of low Q stretches north eastwards around the westerly vortex. A closed anticyclonic circulation forms near the central axis of this tongue, isolating a region of low Q at mid latitudes and drawing out a tongue of high Q from the main vortex into low latitudes. The anticyclone lies about 45° downstream of the applied tropospheric low. The Aleutian High in the real stratosphere and the climatological trough in the troposphere over E. Asia are similarly related. The development is similar to the way cut-off anticyclones form in the troposphere during blocking (see Fig. 11 of Hoskins et al., 1985). McIntyre and Palmer (1983, 1984, 1985) apply the term 'wave breaking' to such irreversible buckling of material contours.

McIntyre (1982) and McIntyre and Palmer illustrate irreversible buckling of material contours in stationary waves with wave breaking near a zero-wind line (or where winds are weak), and with analytical theories of critical layers (see section 6(a)). These theories attempt to deal with the breakdown of linear theory near a zero-wind line. Below, we discuss two examples which show that zero-wind lines are not the only sites for irreversible buckling of Q contours by stationary disturbances.

As the perturbations strengthen, the constraint imposed by the conservation of Q has an impact (another illustration of this is given by Killworth and McIntyre, 1985). The amount of Q that can be advected is finite, so as more Q is drawn away from the main cyclone around an anticyclone, we find that the magnitudes of highs in ϕ' increase while lows decrease. Also, the area of the cyclonic circulation decreases systematically as that of the anticyclonic circulation increases - an important element of the major warming that develops later.

The constraint is violated if Q is calculated using the scaled fields of our linear experiment (i.e. by adding scaled perturbation fields to those of the control experiment, then deriving Q from the resultant). Then tongues of high and low Q form, not by advection, but in situ through lack of conservation. Moreover, they form reversibly, not irreversibly as they do in the nonlinear model: if the applied forcing is switched off, the tongues disappear as they formed but with time reversed. The limitations of linear theory are thus exposed where the constraint of conservation of Q is seriously broken.

As the Aleutian anticyclone builds, the westerly vortex elongates and high Q is drawn progressively into the top left quadrant of Fig. 9(a) from the bottom right quadrant. Here another anticyclone develops (Fig. 7). At a point marked in Fig. 9(a) by a heavy arrow, a tongue of low Q is being sucked into a jet stream. By day 29, Fig. 9(b) shows that an incursion of low Q into mid latitudes has turned into a closed anticyclonic circulation which surrounds a second island of low Q detached from low latitudes.

Poleward of the isolated regions of low Q in Fig. 9(b) are two westerly jet streams which strengthen with the widening of the buckling zone - the broad, mid-latitude band wherein Q contours buckle irreversibly. This widening leads to large values in perturbation fields at mid latitudes. Although this gives the appearance of predominantly downstream propagation from the region of forcing, nonlinear advection of Q is involved rather than linear wave propagation.

The importance of nonlinear advection can be determined by comparing terms in the conservation equation for Q, since this equation can be regarded as the basic governing equation according to the invertibility principle. We may write the equation as

$$\frac{dQ}{dt} = \frac{\partial Q}{\partial t} + \underline{v}_c \cdot \nabla Q_c + \underline{v}' \cdot \nabla Q_c + \underline{v}_c \cdot \nabla Q' + \underline{v}' \cdot \nabla Q'$$
$$= \text{non-conservative terms} \qquad (10)$$

where the subscript c refers to the basic state or control experiment, and the primes denote departures therefrom. We find that, in the buckling zone, the nonlinear term ($\underline{v}' \cdot \nabla Q'$) is comparable to or exceeds the linear terms such as $\underline{v}' \cdot \nabla Q_c$ Moreover, the nonlinear term is significant beyond the zone where Q contours are irreversibly deformed; it is also large at high latitudes where elliptical Q contours pass through jet streams. Thus, at the stage of development shown in Figs. 9(a) and (b), there is not a well defined transition between latitudinal bands where the dynamics is linear and nonlinear. We take up this point in section 6(b).

In our basic state, winds are weak through much of the stratosphere above the applied disturbance at mid latitudes. Because the perturbation propagates upwards quickly, nonlinear advection of Q and associated widening of the buckling zone occur simultaneously through a deep layer. One manifestation is the deep, nonlinear coupling found between zonal harmonic waves 1 and 2 (section 7).

(b) Interacting vortices

We integrated the model with strong forcing for 60 days. A major warming was simulated, with zonal easterlies appearing in the stratosphere around day 40. We now describe synoptic developments leading up to the warming. We present evidence that vortex interactions in the stratosphere, subject to a persistent asymmetry in the troposphere, play a role in the dynamics. Our evidence for vortex interactions is descriptive. Mathematical techniques to deal with simplified examples have been developed by Saffman and Baker (1979), Dritschel (1986) and others.

We begin by showing the variation of the maximum geopotential height of the two anticyclones that develop in the stratosphere. We take this height as giving a rough measure of the strength of an anticyclonic circulation (greater height, in this case, corresponds to stronger gradients and winds). Fig. 10(a) applies to 8mb. The curve labelled A is the maximum height in the first downstream anticyclone from the forcing (top left of Fig. 9(b)); curve B is for the second. We shall also refer to the two anticyclones with these labels.

Up to day 30 both curves rise monotonically as the anticyclones systematically strengthen and widen. Curve B rises sharply only when anticyclone A is strong and well into its nonlinear stage of development. This observation, our comparison of the linear and nonlinear wavetrains, and description of how Q is advected, suggest that we are witnessing one form of vortex interaction: an anticyclone, B, forms downstream in response to the nonlinear development of another, A.

As B reaches its maximum height, curve A rises more sharply than before. We account for this second spurt of growth as follows. As B grows the westerly vortex is pressed towards A - the jet stream strengthens on its northern flank. Anticyclone A captures high Q air from deeper within the cyclone.

It seems that there is an interaction between two anticyclones with a deformed cyclone behaving as an active intermediary. The evolution of A at 50 mb, shown in Fig. 10(b), makes this notion more plausible when contrasted with that at 8 mb. At 50 mb, there is only ever one anticyclone, namely A (see Fig. 8). It strengthens rapidly up to about day 20, as it does at 8 mb, but then stops growing just when the second spurt of growth is happening higher up. Without a second anticyclone at 50 mb, the cyclone simply moves off the pole as A develops. At this lower level, the amount of high Q that A captures is limited, and once this has been spread around the anticyclone geopotential heights become quasi-steady.

During the first stage of development of anticyclone A, our analogue of the Aleutian High, the circulation above it near the stratopause remains undisturbed. During its second stage of growth, the closed anticyclonic circulation extends upwards into the upper stratosphere. We then have our first example of irreversible buckling well within a westerly vortex away from a zero-wind line. Fig. 11 is a map of Q and horizontal winds for the 2000 K isentropic surface (near 1 mb) on day 32. Q contours are separating in the top left quadrant near 45°N, where westerly wind speeds were initially about 30 ms^{-1}. A developing anticyclonic circulation is centred there.

Q contours are buckling in a way that has come to be regarded, since the work of McIntyre and Palmer, as a typical signature of a 'wave breaking' event. The heavy arrow in Fig. 11 marks the characteristic formation of a tongue of high Q. At this stage, however, the terms wave propagation and wave breaking seem less appropriate than they might be earlier in the simulation (see also point 12 in McIntyre and Palmer, 1985). We hypothesize instead that what appears here as a new event in the upper stratosphere results from the interaction of non wave-like circulations.

The simulated "Aleutian High" keeps growing as the westerly vortex loses more of its high Q. Fig. 12 shows fields of Q and horizontal wind for day 47 on the 850 K surface. The area of the closed anticyclonic circulation is now much bigger than that of the closed cyclonic circulation. The cyclone is displaced from the pole by the anticyclone, and

redistributed as a band of high Q around low latitudes. Eventually, the cyclonic circulation breaks down altogether (by day 52) and a huge anticyclone covers the pole.

The major warming simulated by our model seems better described by the interplay of vortices subject to a tropospheric asymmetry, rather than by wave concepts and the theory of wave, mean-flow interactions. We emphasize that the breakdown does not merely involve two-dimensional vortex interactions in the stratosphere; the forcing in the troposphere is essential. We repeated the experiment with strong forcing, but we turned off the forcing just when zonal westerlies started to decelerate rapidly. The westerly circulation recovered as anticyclones quickly collapsed in the stratosphere (too fast to be explained by radiative damping).

A crude idea of how two vortices interact comes from the invertibility principle. The principle states that the anomalously low Q associated with an anticyclone can be regarded as a source of anticyclonic circulation, and a region of high Q a source of cyclonic circulation. The circulations thus induced can then act to advect and distort distributions of Q. We would not expect a small anticyclone to be able to break down the circulation of a large cyclone. In our experiment, it takes much longer for the vortices to reach comparable sizes than the week or so of rapid zonal wind deceleration during the major warming. In the real stratosphere, major warmings evolve from highly asymmetric flows. Labitzke (1982) refers to the wave-1 precursor. We return to this topic when we consider so-called pre-conditioning in section 7.

(c) Upward burrowing of tropospheric anticyclones

The coupling of the stratosphere to the troposphere is usually attributed to the upward propagation of planetary waves. We now give an example of coupling which involves the nonlinear, vertical extension of a tropospheric anticyclone - a phenomenon we term upward burrowing. In this section only, we describe an experiment like the one reported above, but with a localised high specified in the upper troposphere at 0°E instead of a low at 180°E. We find that the tropospheric anticyclone (an idealised "block") appears to burrow upwards into the middle of the stratosphere, giving a deep, closed circulation. There is observational evidence that tropospheric blocks can so extend. We show an example of vertical extension during the major warming of February 1979. To compare observed and simulated cases, we show vertical sections of the departure of geopotential height from its current zonal mean (hitherto, a control experiment was used as a reference state for perturbation fields from the model).

In the experiment, a wavetrain develops downstream from the forcing anticyclone. Fig. 13(a) shows the wavetrain on day 21. The tropospheric anticyclone is then very nearly at full amplitude, but the closed anticyclonic circulation above it extends only as far as the lower stratosphere (up to about 25 km). There is a deep anticyclone downstream which forms as Q contours buckle irreversibly in the mid stratosphere.

Once the stratospheric anticyclone is strong, the closed anticyclonic circulation above the forcing appears to burrow upwards. Fig. 13(b) shows that there are two strong anticyclones in the mid stratosphere on day 26. Inspection of the synoptic height maps shows that the closed circulation over the forcing at 45°N now reaches above 10 mb.

The behaviour here is rather like that of the interacting vortices discussed in section 5(b), where we refer to Fig. 11. As there, we can only give a rough description of what seems to happen based on maps of Q (not shown). The downstream anticyclone (near 160°E) in the stratosphere intensifies. As the cyclonic vortex is pressed against the weak anticyclone lying above the forcing in the mid stratosphere, this anticyclone draws a tongue of high Q from the cyclone. The initially weak anticyclone strengthens and high Q progressively surrounds it, and the related closed circulation reaches higher into the stratosphere. The apparent vertical burrowing cannot be thought of solely in local terms; the large-scale nonlinear dynamics of interacting vortices must be considered.

Consider now the atmospheric example. Figure 13(c) shows the departure of the geopotential height from the zonal mean on 16 February 1979 (SSU data have been used). Apart from the region where heights are negative near 100°W, the field is similar to that shown in Fig. 13(a). Notice the incipient anticyclone in the troposphere over the Atlantic. By 20 February, Fig. 13(d) shows that it has intensified; the closed circulation associated with this feature reaches to almost 5 mb.

The similarity of Figs. 13(b) and 13(d) is striking. In particular, both show a baroclinic (westward-sloping) trough immediately downstream from the extending tropospheric block, and also a barotropic trough (little slope) further downstream still.

In our experiment, the changes beween panels (a) and (b) of Fig. 13 are part of a deep nonlinear transition from wave 1 to wave 2 (in the model, the transition is not as deep as it is in the real atmosphere because of the artificial lower boundary condition). In section 7 we discuss a similar transition in more detail. The similarity to the corresponding changes in panels (c) and (d) is circumstantial evidence that nonlinear vortex interactions, giving upward burrowing of anticyclones and nonlinear changes in zonal harmonics, were involved in the major warming of February 1979. This dynamical picture contrasts with that presented by Palmer (1981a) whose diagnosis was based on the theory of wave, mean-flow interactions, taking Eliassen-Palm fluxes to represent the (quasi-linear) propagation of wave activity.

6. EVOLUTION OF BUCKLING ZONE COMPARED WITH THAT OF ANALYTICAL CRITICAL LAYERS

(a) Rearrangement of Q

Solutions for two-dimensional, stationary Rossby waves impinging on a zero-wind line have been obtained by Stewartson (1978) and by Warn and Warn (1978). We shall refer collectively to SWW's solution. Killworth and McIntyre (1985) and Haynes (1985) extended the work by considering the

effect of instabilities on the predicted flow. The analytical solutions are linear everywhere except for a thin, nonlinear region near the zero-wind line, called a critical layer, where Q contours buckle irreversibly. We refer to such regions more generally as buckling zones in our simulations - not all of them are linked with zero-wind lines (section 8).

These solutions have been seen as relevant to the atmosphere in two ways. (1) McIntyre and Palmer (1984) proposed that the irreversible buckling of Q contours that they observed in the stratosphere is "the real-life analogue of the theoretical nonlinear critical layer". They proposed that there is a "surf zone" outside the westerly vortex where the strongest quasi-horizontal mixing of Q occurs, resulting in weak gradients on a large scale. (2) Killworth and McIntyre discussed, in the context of these solutions and also more generally, whether critical layers absorb, reflect or over-reflect wave activity.

SWW's solution relies on restrictive assumptions made to make analytical methods applicable. The theoretical critical layer is but one example of a buckling zone. Its value is that we can learn about the dynamics of other examples by determining which, if any, of the assumptions break down, and what the consequences then are. Our discussion relates to (1) in this section and to (2) in section (b).

Figure 14(a) shows SWW's solution for a two-dimensional, nonlinear critical layer. Contours are isopleths of Q, and are material lines as the flow is taken to be adiabatic and inviscid. We have superimposed on the

field arrows showing the wind direction inferred from the streamlines plotted by SWW. The winds form a closed anticyclonic circulation in the middle of the panel. In this simplified theory, tongues of low and high Q form as the winds twist up the contours. Notice that the winds blow through the tips of the tongues of both high and low Q. If the perturbation is sustained, the twisting is extreme: tongues get thinner and thinner and the critical layer becomes well mixed apart from fine structure (the process is actually very slow in SWW's solution). If the tongues become locally unstable, the gradient of Q in the critical layer is still weakened on the large scale, but Q may then tend to clump into blobs so the mixing is incomplete (according to McIntyre and Palmer, 1984).

Two of the main assumptions of the theory are that (1) there is no dissipation; and (2) perturbations have small amplitude so their longitudinal scale is much bigger than the width of the critical layer; the ordinate's scale is exaggerated in Fig. 14(a). Assumption (1) means that Q contours cannot break or join; (2) can be shown to mean that Q is advected to leading order in the thin critical region as though it were a passive tracer, i.e. winds there are largely unaffected by changes in Q. Assumption (2) also means that the critical layer stays thin.

These assumptions are not valid in our experiment with strong forcing. First, the flow is dissipative owing to radiative damping and numerical truncation, so Q contours break or join. Second, disturbances in the stratosphere are strong. The buckling of Q contours takes place on a large zonal and meridional scale. Q is not advected like a passive tracer - an important point to appreciate - but modifies the winds in a buckling zone

which widens as more Q is entrained. Also, the flows we simulate are baroclinic and three dimensional, a point relevant to our findings in sections 6(b) and 8.

A portion of Fig. 9(a) is reproduced in Fig. 14(b). A given length measured on either axis of the figure corresponds to almost equal distances, unlike in Fig. 14(a). A principal difference is that tongues of low and high Q do not continue to entwine and thereby become thinner and thinner, like they do in SWW's solution. Rather, a cut-off anticyclone is formed centred on an isolated patch of low Q. Winds blow more around this deep feature than through it, so the associated low Q is not advected like a passive tracer, nor is it mixed substantially with higher Q.

We now turn to how the cut-off occurs. The tongues form on the southern flank of the westerly jet where the relative vorticity is anticyclonic. A low Q anomaly adds to the anticyclonic vorticity, whereas high Q subtracts from it. Hence, the anticyclonic circulation does not lie symmetrically between the tongues, but moves polewards to where Q is low. Easterly winds blow through the tongue of high Q drawing it around the anticyclone. At the point marked with an asterisk in Fig. 14(b), Q contours of the same value are about to meet. Dissipation (radiative and numerical) allows them to join, and an elliptical contour is formed. In this way, an island of low Q forms, as in the top left quadrant of Fig. 9(b) (Q decreases slightly at the centre of this anticyclone because the model does not conserve Q exactly even when there is no radiation). The cutting off of anticyclones is not sensitive to the resolution of our model in the range available to us. The behaviour is reproduced with a model

having 72 grid points along a latitude circle instead of 16. Experiments with higher resolution still and realistic dissipation are now needed to check our findings.

In SWW's solution, Q gradients are weakened (apart from small-scale structure) by mixing in the anticyclone, whereas gradients increase on the poleward and equatorward flanks. The persistent anticyclones simulated by our model have a distribution of Q that is similar to this even though strong mixing is not involved. The weakening and tightening of gradients is most clearly seen when the initial gradient of Q is uniform. Fig. 15(a) shows a portion of a Q field in an initially axisymmetric flow (it is for the 2000 K surface of the basic state described in section 6). Fig. 15(b) is the corresponding field when a closed anticyclonic circulation has formed, its centre marked by the cross. The contours labelled A and B move apart and gradients tighten on both sides of the buckling zone. Weak gradients arise because the tongue of low Q widens as the anticyclone strengthens.

These changes in Q gradients are broadly similar to those that would be expected in a poorly resolved view of a mixing region, and are, in effect, irreversible if the forcing persists. So it can be dangerous to identify a mixing region or 'surf zone' by weak gradients on a synoptic map. McIntyre and Palmer (1984) recommend instead that the area contained within a Q contour be plotted as a function of Q, the boundary of the surf zone showing up as a sharp change in the slope of this function. However,

Butchart and Remsberg (1986) and O'Neill and Pope (paper in preparation) note that dynamically induced radiation and mixing can have similar effects on this function.

Our results highlight some limitations of SWW's solution as a model for the development of the Aleutian High in the stratosphere. We expect less mixing of Q to small scales than there would be if the ordinate in Fig. 14(a) could be stretched to represent the width of the Aleutian High, and the solution depicted still applied. The term "surf zone", with its connotation of strong mixing, seems less appropriate for the buckling zone in our experiment than it does for the critical layer in SWW's analytical model. The situation in the real stratosphere remains to be clarified.

(b) The signature of a widening buckling zone in $\underline{F}$ and D_F

Killworth and McIntyre (1985) ask whether a nonlinear critical layer based on SWW's solution absorbs, reflects or over-reflects wave activity. This might matter for the dynamics of the stratosphere because reflection from a critical layer - or more generally a buckling zone - could be an important mechanism for inducing strong polar warmings through focusing of wave activity or resonant growth of wave amplitudes or both (McIntyre, 1982).

We discuss the question in this section by contrasting the evolution of $\underline{F}$ and D_F in SWW's analytical model with that of the buckling zone in the simulation discussed in sections 5(a) and 5(b). We consider in particular two features of these diagnostics: (1) a dipole pattern in D_F develops as

the buckling zone starts to widen; (2) later on, $\underline{F}$ points upwards and polewards at high latitudes which would imply, if linear theory were valid, that wave activity is focused into the polar cap.

SWW's solution applies to a two dimensional, quasi-horizontal flow. Its counterpart in three dimensions would have a vertically aligned zero-wind line with Rossby waves striking it perpendicularly (e.g. by having been strongly refracted so that they propagate horizontally). Killworth and McIntyre summarise the properties of SWW's solution in their Figs. 1 and 2. Whether the critical layer absorbs, reflects or over-reflects wave activity is determined by the divergence of $\underline{F}$ across it, or, equivalently, by the average meridional flux of quasi-geostrophic potential vorticity within it. These quantities evolve through nonlinear advection of Q in the critical layer. Advection of high and low Q in the critical layer moves ridges and troughs east-west, thereby changing the meridional phase gradient of the disturbance. By a well-known result of quasi-geostrophic theory, the associated horizontal momentum flux changes, as do D_F and the direction of $\underline{F}$. In the idealised conditions of SWW's problem, a wave of varying amplitude returning from the critical layer is superimposed on a steady wave propagating towards it. The direction of $\underline{F}$ depends on the relative amplitude of these waves.

The critical layer begins as a wave absorber, i.e. it is only partially reflecting because the returning wave has smaller amplitude than the incoming wave. $\underline{F}$ points towards and converges on the critical layer. As nonlinear advection of Q proceeds, $\underline{F}$ tends to zero (together with the phase gradient of the disturbance), and the critical layer turns

momentarily into a perfect reflector (waves coming in and out have equal amplitude). Then it becomes over-reflecting as Q contours continue to twist up. $\underline{F}$ points away from the critical layer where there is now divergence. In SWW's solution, the cycle repeats (though less strongly). Killworth and McIntyre, and Haynes (1985) have shown however, that an instability develops in the flow, and suggested that it probably inhibits these oscillations, so that the critical layer approaches a reflecting state but may never become strongly over-reflecting.

Thus, if these results applied, a circumpolar westerly vortex surrounded by easterlies would form an imperfect but self-tuning cavity. Waves might grow resonantly as the critical layer becomes more reflecting.

The terms wave absorption and reflection have a clear physical meaning in SWW's problem because there is a well defined, linear "far-field" outside the critical layer where concepts of wave propagation apply. In our simulation, however, such concepts are not clear-cut - the buckling zone is wide. Moreover, there need not be a correspondence between the meridional direction of $\underline{F}$ and the sign of D_F, as we later explain.

Figure 16 shows the evolution of D_F at 8 mb for our experiment. As discussed in section 4(b), the buckling zone starts as an over-reflector as indicated by divergence at mid-latitudes (shaded) until day 10. It would also do so in SWW's solution if the gradient of Q in the critical layer were reversed (this may be inferred from Eqs (2.31) to (2.36) in Killworth and McIntyre, 1985). In the upper stratosphere, by contrast, it begins as an absorber; Q increases monotonically polewards as in SWW's solution. By

day 16, the mid latitude divergence at 8 mb vanishes. The band of strong convergence moves south from high latitudes as the over-reflecting barrier is smeared out (section 5(a)). $\underline{F}$ leans equatorwards, apparently defocused from high latitudes. The buckling zone becomes an absorber; disturbances originating at mid latitudes do not penetrate to low latitudes.

There is a dipole in D_F from about day 17 to day 27 with divergence at high latitudes and convergence at mid latitudes, Geller et al. (1983) and Hartmann et al. (1984) find such dipoles using observational data. (Robinson, 1986, notes that divergence is stronger when calculated from geostrophic rather than from, as here, actual winds.) In our experiment, the divergence is not due to the decay of wave activity as given in Eq. (6). Hartmann (1983) suggests that, for linear, growing waves, divergence in the stratosphere might imply a source of wave activity there. The argument relies on there being a region where D_F is positive and $\overline{q}_Y$ is negative; consider Eqs. (5) and (6). There is no such region at high latitudes in our simulated fields. Alternatively, divergence might be induced by dissipation of linear waves, by ageostrophy or by nonlinear effects (Andrews, 1987).

To see how the dipole arises, we now relate the divergence of $\underline{F}$ to local features on synoptic charts. We make a local connection by using Plumb's flux, $\underline{P}$, the zonal mean of which is $\underline{F}$. It proves simpler to use the 1 mb level for illustration. Our synoptic discussion focuses on localised jet streams, and there is only one to contend with at 1 mb, whereas there are two at 8 mb. However, D_F and $\underline{F}$ evolve similarly at the two levels for the period of interest.

Figure 17(a) is a map of Q and horizontal wind vectors for day 21, when divergence is largest at high latitudes. Q contours in the buckling zone have a pattern similar to that of the theoretical critical layer at its absorbing stage. There is a strong jet stream near 60°N on the poleward flank of the developing anticyclone. Notice that the jet crosses lines of longitude from the south-west to the north-east.

Figure 17(b) is a map of the horizontal projection of $\underline{P}$. The magnitude of $\underline{P}$ is largest near the jet entrance, and the orientation of the jet corresponds to $\underline{P}$ having an equatorward direction. $\underline{P}$ has much smaller magnitude on either side of the jet stream. Consequently, the equatorward component of $\underline{F}$ is largest near the latitude of the localised jet, and D_F changes sign there. We therefore conclude that the dipole has its origin in the formation of a localised jet, a process that involves nonlinear dynamics as we have already noted.

If the tropospheric forcing is not too strong, the dipole could be sustained, as it is in the southern hemisphere (Mechoso et al., 1985). Then, the widening of the buckling zone is inhibited by radiative damping, and a quasi-steady flow like that in Fig. 17(a) might persist. In our experiment, however, radiative and numerical damping are too weak for this.

Maps of Q, winds and the horizontal component of $\underline{P}$ for day 29 are shown in Fig. 17(c) and (d). Compared with Fig. 17(a), the anticyclone in Fig. 17(c) has moved north eastwards as the low Q associated with it is advected in a widening buckling zone. At high latitudes (polewards of

about 60°N), the jet is roughly mirror symmetric about a reference line of longitude through the centre of the anticyclone. The symmetry is reflected in the horizontal component of $\underline{F}$. As the jet rotates clockwise with respect to the reference line, arrows of $\underline{F}$ point upwards because the meridional phase gradient of the disturbance reduces (and hence the eddy momentum flux term in $\underline{P}$ and $\underline{F}$). This aspect is analogous to the changing meridional gradient of phase in the theoretical critical layer. Notice at high latitudes that the magnitudes of $\underline{P}$ in Fig. 17(d) are now similar at the jet entrance and exit (they were shorter at the exit in Fig. 17(b)). The contributions to $\underline{F}$ are opposed at these places. Even slight changes in jet structure at this stage can lead to a flip in the direction of $\underline{F}$ at high latitudes, as we find in our experiment and has been found in the atmosphere by Palmer (1981a) and others.

Likewise, nonlinear advection alters the phase gradient in the vertical. At high levels, eastward advection of the anticyclone can reduce the westward tilt with height, since the phase of the disturbance at the lower boundary is fixed. Such a tendency towards barotropy should inhibit the vertical penetration of disturbances.

The band of convergence in Fig. 16 moves polewards and arrows representing $\underline{F}$ point upwards as the buckling zone widens. The sequence of divergence followed by convergence with $\underline{F}$ apparently focused into polar latitudes is typical of the real atmosphere during highly disturbed conditions (Palmer, 1981a; O'Neill and Youngblut, 1982; Shiotani and Hirota, 1985).

This change in sign of the meridional component of $\underline{F}$ prompts the question: has the buckling zone turned from being an absorber (equivalently, a partial reflector) into an over-reflector of wave activity? The strong convergence of $\underline{F}$ across the buckling zone (Fig. 16, days 25 to 45) shows that it has not. It stays absorbing by widening and entraining more high Q (see also McIntyre, 1982, section 5). Correspondingly, the distribution of Q does not look like that of the critical layer at its reflecting or over-reflecting stage (compare Fig. 17(c) with Fig. 2(d) in Killworth and McIntyre).

In the case of the two dimensional critical layer, poleward pointing $\underline{F}$ must correspond to divergence across the critical layer ($\underline{F}$ can be neglected on the southern flank of the critical layer in easterly winds), and hence over-reflection. There is no such restriction on a three-dimensional flow. There is convergence of $\underline{F}$ in the vertical, as well as in the horizontal because (1) the zero-wind line slopes with height in our initial state, and (2) there is vertical convergence through transience and dissipation. Vertical convergence of $\underline{F}$ allows $\underline{F}$ to be poleward pointing when the buckling zone is still absorbing.

The main point of similarity between the theoretical critical layer and the buckling zone is that nonlinear advection of Q changes the meridional phase gradient and hence the direction of $\underline{F}$. Beyond that, too close an analogy should not be made. In particular, when $\underline{F}$ appears focused polewards in the simulation, there is no linear far field, so the concepts

of reflection and focusing are not well defined. It would not be easy, in such circumstances, to decide whether resonance was important in amplifying what waves there were.

The breakdown of the polar vortex in a stratospheric warming has been attributed to the polar focusing of $\underline{F}$ by an evolving critical layer (e.g. Dunkerton et al, 1981). According to this picture, the breakdown at high latitudes results from wave, mean-flow interactions promoted by the configuration of the flow at lower latitudes. In our view, the account of vortex interactions given in section 5(b) is a more appropriate description when the buckling zone is very wide. Even if it were possible to define waves propagating on the westerly vortex, their dynamics would be highly entangled with that of vortex interactions.

7. VACILLATION CYCLES AND PRE-CONDITIONING

(a) Introduction

Though there has recently been a turn towards a synoptic description of the stratosphere using maps of Q (following the work of McIntyre and Palmer, 1983, 1984, 1985), dynamical thinking remains strongly influenced by arguments based on zonal averaging. Theories of wave, mean-flow interaction developed, for example, by Andrews and McIntyre (1976, 1978) provide the framework. Since the work of Matsuno (1971) diagnostic studies and idealised numerical simulations of stratospheric warmings are often concerned with explaining changes in zonal mean winds. Such changes are connected with pulses in the amplitudes of wavenumbers 1 or 2. The wave

pulse initiating a stratospheric warming is usually assumed to have its origin in a pulse in the troposphere which then propagates upwards. The troposphere is thus regarded as a wavemaker, generating large-scale planetary waves by some means or another. The response of the stratosphere to such pulses, it has been argued, is governed by zonally averaged quantities such as the refractive index (e.g. Kanzawa, 1980; Butchart et al., 1982; O'Neill and Youngblut, 1982), determing whether waves are refracted into low latitudes, or are focused into polar regions leading to a strong warming. McIntyre and Palmer (1983) have extended this idea to treat waves propagating on a cyclonic vortex displaced from the pole. The concept of pre-conditioning has been introduced (Butchart et al.; Kanzawa; Palmer, 1981b). A defocused tropospheric pulse gives only a minor stratospheric warming but changes the stratosphere - its 'basic state' - so that a later tropospheric pulse is more focused and a major warming is more likely to ensue.

So it is tacitly assumed that, at some point prior to a warming, the stratosphere can be described in terms of disturbances on a quasi-steady state for the usual ideas of wave propagation to apply, and that a simple property of this state (zonal wind distribution, or area of the cyclonic vortex) determines whether a major warming is favoured when the next tropospheric pulse comes along. Minor and major warmings are thus thought of as distinct events forced by distinct upward propagating pulses from a tropospheric wavemaker.

Our purpose in this section is to relate the zonally averaged and synoptic pictures. We show that the above theoretical interpretation of sudden warmings could be misleading. Our arguments are based on warmings simulated under controlled conditions. Warmings in the real atmosphere are probably more complicated still; shortcomings of the theories, as they now stand, are unlikely to be limited to our simulations.

Long after the strong tropospheric perturbation we apply becomes steady, the simulated stratosphere undergoes a sequence of large oscillations, or vacillations, in the zonal mean wind and wave amplitudes. These vacillations resemble changes observed in the real stratosphere. We relate them to localised changes in the flow. The sequence of a major warming following a minor warming is reproduced, as are the often-observed polar confinement of the zonal mean jet, and the shrinking of the westerly vortex. Travelling zonal harmonics, observed to accompany warmings (O'Neill and Taylor, 1979; Madden and Labitzke, 1981), are also reproduced.

We argue, however, that concepts of wave propagation and the attendant theory of wave, mean-flow interaction are not useful at this stage of the experiment (though they are during the first ten days or so). We have already mentioned our inability to identify a linear wave domain where theories of wave propagation can be applied. Moreover, the zonal mean flow varies on the same timescale as the amplitude of the waves, not much more slowly as required in order for wave, mean-flow theory to be simple. In our experiment, the minor and major warmings should not be viewed as separate events for the following reasons. (1). There is no quasi-steady state between them when the stratosphere is evolving only slowly. (2) The

forcing is steady during the sequence (and has been for much longer than it takes planetary waves to propagate from the troposphere through the stratosphere), so there is no new tropospheric wave pulse (as defined by the 300 mb geopotential) to propagate on a supposedly pre-conditioned state. Rather there are deep nonlinear transitions which alter the zonal wind, and amplitudes and phases of zonal harmonics. (3) Such oscillations notwithstanding, we noted in section 5(b) that there are systematic changes in the circulation when viewed locally (anticyclones build steadily, cyclone shrinks steadily).

(b) A simulated vacillation cycle

We recall that two anticyclones develop monotontically during the first 40 days of the integration. The variation in zonal harmonic wave amplitudes is not monotonic, however, but oscillatory.

Figure 18 shows the variation in amplitude of harmonic waves 1 and 2 at 62.5°N. Their evolution is readily described in terms of more localised developments. Referring to Figs. 9(a) and 10(a), wave-1 increases at first when a single developing anticyclone is dominant. From about day 16, it decreases rapidly in the middle stratosphere, attaining smallest amplitudes when those of wave 2 are at a maximum. These changes coincide with the growth of a second anticyclone separated in longitude by about 180° from the first. (The decrease in wave 2 between days 15 and 20 is related to the merging of anticyclones described in section 5(a)).

The anticyclones are deep and wide. The wave-1 to wave-2 transition occurs simultaneously from 25 km to above 48 km (Fig. 18), and from 40°N to 80°N (not shown). There can be no such oscillation in the lower stratosphere because no provision is made for downstream effects from the localised disturbance at the lower boundary. This restriction appears to influence the stratosphere up to a scale height (7 km) or so above the boundary.

The anticorrelation in time of the amplitudes of the two harmonics implies that they are nonlinearly coupled. There are several pieces of evidence to support this contention. (1) There is no such phase relationship between the harmonics in our experiment with weak forcing. (2) We have shown that nonlinear advection of Q is involved in the formation of cut-off anticyclones. (3) There is a region in the lower stratosphere at mid latitudes where the wave-2 component of D_F is divergent even though wave 2 is growing, contradicting the linear result, Eq. 5. (Note: such divergence in the stratosphere is not necessarily a pre-requisite for the nonlinear generation there of a particular harmonic, especially if the transition between harmonics extends down to the upper troposphere.)

Palmer and Hsu (1983) also demonstrated that strong wave 2 can be generated nonlinearly in the stratosphere when the forcing is pure wave 1. In interpreting a wave-1 to wave-2 transition in the real stratosphere, they argued that the development was nonlinear with respect to latitude circles, but might be explained by linear, upward propagation of wave 1 on a displaced polar vortex. By contrast, we suggested (section 5(b)) that

the transition in our experiment could be viewed as a form of vortex interaction - an inherently nonlinear process, not an artefact of an injudicious choice of co-ordinate system for defining propagating waves. Indeed, Juckes (personal communication) finds that wave-2 generation is a characteristic feature of experiments with a barotropic model forced by wave-1 topography. Details of vertical propagation are inessential in his experiments.

What might be termed a sequence of minor and major warmings can be seen in the zonal winds at 1 mb, shown in Fig. 19. First winds decelerate as the westerly vortex moves off the pole and the first downstream anticyclone from the forcing develops (wave 1 builds). As the second anticyclone grows, zonal winds at high latitudes accelerate as the westerly vortex, now elliptical, moves back towards the pole. The zonally averaged jet is confined to high latitudes; zonal winds are weak westerly or easterly at latitudes containing the southern flanks of the anticyclones.

A northward movement of the zonal mean jet has been held significant for the dynamics of later warmings (e.g. Quiroz et al., 1975; Kanzawa, 1980). Palmer and Hsu refer to a rapid re-acceleration of zonal winds after a minor warming as a sudden cooling. They argue that a sudden cooling can produce a so-called pre-conditioned, narrow jet that will focus planetary waves, thereby promoting a major warming.

For our case, the term sudden cooling would be misleading if it were taken to mean that the stratosphere, after being disturbed, had quickly settled to a new, relatively undisturbed state (so that the zonal mean may

be taken as a 'basic state') awaiting the next impulse from below. Consider the synoptic pattern when the confined zonal mean jet is strongest (day 26, Fig. 19). It is highly distorted by two anticyclones which, up till then, have developed systematically. It is not quasi-steady but rapidly evolving, and the relevance of the current zonal mean state as a basic state for wave propagation is unclear.

McIntyre and Palmer (1983) propose that it is not propagation on the zonal mean state that matters but propagation on the cyclonic vortex, wherever it lies, since only a cyclonic vortex can support the propagation of stationary Rossby waves. They suggest that irreversible mixing by breaking, planetary waves can erode the vortex. A small vortex, they argue is more susceptible to disruption than a large one. They predict that conditions prior to major warmings will be found to be characterized by an unusually small cyclonic vortex in the stratosphere.

Their reasoning is based on considerations of wave 'focusing'. We suggest that it is not just the size of the cyclonic vortex that matters. Moreover, it is not enough to consider, as McIntyre (1982, section 8) does, wave propagation on a vortex made symmetric in such a way that Q contours enclose the same area. It happens that the area enclosed by given Q contours changes little in the stratosphere in our experiment between the start and day 30 (though the size of the cyclone on a synoptic map does decrease). The response of the stratosphere to a new tropospheric pulse growing from day 30 is, however, markedly different from that described

above. In one experiment, a major warming ensued just 5 days after a new pulse reached full amplitude, compared with 35 days starting from symmetric conditions.

We contend that asymmetries in the flow and accompanying vortex interactions are relevant at the onset of a major warming (often taken to be when zonal winds start to decelerate rapidly), though a small cyclone is indeed more liable to be displaced and stretched out by a large anticyclone. Unless the size of the cyclonic vortex is the dominant factor in promoting its breakdown, there is no reason to suppose that it need be unusually small before a major warming. Fairlie and O'Neill (1987) note that the stratospheric cyclone was strongly distorted but not unusually small before the major warming of 1984/85 (at the start of rapid deceleration of the zonal-mean wind), and remark that wave amplitudes in the upper troposphere were large, but not unsually so compared with winters not having major warmings.

(c) Travelling harmonic waves

Travelling zonal harmonic waves of large amplitude have been identified in the real stratosphere. Madden and Labitzke (1981) found a westward travelling wave 1 in the stratosphere in January 1979, and argued that its structure was similar to a free Rossby wave with a 16-day period. They proposed that interference between travelling and stationary waves could account for observed variations in total wave amplitude.

We use fields from our model to show how travelling harmonics with varying amplitude can arise when two quasi-stationary anticyclones form at different times. The anticyclones develop nonlinearly, so we do not expect the travelling harmonics to be free Rossby waves (normal modes).

Figure 20 is a longitude-time section of the wave 1 component of the height field at 1 mb and at 62.5°N. The phase variation is readily seen from the changing longitude of the zero contour. During the first 10 days, wave 1 travels rapidly westwards as linear, travelling waves are excited by switching on the forcing. We shall concentrate on the next period of fast westward travel, roughly between days 18 and 26. There are two features to discuss. First, the largest westward phase speed occurs when the amplitude of wave 1 is decreasing and that of wave 2 is increasing (see also Fig. 18). Second, the phase speed decreases as wave 1 starts to build again.

We account for both of these aspects by referring to an Argand diagram, Fig. 21. At 1 mb the amplitude of wave 2 is increasing; geopotential heights associated with one anticyclone are quasi-steady at 62.5°N while there is a rapidly developing anticyclone about 140° away in longitude. We represent the wave-1 component of both by nearly oppositely directed vectors $\underline{A}$ and $\underline{B}$ in Fig. 21. The length of $\underline{A}$ is constant and that of $\underline{B}$ is increasing at a roughly constant rate. Because the anticyclones are stationary in the period of interest, the directions of both are fixed.

The total wave-1 component is the vector sum of $\underline{A}$ and $\underline{B}$. This resultant is represented by the vector $\underline{C}$. Imagine $\underline{B}$ starting with zero length. As it lengthens, $\underline{C}$ get shorter and the phase angle, θ, decreases

(θ is the phase in degrees east), i.e. the resultant harmonic travels westwards as total wave 1 decreases in amplitude. It reaches a minimum amplitude when $\underline{C}$ is orthogonal to $|\underline{B}|$, as it is in the figure. This is when total wave 1 is travelling westwards most rapidly, because at this point a given increment in $|\underline{B}|$ subtends a bigger angle at the origin 0 than it would either side.

This deals with the first aspect of Fig. 20 that we noted. As for the second, clearly beyond the point where $\underline{B}$ and $\underline{C}$ are orthogonal in Fig. 21, the amplitude of total wave 1 increases and the phase speed decreases until $\underline{B}$ stops lengthening.

We can apply a similar argument to total wave-2. We find that wave 2 pulsates in amplitude but travels little. The wave-2 components of the two anticyclones are nearly in phase, so the phase of the resultant is insensitive to the length of vectors in the Argand diagram.

Whether wave 1 travels westward or eastward, and whether its amplitude is increasing or decreasing as the phase speed slows depends sensitively on the relative positions and strengths of the anticyclones. For example, between days 26 and 42 wave 1 is eastward travelling.

Plumb (1981a, b) has suggested that a slowing down of the travelling wave as wave amplitudes are increasing might indicate an approach to resonance. The idea is that a normal mode of the atmosphere becomes stationary (when the basic state is modified, say), and then there is

resonant growth because the forcing is also stationary. This argument may work for simple models such as that of Plumb, but it is hard to see its relevance to our case.

We have used SSU data to study the period analysed by Madden and Labitzke (1981). Referring to Fig. 3 of their paper, the westward travelling wave 1 that they identify in the lower stratosphere also has smallest amplitude when it is travelling fastest (about 16 January 1979). This is when SSU measurements show that wave 2 is building. At 10 mb, however, wave 1 is eastward travelling in SSU fields. We have studied the synoptic development. The evolution is more complicated than in our case, but a common feature is that both flows have an elliptical westerly vortex straddled by two anticyclonic regions. This similarity, and the large amplitude of the wave 1 (exceeding 500 gpm at 30 mb), suggest that the travelling wave analysed by Madden and Labitzke is not a linear normal mode but an harmonic whose phase varies as the flow evolves nonlinearly.

(d) Discussion

In our model, vacillations in zonal mean winds and harmonic waves are connected with the nonlinear development and mutual interaction of deep, closed, anticyclonic circulations which extend from low to high latitudes. The period of these variations is about 3 weeks. Vacillations with periods observed in the real stratosphere are simulated with much smaller harmonic amplitudes at the forcing level than were needed in the highly truncated model used by Holton and Mass (1976) (about 100 gpm rather than about 300 gpm) . Our simulation has strong localised forcing.

Our idealised simulation reproduces the type of oscillatory behaviour observed in the stratosphere. For example, the stratosphere in January 1982 evolved in a similar way to our experiment, both synoptically and in zonal mean winds and wave amplitudes (compare Figs. 2(a) and 2(e) of Naujokat et al, 1982, with our Figs. 19 and 18). Labitzke (1982) surveyed many northern winters and recorded the following. First, height wave 1 amplifies concurrently with a minimum in height wave 2 before a major warming. Second, growth of wave 2 often accompanies the breakdown of the westerly circulation. Our simulation has reproduced both these features.

In our experiment, the vortex is advected off the pole but does not split. There is evidence that nonlinear interaction of wave 2 with wave 1 is important during the build up of wave-2 warmings when the vortex does split. Labitzke (1977) finds that strong wave 1 (maps show an intense Aleutian High) is a precursor to a major warming of both kinds. SSU data show the intense wave 2 warmings of 1979, 1982 and 1984/85 were all preceded by large amplitudes in wave 1 (the transition between harmonics taking longer in 1979). Labitzke classifies winter months into disturbed wave-1 and cold wave-2 types. One reason that polar temperatures and winds are more disturbed in the former case is that, given strong wave 1, nonlinear harmonic coupling with wave 2 is possible so the stratospheric cyclone is jostled about the polar cap. In the latter case, symmetry precludes such coupling if wave 1 is weak to start with. Apparently, wave 2 does not amplify to split the westerly vortex from a cold wave-2 pattern.

In the observed examples just quoted, the transition in time from wave 1 to wave 2 extends from 100 mb well into the stratosphere. Fairlie and O'Neill (paper in preparation) studied the 1984/85 case and also noticed a similar transition in the troposphere. They show that wave 2 grows when a deep anticyclone develops over the Atlantic in the stratosphere already containing an intense Aleutian High and an elliptical cyclonic vortex.

There is some evidence which, at first sight, contradicts our suggestion that coupling between zonal harmonics is important during actual wave-2 warmings. Butchart et al. (1982) claim that their idealised experiment (I) shows that wavenumber 1 and wave-wave interactions were not crucial in the wave-2 warming of February 1979. This experiment was initialised on 16 February 1979 (there were zonal easterlies by 22 February) with all components except the zonal mean and wave 2 subtracted from observed fields. The reproduction of zonal easterlies notwithstanding, there is no direct evidence from this experiment that nonlinear coupling can be neglected in the actual warming. Moreover the experiment was initialised late in a vacillation cycle of the real stratosphere. The transition to wave 2 was already effected to a large extent in the lower stratosphere, as Fig. 13 shows (discussed in section 5(c)).

They also claim that the essential features of the warming were reproduced in another of their idealised experiments (IV) in which a growing, eastward-travelling perturbation in wavenumber 2 was applied to the zonal mean (symmetric) state on 16 February. This experiment apparently contradicts our assertion that initial asymmetry in the flow is

relevant to the dynamics of the rapid breakdown of the westerly circulation. We repeated the experiment, using the same model with minor improvements, and found what we judge to be significant dynamical differences between the three-dimensional evolutions of the real warming and this simulation. In particular, when zonal easterlies appear in the simulated stratosphere, the cyclonic vortices at 10 and 100 mb are stretched along axes orthogonal to each other, whereas in the real case the axes are almost aligned. These differences are masked by zonal averaging.

The deep, wide, apparently nonlinear pulsations that characterize the winter stratosphere imply that it is a considerable over-simplification to regard troposphere-stratosphere coupling as comprising a tropospheric wavemaker and a stratospheric 'basic state' upon which waves propagate at first linearly, later to become nonlinear when they 'break'. Such a description is applicable for the early stages of idealised experiments starting with an axisymmetric flow and with prescribed forcing (such as our experiments, and the series of idealised experiments designed by Butchart et al.). Stratospheric major warmings do not ensue from such convenient initial states.

In our experiment, there is no natural way to think of the flow as being pre-conditioned just before the major warming. No obvious basic state presents itself, and there is no new tropospheric pulse. We do not claim that real stratospheric warmings are associated with a steady tropospheric flow pattern. On the contrary, pulsations in the real troposphere are an added complication.

8. IRREVERSIBLE BUCKLING AWAY FROM ZERO-WIND LINES

Zero-wind lines (critical lines) are not the only places where stationary disturbances irreversibly buckle Q contours. In section 5(b), we described how this can happen within a westerly vortex. The flow was already highly nonlinear at a lower level when buckling started higher up as a closed anticyclone extended upwards.

In simpler, idealised flows we can use the properties of linear stationary waves to predict sites for irreversible buckling well away from a zero-wind line (see also Marks, 1986). Wave amplitudes can get big enough in the rarefied high atmosphere to produce easterlies locally where there were once strong westerlies. Lower down, the density is greater, so irreversible buckling is favoured where winds are weak.

We show the density effect operating by choosing as an initial state a flow with a very broad westerly jet. In the upper stratosphere, the zero-wind line is in a different hemisphere from the forcing. We repeated the experiment described in section 5, but choosing the initial field during a southern winter and centring the forcing at 45°S, 180°E.

Figure 22 shows the initial wind, the zonal mean wind for the southern hemisphere on 12 September, 1981. We computed it from SSU measurements. Zonal easterlies are confined to low latitudes and to the mid stratosphere. The negative of Q decreases monotonically from the south pole to the equator (not shown).

We use the displacement field introduced in section 3(c) to examine the meridional movement of Q contours when the wavetrain produced by the forcing is still linear at middle and high latitudes (linearity checked as before). Fig. 23 shows the displacement on the 2000 K isentropic surface (near 0.7 mb) on day 11.

The displacement field results from waves radiating downstream and equatorward from the forcing, as may be inferred from the phase gradient. Just downstream from the cyclonic forcing at 180°E, displacements are largest over a broad latitudinal band centred at mid latitudes; wave activity has not yet dispersed very much. Further downstream, wave activity is more dispersed, and the largest displacements are confined to a narrower band at low latitudes where winds are weak.

There is one site, labelled B on the figure, where Q contours have already buckled far enough that the meridional variation of Q is no longer monotonic locally (i.e. the Q contour makes an s-turn). Values of displacement cannot be computed with our algorithm in the blanked out rectangle because of this.

At the site labelled A, Q contours are just about to make an s-turn. They do so where the meridional gradient of the displacement field is large and positive, which is where Q contours move furthest apart. Notice that A is well separated from B; the irreversible buckling at A is not because of encroachment by the buckling zone at B.

At A, the disturbance is quasi-stationary and westerly winds are about 40 ms^{-1} initially, but displacements become large enough for Q contours to buckle irreversibly and the wind direction to reverse locally. Fig. 24 shows for day 16 the distribution of Q and wind vectors on the 2000 K isentropic surface. The points labelled A and B correspond to the sites thus labelled in Fig. 23. At A, the westerly jet divides around adjacent tongues of high and low Q. The buckling region at B is nearer the edge of the westerly vortex. As it widens, another example of the nonlinear coupling between harmonic waves 1 and 2 is reproduced.

Irreversible buckling well within the vortex can happen even in the lower stratosphere in early winter, as Clough et al. (1985) noticed. Refraction of wave activity (in cases where these concepts are relevant) is not always strong enough for disturbances to impinge on the zero-wind line before the density effect comes into play.

9. CONCLUSIONS

We have examined the relevance of linear and weakly nonlinear theories of stratospheric dynamics for interpreting the results of idealised numerical experiments. Linear theory can be used for initially axially symmetric flows when the forcing at the lower boundary of our model is weak, or in the early stages of experiments with strong forcing. There are identifiable Rossby wavetrains emanating from a localised forcing. Since the zonal mean flow changes only slowly early on and wave amplitudes are small, we can use theories of linear wave propagation and wave, mean-flow interaction. However, once the disturbances attain large amplitude, there

is no obvious wave propagation, and the evolution in our experiments is more usefully described (but not treated so simply mathematically) in terms of three-dimensional vortex interactions subject to tropospheric asymmetry. The real stratosphere is rarely close to being zonally symmetric during winter in the northern hemisphere, particularly in the week or so preceding a major warming. The real flow is typically more like that 30 days into our integrations with strong forcing, when the dynamics is highly nonlinear with respect to our chosen reference or basic state. The nonlinearity does not seem to be an artefact of this particular choice (there is not a clear separation in timescales for waves and zonal mean flow for the current zonal mean to be a suitable basic state).

Experiments with weak forcing show that the propagation of linear waves is sensitive even to fine details of the basic state they propagate on. In particular, a narrow region where the gradient of potential vorticity, Q, is negative near a zero-wind line forms an over-reflecting barrier which confines waves in a waveguide. Consequently, the wavetrain wraps right round the hemisphere, leading locally to constructive and destructive interference. As a result of latitudinal (and also vertical) trapping, the wavetrain is not well dispersed, as it has to be for Plumb's flux to be a straightforward diagnostic of linear, stationary wave propagation. With strong forcing, the latitudinal barrier quickly disappears, so that properties of initial wave propagation are not necessarily a good predictor for the eventual nonlinear evolution - for example, whether a major warming is favoured or not.

We compared the disturbances generated with weak and strong forcing, the perturbation height for the former being scaled to obtain approximately the response in a model with no nonlinear terms. In geopotential height, nonlinearity begins to manifest itself by the weakening of cyclones and strengthening of anticyclones compared with their linear counterparts, and by the eastward advection and merging of anticyclones. These features are associated with the nonlinear advection of Q on isentropic surfaces. As nonlinearity builds, cyclonic and anticyclonic vortices advect and distort one another. There are a number of examples in our experiments of closed anticyclonic circulations developing apparently through the interaction of deep vortices. Closed anticyclonic circulations seem to burrow upwards in this way. The eventual breakdown of the stratospheric westerly vortex in the simulation we see as a prime example of the interaction of large vortices subject to steady tropospheric asymmetry. In the real atmosphere, the troposphere is not steady during major warmings, which means that the nonlinear domain may be deeper than it is in our experiments. The time taken for breakdown may seem long compared with the timescale of a week or so that might be deduced by monitoring zonal mean winds. However, we emphasized that major warmings do not develop in the real atmosphere in a week starting from an axially symmetric state. It takes much longer than this in our experiment for the "Aleutian High" to build to a size comparable to that of the cyclone, apparently a requirement for the disruption of the cyclonic vortex.

We compared the synoptic view of the flow in our experiments with the zonal mean picture. In contrast with the systematic build-up of anticyclones and the systematic weakening of the main cyclone, there are

strong vacillations in zonal mean winds and zonal harmonic amplitudes long after the forcing is steady. The oscillations in these diagnostics are strongly coupled: we argue that they develop nonlinearly through the mutual interaction of deep vortices (whose depth is limited by the prescribed lower boundary). The theory of wave, mean-flow interaction, in which propagating waves are regarded as forcing changes in the mean flow, is not a suitable framework to consider such processes. One manifestation of the nonlinearity, also observed in the real atmosphere, is the anticorrelation in time between amplitudes of harmonic waves 1 and 2. This arises from nonlinear development of well separated, localised anticyclones, a further consequence of which is the production of travelling zonal harmonics. In considering the question posed by McIntyre (1982) - "How and why do planetary wave amplitudes become anomalously large?" - we should bear in mind that harmonic amplitudes can change cyclically when the external forcing is steady.

Another question raised by McIntyre is: "... for what stratospheric conditions is a major warming likely to occur ...?" The usual way the question is answered is in terms of a so-called pre-conditioned, quasi-steady state having a simple property which promotes disruption by a wave pulse that is supposed to propagate on it (the westerly vortex is small or the zonal-mean jet is confined to high latitudes). Such a state, it is held, can be produced by an earlier minor warming.

Our experiments and independent observations suggest a contrary view; one that is not based on a causal chain of wave, mean-flow interactions. Warmings evolve from highly asymmetric states containing pre-existing

anticyclones. If the troposphere gets more disturbed (as is usual in real major warmings), there would be a complicated mixture of vortex interaction and wave propagation - if waves could be identified at all. The sequence in our experiments of minor warming followed by major warming cannot be split up into distinct events connected with new wave pulses from the troposphere. First, the forcing is steady during the sequence; secondly, anticyclones grow systematically at the expense of the cyclone; and thirdly, there is no quasi-steady state between minor and major warmings for waves to propagate on even if there were any. The lesson is that zonally averaged diagnostics on their own do not readily discriminate between simple flows for which the theory of wave, mean-flow interactions works well, and flows that are highly nonlinear in any spatial frame over a sensible period of time.

We can learn about the dynamics of the stratosphere by looking at how and why idealised theoretical models break down when they are applied to more realistic conditions. We compare the evolution of the theoretical, weakly nonlinear critical layer (studied by Stewartson, 1978; Warn and Warn, 1978; Killworth and McIntyre, 1985; Haynes, 1985) with "buckling zones" simulated by our model. One of the main findings is that it is not possible for large amplitude disturbances to define a narrow nonlinear zone where Q is advected and subsequently mixed as though it were a passive tracer. The buckling zone widens and a cut-off island of low Q is formed with anticyclonic winds blowing approximately around it, reminiscent of the formation of a blocking anticyclone in the troposphere. We show that gradients of Q in the anticyclone are weak even in the absence of strong mixing. We argue that the term "surf zone" (introduced by McIntyre and

Palmer, 1984), connoting strong mechanical mixing of air parcels which remain on an isentropic surface, is less appropriate for the buckling zones in our experiments than it is for the idealised critical layer. We also show that the evolution near a zero-wind line is only one example of irreversible buckling of Q contours; the phenomenon can occur well away from a (Doppler shifted) zero-wind line if disturbances get big enough with height as density decreases.

Another aspect of critical layer theory whose possible relevance to the stratosphere has been suggested by several authors (e.g. Killworth and McIntyre, 1985) is that critical layers can become reflecting, thereby focusing wave activity and possibly also giving resonant growth of wave amplitudes. We show that the apparent focusing of EP fluxes is a signature of a widening buckling zone and the associated nonlinear dynamics near a developing, localised jetstream. "Focusing" is a symptom of a strong warming; there is no unequivocal justification for its being regarded as a cause. Likewise, the poleward movement of the band of EP flux convergence is a manifestation of this widening. If the concept of reflection is relevant at all, the buckling zone acts only as a partial reflector, because radiative damping and widening keeps it so. In fact, the buckling zone is so wide when westerlies break down that concepts of focusing, reflection and resonance cannot be defined unambiguously as there is no linear "far field".

We do not try to explain the poleward focusing of EP fluxes, the poleward movement of the zonal-mean jet and the poleward movement of convergence in terms of a wave, mean-flow interaction. The large amplitude

of the disturbance precludes the perturbation expansion in wave amplitude that is central to the causal arguments based on wave, mean-flow thoery. In particular, there is nothing special about the current zero-wind line when the flow is highly distorted, and there is no justification for treating it as a critical line for propagating, stationary planetary waves.

The basic notion underlying much dynamical thinking about the stratosphere is that the troposphere acts as a wavemaker and disturbances propagate quasi-linearly into the stratosphere where, according to McIntyre and Palmer (1983, 1984, 1985), they 'break'. We argue that such a model is too simple when the stratosphere is as disturbed as it is often found to be in northern mid winter (that is not to say that quasi-linear theory is never of use). The nonlinear domain is wide and deep, and the pattern of Q contours that is supposedly the signature of wave breaking can result from the interaction of large, deep vortices. In these circumstances, a liberal conception of a wave would have to be allowed in order to use the terms wave propagation and wave breaking.

Our account of experiments with strong forcing emphasises local dynamical changes and is descriptive. We draw attention to the limitations of some simple analytical and conceptual models but do not offer a substitute for them as a framework on which to build causal explanations. Without the justification for causal arguments that a perturbation expansion brings, diagnostic studies based on wave, mean-flow theory are no less descriptive than our synoptic account - the language is just different and the vocabulary more limited.

ACKNOWLEDGEMENTS

We thank Drs D G Andrews, N Butchart, P H Haynes, C J Marks, M E McIntyre, T N Palmer and K Rose for carefully reading our paper and suggesting improvements. Mrs B C Kingston's diligent work preparing the figures is appreciated. The idea for this study arose in discussions with Dr N Butchart. We relied on Dr D G Andrews for sound advice as the work progressed.

APPENDIX

SYMBOLS USED IN THE TEXT

A	Eliassen-Palm wave activity
B	Perturbation amplitude
(C_{gy}, C_{gz})	Group velocity
$f(t)$	Growth function for perturbation
$\underline{F}$	Eliassen-Palm flux
D_F	The divergence of $\underline{F}$ normalized as an effective zonal force per unit mass, given by Eq. (4.3) in Dunkerton et al. (1981)
$\underline{P}$	Flux of three-dimensional wave activity (Plumb, 1985)
Q	Ertel's potential vorticity
q	Quasi-geostrophic potential vorticity
$\overline{q}_y$	Meridional isobaric gradient of the zonal mean q (proportional to isentropic gradient of Q)

q'	Difference between q and its zonal mean
$\underline{v}$	Three-dimensional velocity
t	Time
α	Half width of 300 mb forcing function (Eq. 1)
η'	Meridional particle displacement (Eq. 8)
θ	Co-latitude
ρ_o	Density in standard atmosphere
τ	e-folding time
ϕ	Geopotential height
ϕ'_B	Perturbation geopotential height at 300 mb boundary (Eq. 1)

Subscript c denotes quantities in the control experiment.

Primed quantities are differences from the control, except q'.

Overbar denotes zonal mean quantities.

REFERENCES

Andrews, D.G. 1987 On the interpretation of the Eliassen-Palm flux divergence. Quart. J. R. Met. Soc. 113, 323-338.

Andrews, D.G. and McIntyre, M.E. 1976 Planetary waves in horizontal and vertical shear: the generalised Eliassen-Palm relation and the mean zonal acceleration. J. Atmos. Sci., 33, 2031-2048.

1978 Generalised Eliassen-Palm and Charney-Drazin theorems for waves on axisymmetric flows in compressible atmospheres. J. Atmos. Sci., 35, 175-185.

Butchart, N., Clough, S.A. Palmer, T.N. and Trevelyan, P.J. 1982 Simulations of an observed stratospheric warming with quasigeostrophic refractive index as a model diagnostic. Quart. J. R. Met. Soc., 108, 475-502.

Butchart, N. and Remsberg, E.E. 1986 The area of the stratospheric polar vortex as a diagnostic for tracer transport on an isentropic surface. J. Atmos. Sci., 43, 1319-1339.

Charney, J.G. and Drazin, P.G. 1961 Propagation of planetary-scale disturbances from the lower into the upper atmosphere. J. Geophys. Res., 66, 83-109.

Charney, J. and Stern, M. 1962 On the stability of internal baroclinic jets in a rotating atmosphere. J. Atmos. Sci., 19, 159-172.

Clough, S.A., Grahame, N.S. and O'Neill, A. 1985 Potential vorticity in the stratosphere derived using data from satellites. Quart. J. R. Met. Soc., 111, 335-358.

Dritschel, D.G. 1986 The nonlinear evolution of rotating configurations of uniform vorticity. J. Fluid Mech., 172, 157-182.

Dunkerton, T., Hsu, C.P. and McIntyre, M.E. 1981 Some Eulerian and Lagrangian diagnostics for a model stratospheric warming. J. Atmos. Sci., 38, 819-843.

Edmon, H.J., Hoskins, B.J. and McIntyre, M.E. 1980 Eliassen-Palm cross sections for the troposphere. J. Atmos. Sci., 37, 2600-2616. (Corrigendum 38, 1115).

Fairlie, T.D.A. and O'Neill, A. 1987 Aspects of dynamics of the middle atmosphere inferred using data from a satellite and from a numerical model. Submitted to Phil. Trans. Roy. Soc.

Geller, M.A., Wu, M.-F. and Gelman, M.E. 1983 Troposphere-stratosphere (surface - 55 km) monthly winter general circulation statistics for the Northern Hemisphere - four year averages. J. Atmos. Sci., 40, 1334-1352.

Hartmann, D.L. 1983 Barotropic instability of the polar night jet stream. J. Atmos. Sci., 40, 817-835.

Hartmann, D.L., Mechoso, C.R. and Yamazaki, K. 1984 Observations of wave-mean flow interaction in the southern hemisphere. J. Atmos. Sci., 41, 351-362.

Haynes, P.H. 1985 Nonlinear instability of a Rossby-wave critical layer. J. Fluid Mech., 161, 493-511.

Holton, J. 1976 A semi-spectral numerical model for wave, mean-flow interactions in the stratosphere: application to sudden stratospheric warmings. J. Atmos. Sci., 33, 1639-1649.

Holton, J.R. and Mass, C. 1976 Stratospheric vacillation cycles. J. Atmos. Sci., 33, 2218-2225.

Hoskins, B.J., McIntyre, M.E. and Robertson, A.W. 1985 On the use and significance of isentropic potential vorticity maps. Quart. J. R. Met. Soc., 111, 877-946.

Kanzawa, H. 1980 The behaviour of mean zonal wind and planetary-scale disturbances in the troposphere and strtosphere during the 1973 sudden warming. J. Meteor. Soc. Japan, 58, 329-356.

Killworth, P.D. and McIntyre, M.E. 1985 Do Rossby-wave critical layers absorb, reflect or over-reflect? J. Fluid. Mech., 161, 449-492.

Labitzke, K. 1977 Interannual variability of the winter stratosphere in the northern hemisphere. Mon. Wea. Rev., 105, 762-770.

1982 On the interannual variability of the middle stratosphere during the northern winters. J. Met. Soc. Japan, 60, 124-139.

Lindzen, R.S. and Tung, K.K. 1978 Wave overreflection and shear instability. J. Atmos. Sci., 35, 1626-1632.

Madden, R.A. and Labitzke, K. 1981 A free Rossby wave in the troposphere and stratosphere during January 1979. J. Geophys. Res., 86, 1247-1254.

Marks, C.J. 1986 Models of planetary waves in the winter stratosphere. D. Phil. thesis, University of Oxford, pp. 236.

Matsuno, T. 1970 Vertical propagation of stationary planetary waves in the winter northern hemisphere. J. Atmos. Sci., 27, 871-883.

1971 A dynamical model of the stratospheric sudden warming. J. Atmos. Sci., 28, 1479-1494.

McIntyre, M.E. 1982 How well do we understand the dynamics of stratospheric warmings? J. Met. Soc. Japan, 60, 37-65.

McIntyre, M.E. and Palmer, T.N. 1983 Breaking planetary waves in the stratosphere. Nature, 305, 593-600.

1984 The 'surf zone' in the stratosphere. J. Atmos. Terr. Phys., 46, 825-849.

1985 A note on the general concept of wave breaking for Rossby and gravity waves. PAGEOPH, 123, 964-975.

Mechoso, C.R., Hartmann, D.L. and Farrara, J. 1985 Climatology and interannual variability of wave, mean-flow interaction in the southern hemisphere. J. Atmos. Sci., 42, 2189-2206.

Naujokat, B., Petzoldt, K., Labitzke, K. and Lenschow, R. 1982 The fourth winter of PMP-1, 1981/82: A winter with several interesting features. Beilage zur Berliner Wetterkarte, 35, pp. 12.

O'Neill, A. and Taylor, B.F. 1979 A study of the major stratospheric warming of 1976-77. Quart. J. Roy. Met. Soc., 105, 71-92.

O'Neill, A. and Youngblut, C.E. 1982 Stratopsheric warmings diagnosed using the transformed Eulerian-mean equations and the effect of the mean state on wave propagation. J. Atmos. Sci., 39, 1370-1386.

Palmer, T.N. 1981a Diagnostic study of a wavenumber-2 stratospheric sudden warming in a transformed Eulerian-mean formalism. J. Atmos. Sci., 38, 844-855.

1981b Aspects of stratospheric sudden warmings studied from a transformed Eulerian-mean viewpoint. J.Geoph. Res., 86, 9679-9687.

Palmer, T.N. and Hsu, C.-P.F. 1983 Stratospheric sudden coolings and the role of nonlinear wave interactions in preconditioning the circumpolar flow. J. Atmos. Sci., 40, 907-928.

Plumb, R.A. 1981a Forced waves in a baroclynic shear flow, Part 2: Damped and undamped response to weak near-resonant forcing. J. Atmos. Sci., 38, 1856-1869.

1981b Instability of the distorted polar night vortex: a theory of stratospheric warmings. J. Atmos. Sci., 38, 2514-2531.

1985 On the three-dimensional propagation of stationary waves. J. Atmos. Sci., 42, 217-229.

Quiroz, R.S., Miller, A.J. and Nagatani, R.M. 1975 A comparison of observed and simulated properties of sudden stratopsheric warmings. J. Atmos. Sci., 32, 1723-1736.

Robinson, W.A. 1986 The application of the quasi-geostrophic Eliassen-Palm flux to the analysis of stratospheric data. J. Atmos. Sci., 43, 1017-1023.

1987 The behaviour of planetary wave 2 in preconditioned zonal flows. Submitted to J. Atmos. Sci.

Saffman, P.G., and Baker, G.R. 1979 Vortex interactions. Ann. Rev. Fluid Mech., 11, 95-122.

Shiotani, M. and Hirota, I. 1985 Planetary wave, mean-flow interaction in the stratosphere: a comparison between northern and southern hemispheres. Quart. J. R. Met. Soc., 111, 309-334.

Simmons, A.J. 1974 Planetary-scale disturbances in the polar winter stratosphere. Quart. J. R. Met. Soc., 100, 76-108.

Stewartson, K. 1978 The evolution of the critical layer of a Rossby wave. Geoph. Astrophys. Fluid Dyn., 9, 185-200.

Warn, T. and Warn, H. 1978 The evolution of a nonlinear critical level. Studies in Appl. Math., 59, 37-71.

FIGURES

Fig. 1. The initial field. (a) Cross-section of zonal mean wind (ms^{-1}, with easterlies shaded) for the northern hemisphere on 19 January 1982. On this and other vertical sections, the height co-ordinate, z, is given by z = H ln (1000/p) where p is the pressure in mb and H = 6.95 km. (b) Polar-stereographic map of Ertel's potential vorticity, Q, and winds on the 850 K isentropic surface. The units are 10^{-4} K m^2 kg^{-1} s^{-1}. The heavy dashed curve gives the location of the zero-wind line. In the above units the contour interval is 0.2 between values 1 and 3, while the interval is 2 for values of 4 and above. Values less than 2 are shaded and the region where the poleward gradient of Q is negative is stippled. The frame surrounding the figure is tangential to latitude 20°N.

Fig. 2. Longitude-height section at 62.5°N of the perturbation field in geopotential height for day 11 of the experiment with a 'low' of amplitude 100 gpm at the lower boundary. The perturbation field is scaled by a factor of 6 for comparison with the experiment where the forcing has amplitude 600 gpm (see section 2(b) for discussion). The units are in geopotential decametres and negative values are shaded. The contour interval is 20 in the above units. The dashed line is the 10 contour.

Fig. 3. Polar-stereographic maps at 8 mb of the perturbation field in geopotential height for day 16 of the experiments with local forcing of amplitude 100 gpm at the lower boundary. The units, scaling and shading are as in Fig. 2. (a) The experiment with a 'low' at the lower boundary. (b) The experiment with a 'high' at the lower boundary.

Fig. 4. As Fig. 2 but on day 29.

Fig. 5. The direction of the Eliassen-Palm flux and its 'divergence' on day 11 for the experiment with a 'low' of amplitude 100 gpm at the lower boundary. Note that the divergence has not been scaled. Contours are drawn at intervals of $.4 \times 10^{-6}$ ms^{-2} with regions of positive values shaded.

Fig. 6. Polar-stereographic map at 8 mb of the Plumb's flux, $\underline{P}$, on day 16. The arrows represent the horizontal projection of $\underline{P}$ and contours give the vertical component. Regions where the flux is downward are shaded. The units are 10^{-4} m^2 s^{-2}.

Fig. 7. Polar-stereographic map at 8 mb of the perturbation in geopotential height on day 16 for the experiment with a 'low' of 600 gpm at the lower boundary. The units are geopotential decametres and negative values are shaded. The contour interval is 20 in the above units. Compare Fig. 3.

Fig. 8. As Fig. 7, but longitude height section at 62.5°N on day 29.

Fig. 9. Polar-stereographic maps of Ertel's potential vorticity, Q, and winds on the 850 K isentropic surface. Units and contour interval are as in Fig. 1(b). Values less than 2 are shaded. (a) For day 16. The arrow marks the developing anticyclone discussed in the text. (b) For day 29.

Fig. 10. Evolution with time of the maximum geopotential height of anticyclones. The units are geopotential kilometres. (a) For the two anticyclones at 8 mb. The contour labelled A is for the anticyclone at 50°N, 135°W and the contour labelled B is for the anticyclone at 40°N, 30°W. (b) For the anticyclone at 50 mb (which corresponds to A at 8 mb).

Fig. 11. Polar-stereographic map of Q on the 2000 K isentropic surface (near 1 mb) on day 32. The units are 10^{-4} K m^2 kg^{-1} s^{-1}. Shading is between 40 and 70 in these units. The arrow marks the tongue of high Q discussed in the text.

Fig. 12. As Fig. 9 but on day 47.

Fig. 13. Longitude-height cross sections of the difference of the geopotential height from its zonal mean. The units are in geopotential decametres and negative values are shaded. The contour interval is 20 in the above units. (a) For day 21 at 62.5°N for the experiment with a 'high' of 600 gpm at 45°N, 0°E at the lower boundary. (b) As (a) but for day 29. (c) For 16 February 1979 at 60°N using data from stratospheric sounding units on board the Tiros-N satellite. (d) As (c) but for 20 February 1979.

Fig. 14. (a) Theoretical nonlinear critical layer solution of Stewartson (1978) and Warn and Warn (1978). Picture taken from McIntyre and Palmer (1983) with wind arrows marked on by hand from the streamlines given by

Warn and Warn (1978). Note that the ordinate's scale is exaggerated. (b) Portion of Fig. 9(a) using a Mercator projection. The asterisk marks the point where Q contours are about to meet, as discussed in the text.

Fig. 15. Portion of a map of Q on the 2000 K isentropic surface for the experiment described in section 8. The units are -10^{-4} K m^2 kg^{-1} s^{-1}. The contour interval is 10 and shading is between 40 and 60. (a) For day 0. (b) For day 29. The cross marks the centre of the anticyclone. The contours labelled A and B are those referred to in the text.

Fig. 16. Latitude-time series at 10 mb of D_F for the experiment with a 'low' of 600 gpm at the lower boundary. Contours are drawn at intervals of 20×10^{-6} ms^{-2}. The pecked line is the contour 10×10^{-6} ms^{-2} and regions of positive values are shaded.

Fig. 17. (a) Map of Q and winds on the 2000 K isentropic surface on day 21. The units are 10^{-4} K m^2 kg^{-1} s^{-1} and shading is between 40 and 70 in these units. (b) Map of the horizontal projection of $\underline{P}$ at 1 mb on day 21. The units are 10^{-4} m^2 s^{-2}. (c) As (a) but for day 29. (d) As (b) but for day 29.

Fig. 18. Height-time series at 62.5°N of wave amplitudes. The units are geopotential decametres and values larger than 35 are shaded. (a) For wave 1. (b) For wave 2.

Fig. 19. Latitude-time series at 1 mb of the zonal mean wind. The units are ms^{-1} and negative values are shaded.

Fig. 20. Longitude-time series at 1 mb of the amplitude of wave 1 at 62.5°N. The units are geopotential decametres and negative values are shaded.

Fig. 21. Argand diagram representing the addition of the wave 1 components of two anticyclones positioned 140° apart. The notation is described in the text.

Fig. 22. Cross-section of zonal mean wind (ms^{-1}, with easterlies shaded) for the southern hemisphere on 12 September 1981.

Fig. 23. Displacement field on the 2000 K isentropic surface for the southern hemisphere on day 11 for the experiment with a 'low' of amplitude 600 gpm at 45°S, 180°E at the lower boundary and the initial field shown in Fig. 22. The contour interval represents a displacement of 4 degrees of latitude and regions of movement away from the pole are shaded. The displacement field cannot be calculated with our algorithm in the rectangle that is blanked out. The letters A and B mark developing anticyclones.

Fig. 24. Polar-stereographic map of Q and winds on the 2000 K isentropic surface. The units are -10^{-4} K m^2 kg^{-1} s^{-1} and shading is between 40 and 70 in these units. The letters A and B mark developing anticyclones.

(a)

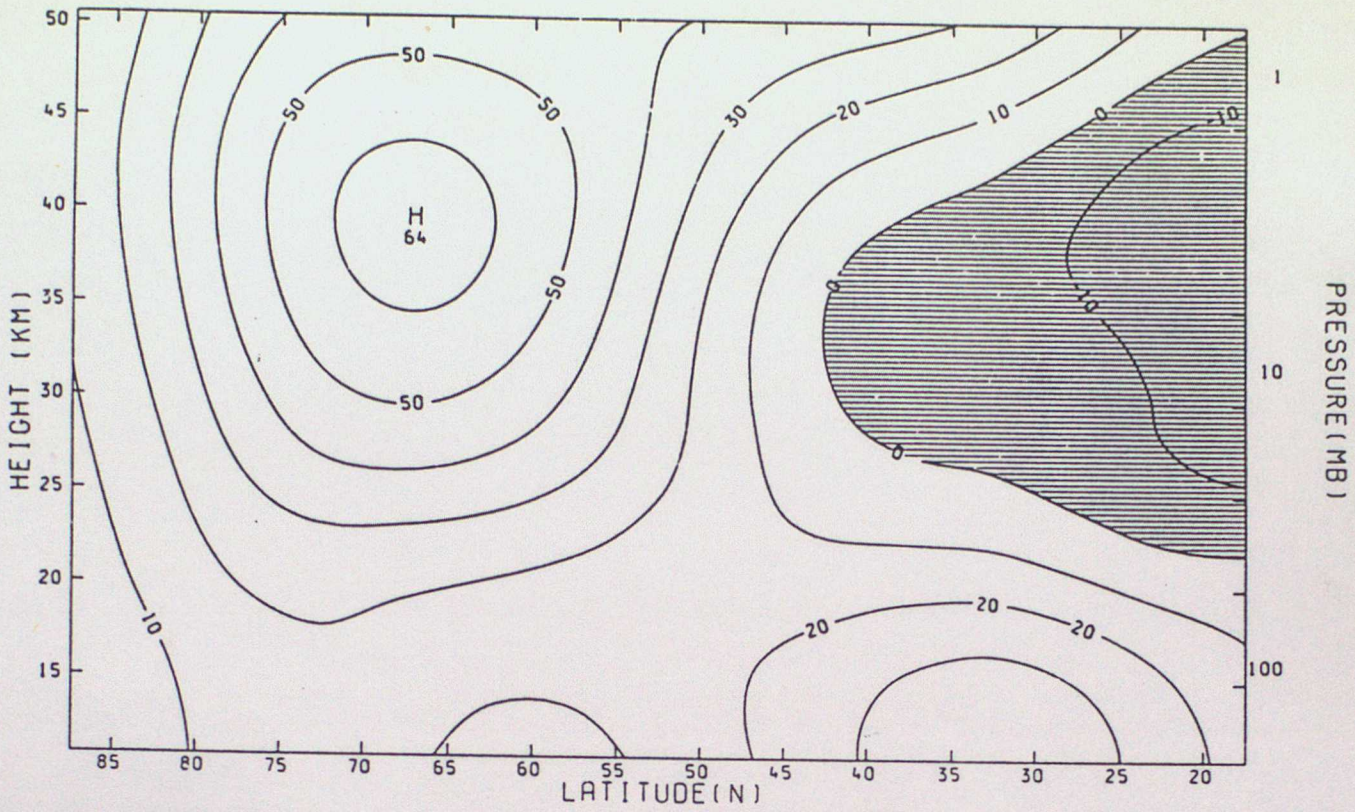
HEIGHT (KM)
PRESSURE (MB)
LATITUDE (N)
H
64
50
45
40
35
30
25
20
15
1
10
100
85
80
75
70
65
60
55
50
45
40
35
30
25
20
50
30
20
10
0
-10
-20

(b)

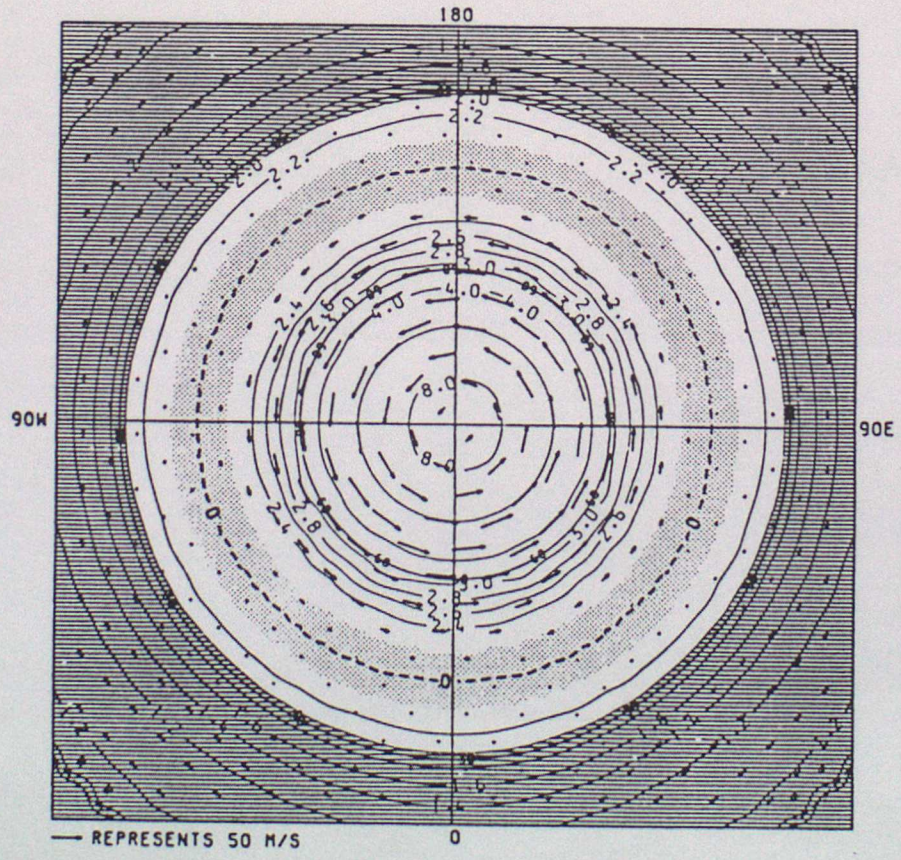
180
90W
90E
0
REPRESENTS 50 M/S

Fig. 1

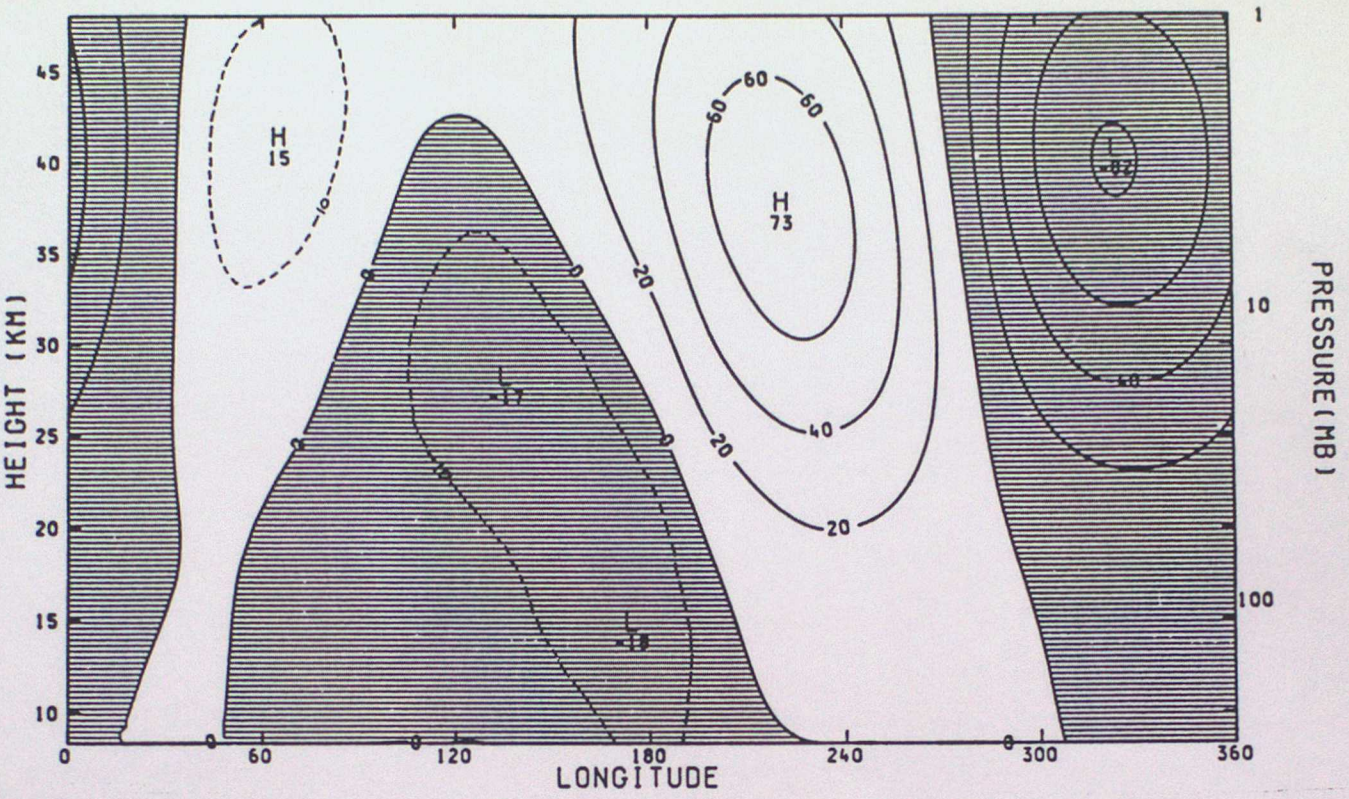
HEIGHT (KM)
PRESSURE(MB)
LONGITUDE
H
15
H
73
L
-17
L
-18
L
-82
0
60
120
180
240
300
360
10
15
20
25
30
35
40
45
1
10
100

Fig. 2

(a)

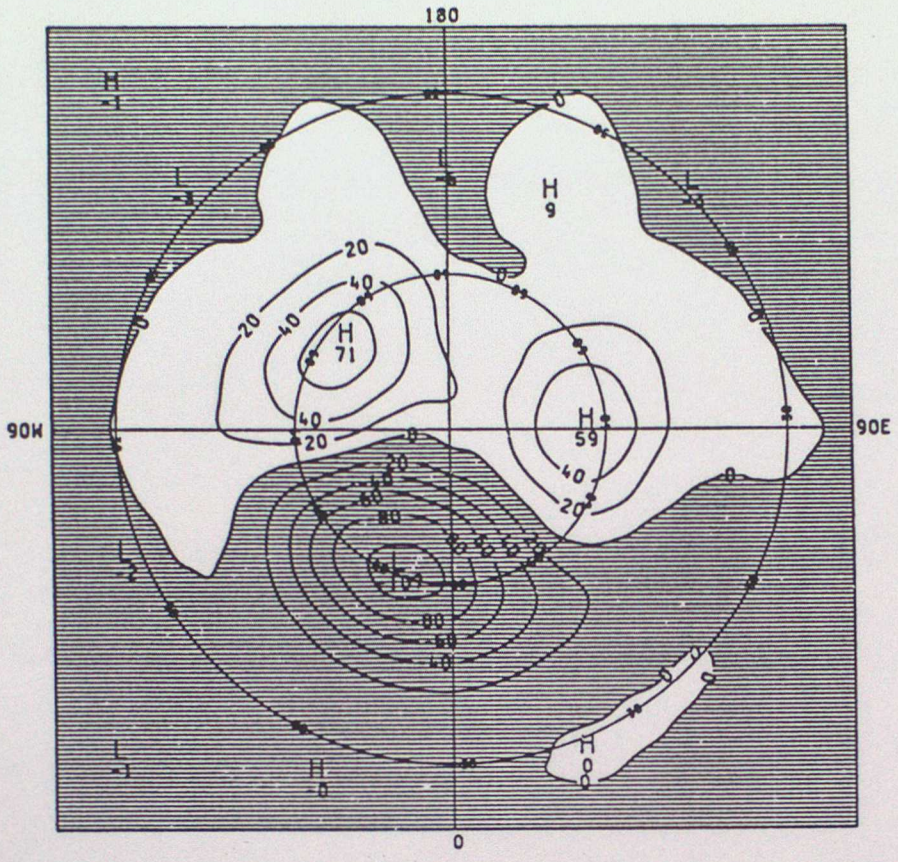
180
90W
90E
0
H
9
H
71
H
59
H
0
L
-1
L
-2
L
-3
L
-4
L
-5
L
-6
H
-1
H
-0
20
40
60
80
-20
-40
-60
-80
0

(b)

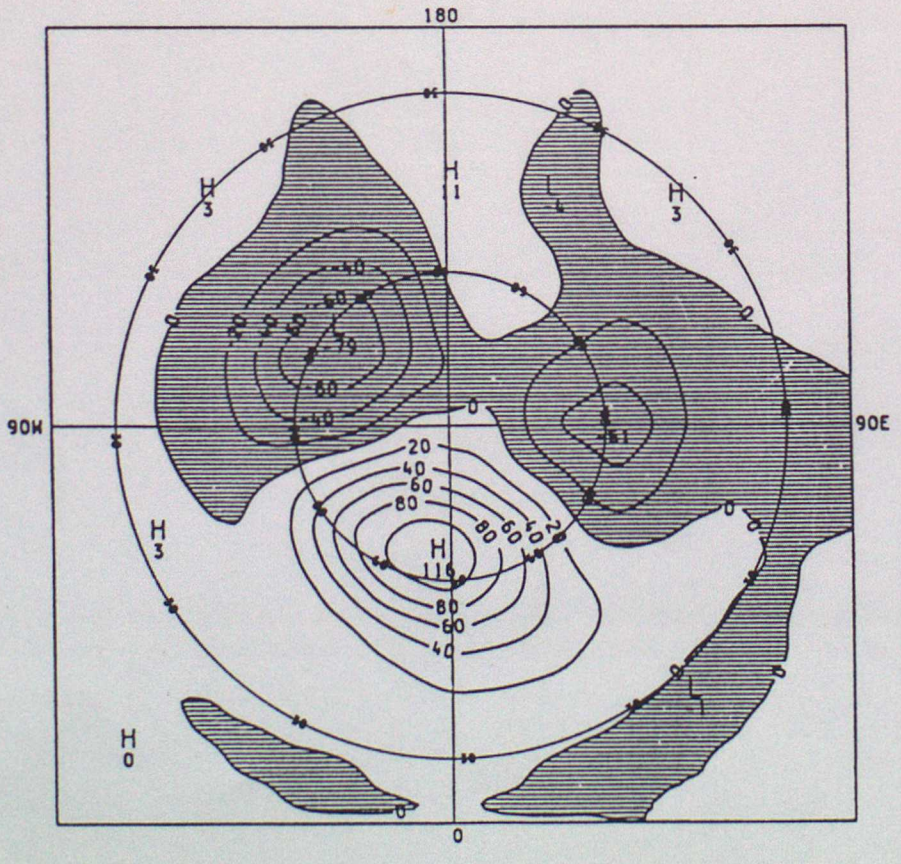
180
90W
90E
0
H
11
H
3
H
3
H
3
H
116
H
0
L
-4
L
-79
L
-61
L
-1
20
40
60
80
-20
-40
-60
-80
0

Fig. 3

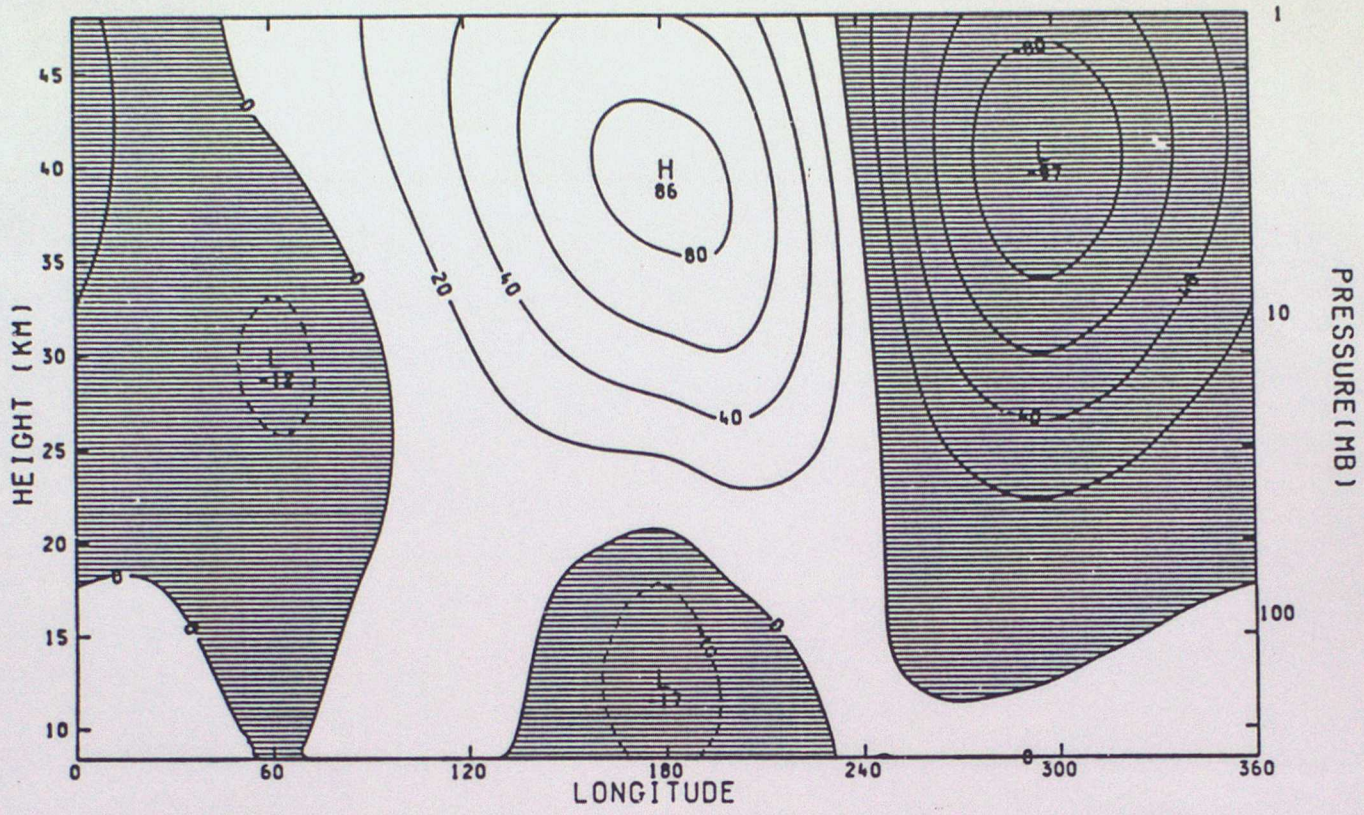
HEIGHT (KM)
45
40
35
30
25
20
15
10
0
60
120
180
240
300
360
LONGITUDE
1
10
100
PRESSURE(MB)
H
86
80
40
20
0
-40
-80

Fig. 4

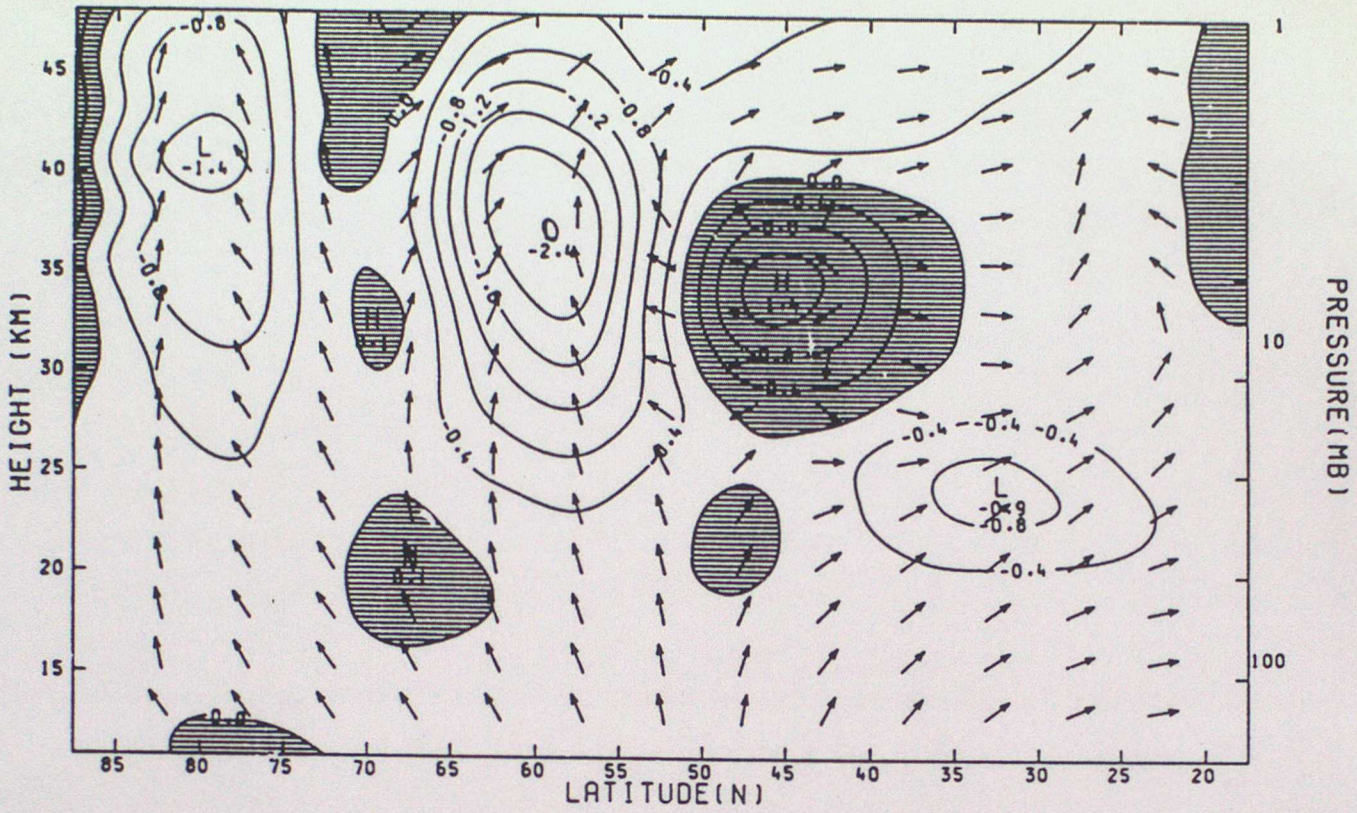
HEIGHT (KM)
PRESSURE (MB)
LATITUDE (N)
45
40
35
30
25
20
15
1
10
100
85
80
75
70
65
60
55
50
45
40
35
30
25
20

Fig. 5

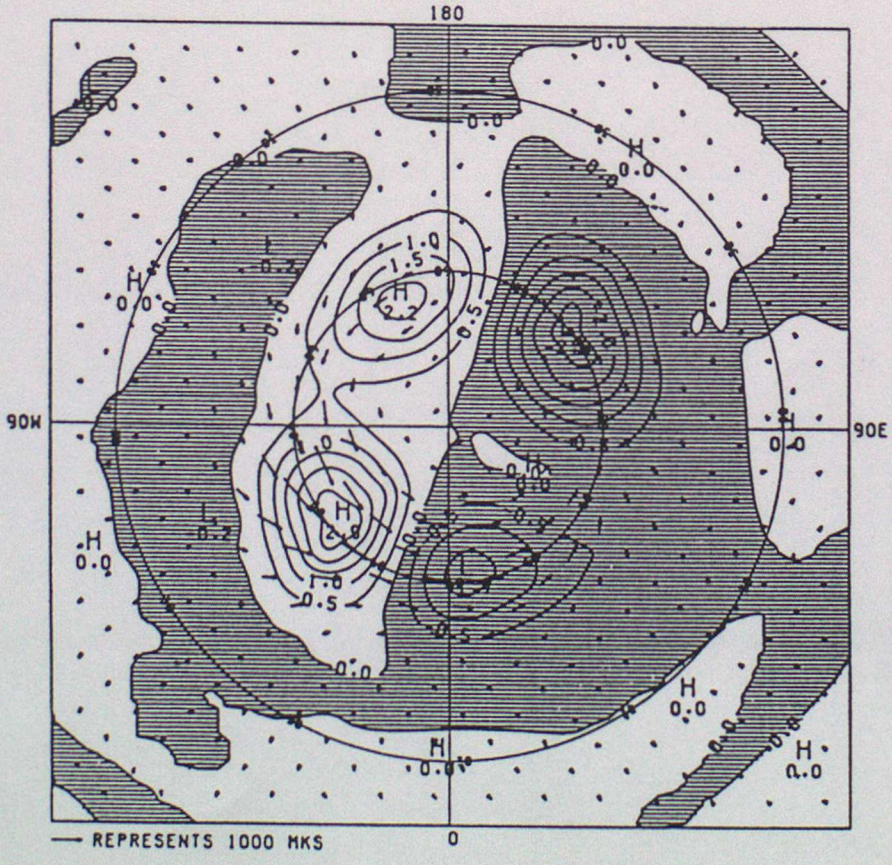
180
90W
90E
0
REPRESENTS 1000 MKS

Fig. 6

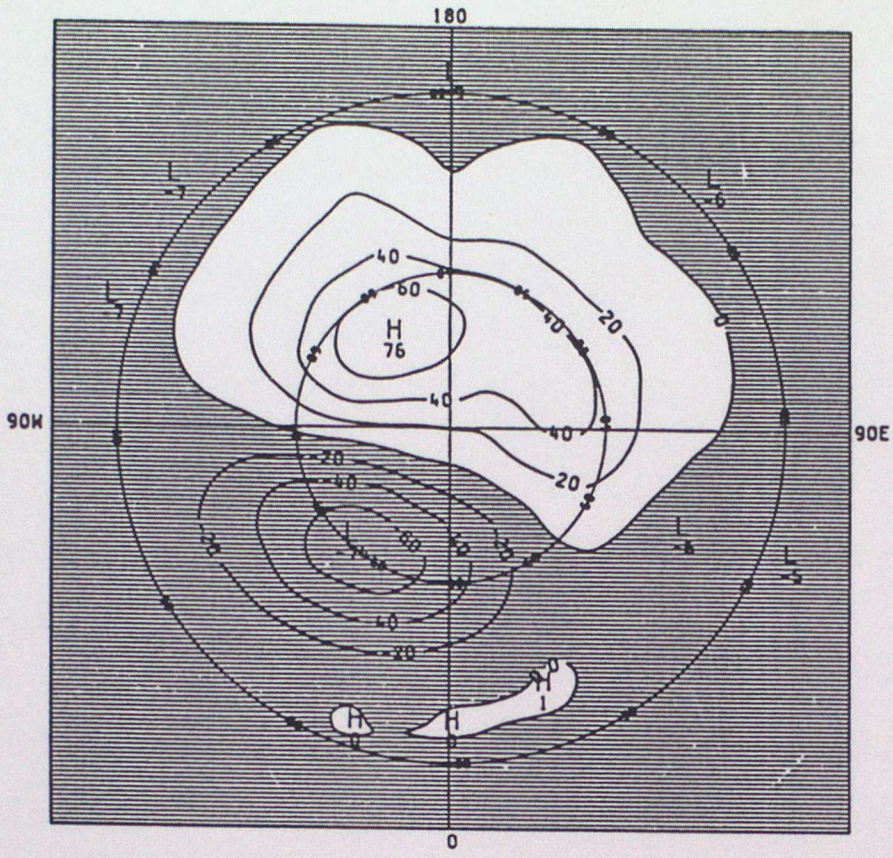

Fig. 7

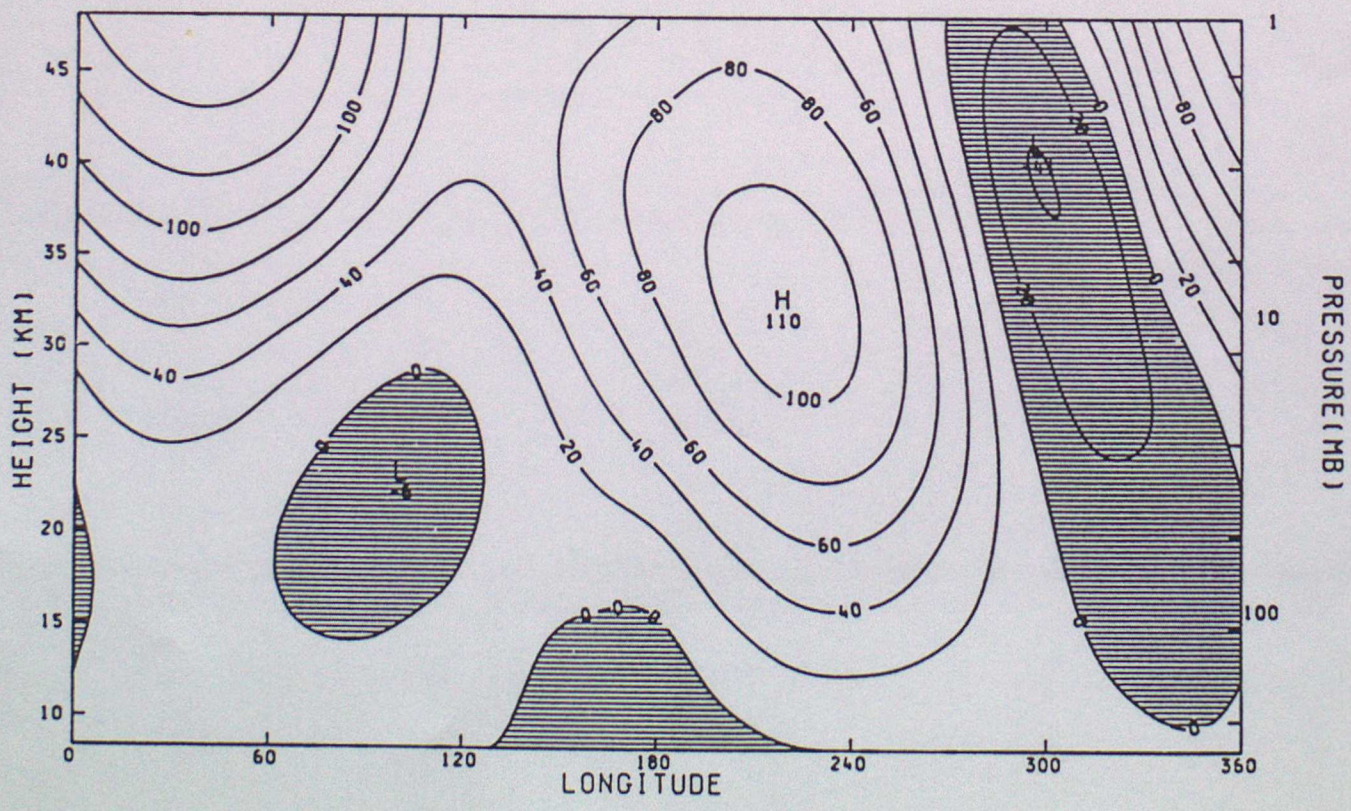
HEIGHT (KM)
PRESSURE(MB)
LONGITUDE
0
60
120
180
240
300
360
45
40
35
30
25
20
15
10
1
10
100
H
110
80
80
80
60
100
100
40
40
40
60
80
60
40
20
40
60
60
40
0
0
0

(a)

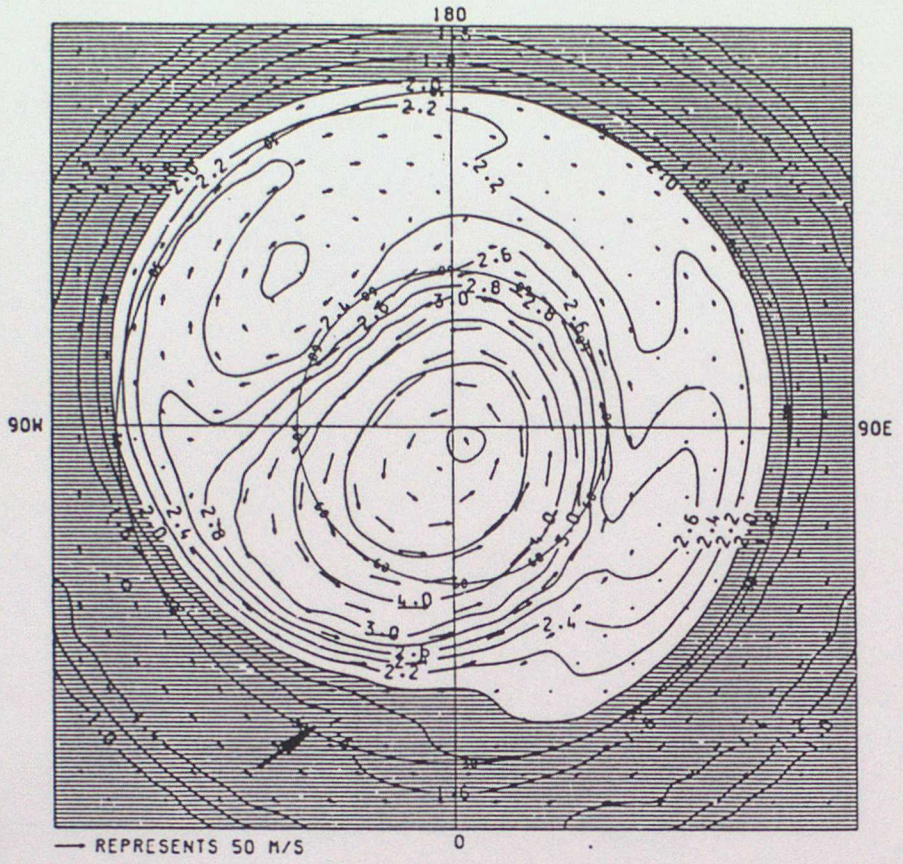

(b)

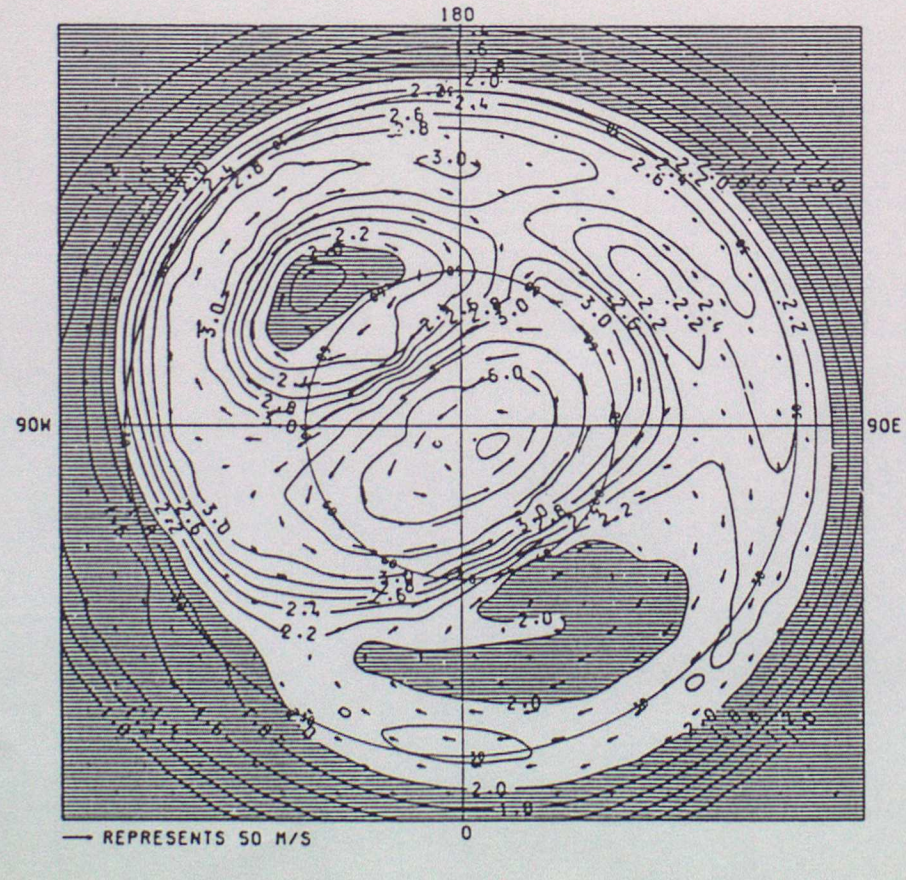

Fig. 9

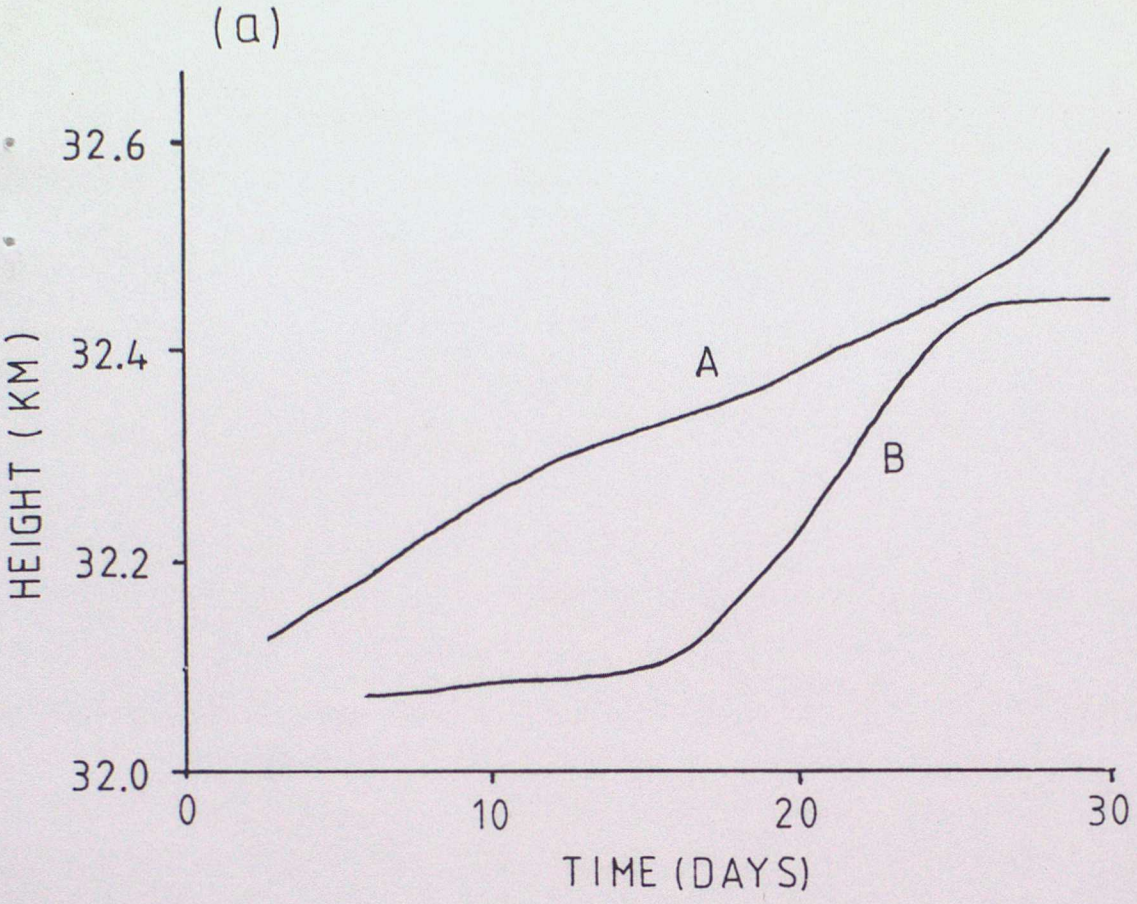
(a)
32.6
32.4
32.2
32.0
HEIGHT (KM)
A
B
0
10
20
30
TIME (DAYS)

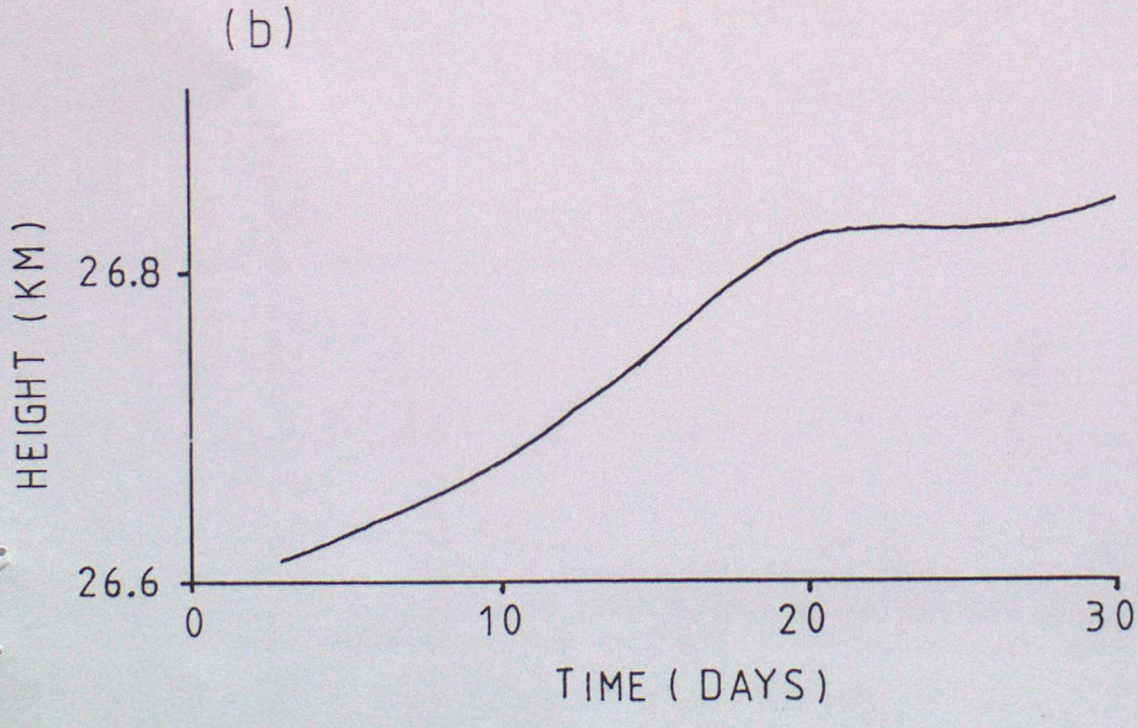
(b)
26.8
26.6
HEIGHT (KM)
0
10
20
30
TIME (DAYS)

Fig. 10

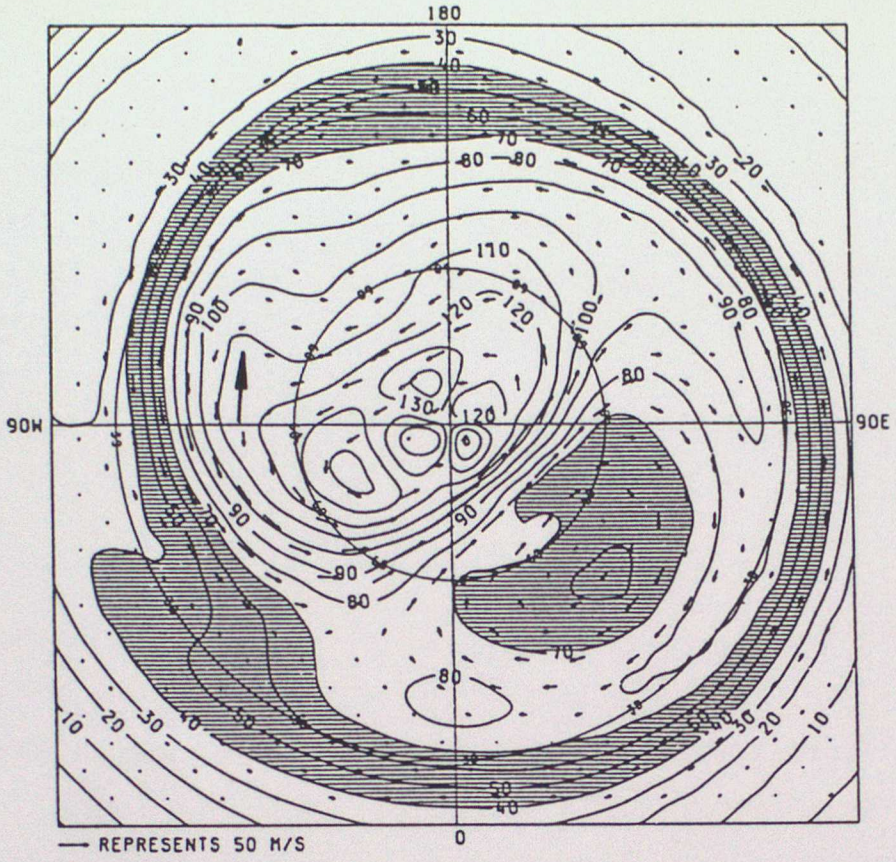

Fig. 11

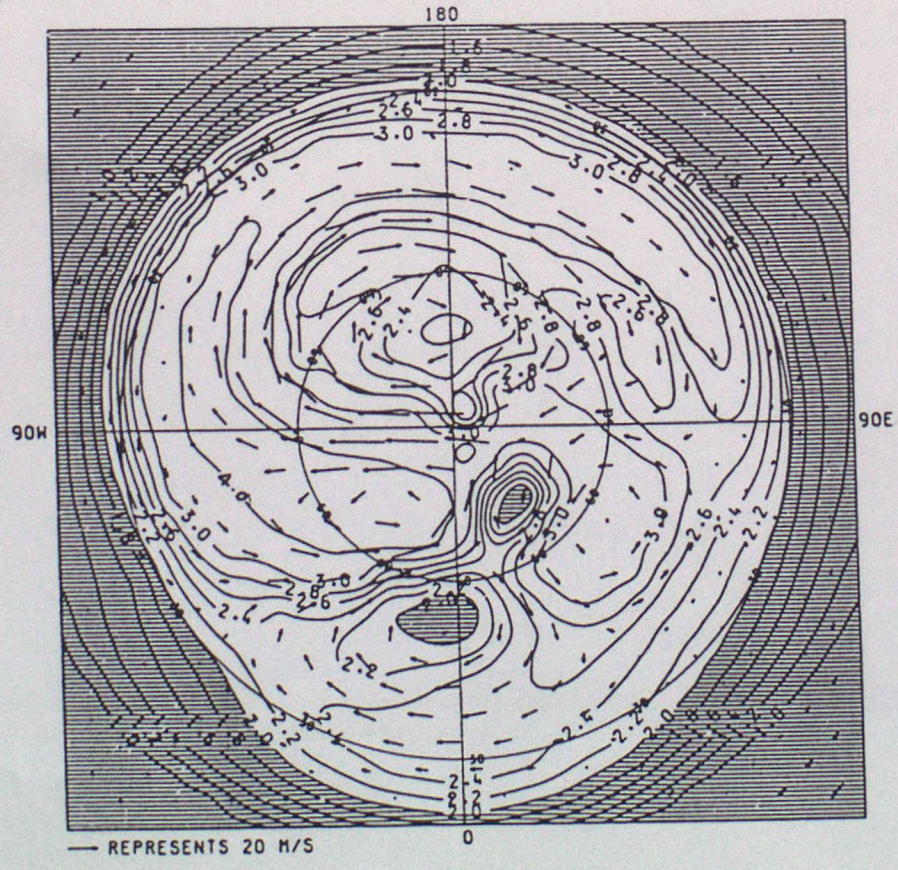

Fig. 12

(a)

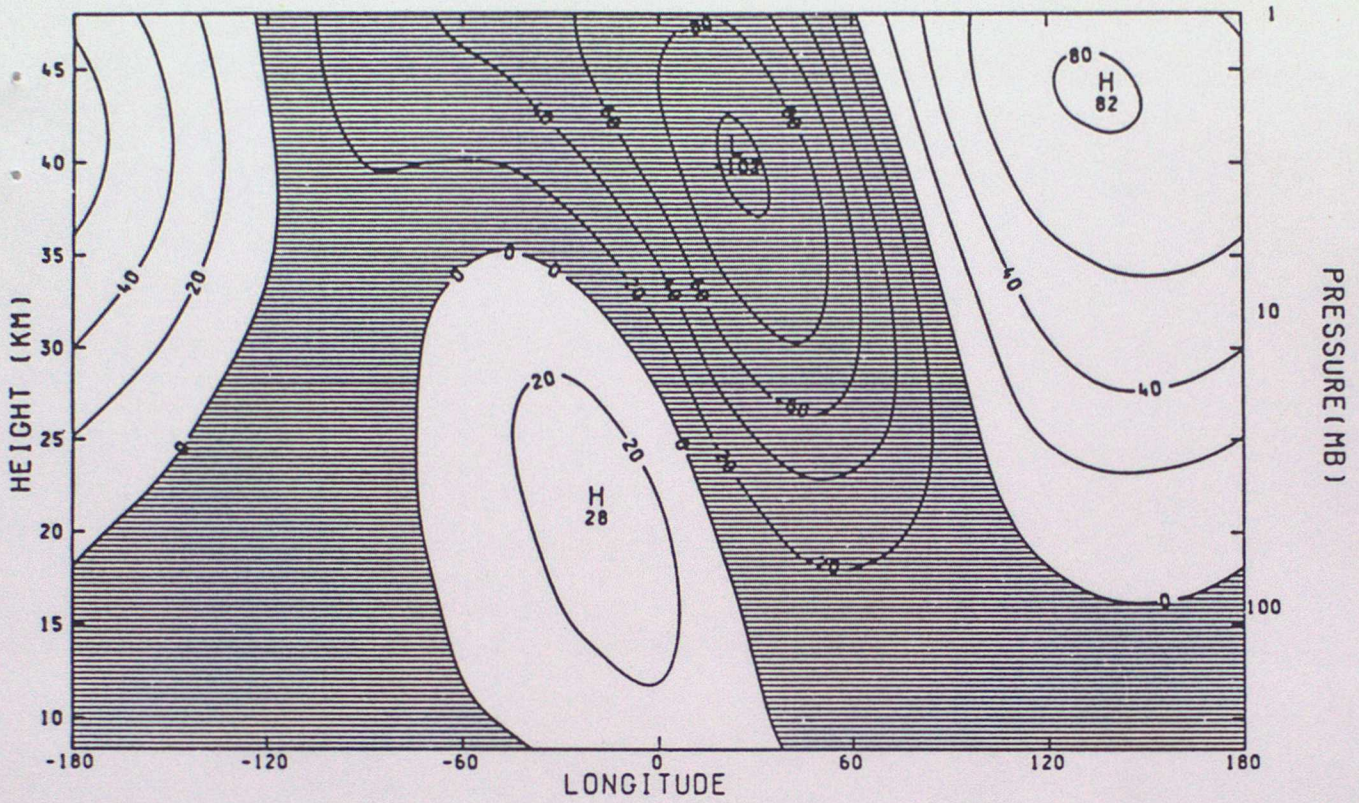
HEIGHT (KM)
PRESSURE (MB)
LONGITUDE
H
82
H
28
-180
-120
-60
0
60
120
180
1
10
100

(b)

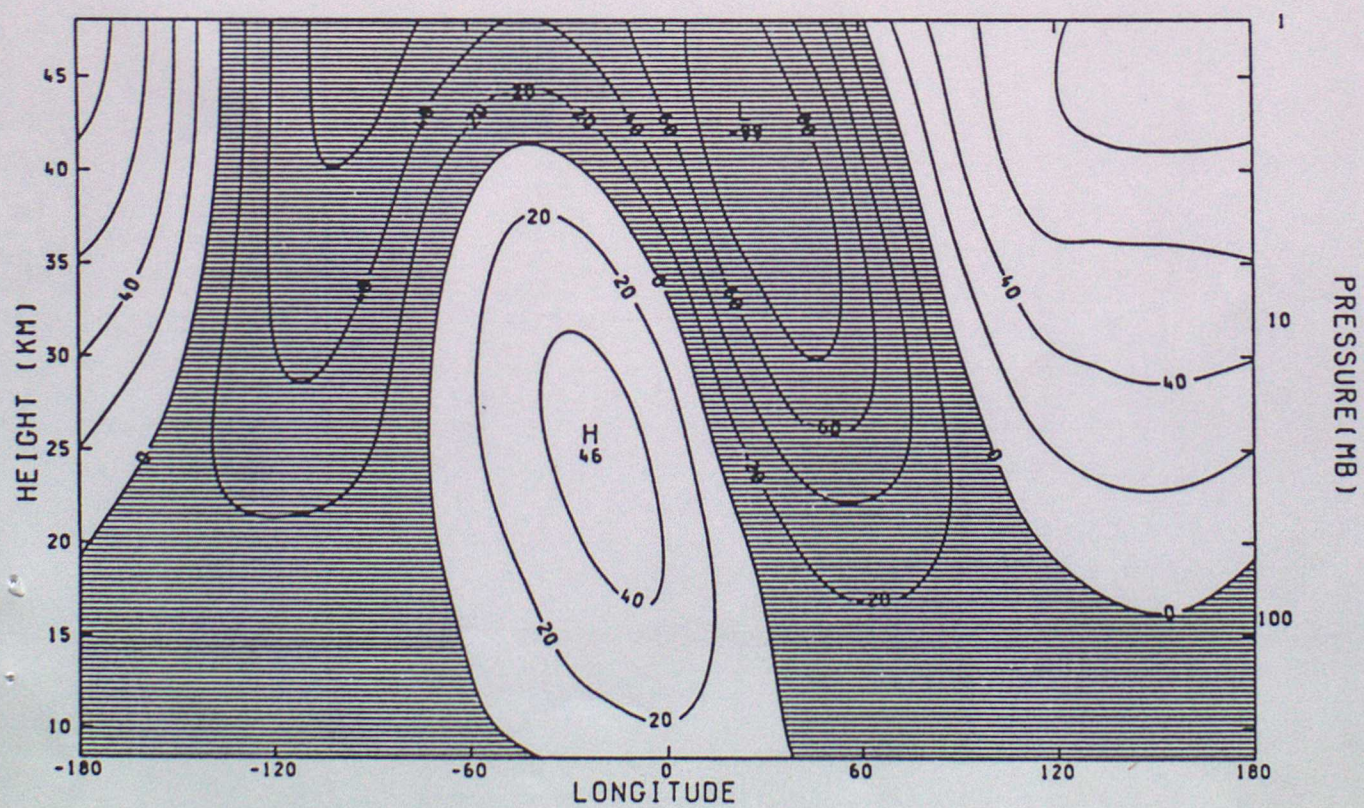
HEIGHT (KM)
PRESSURE (MB)
LONGITUDE
H
46
-180
-120
-60
0
60
120
180
1
10
100

Fig. 13

(c)

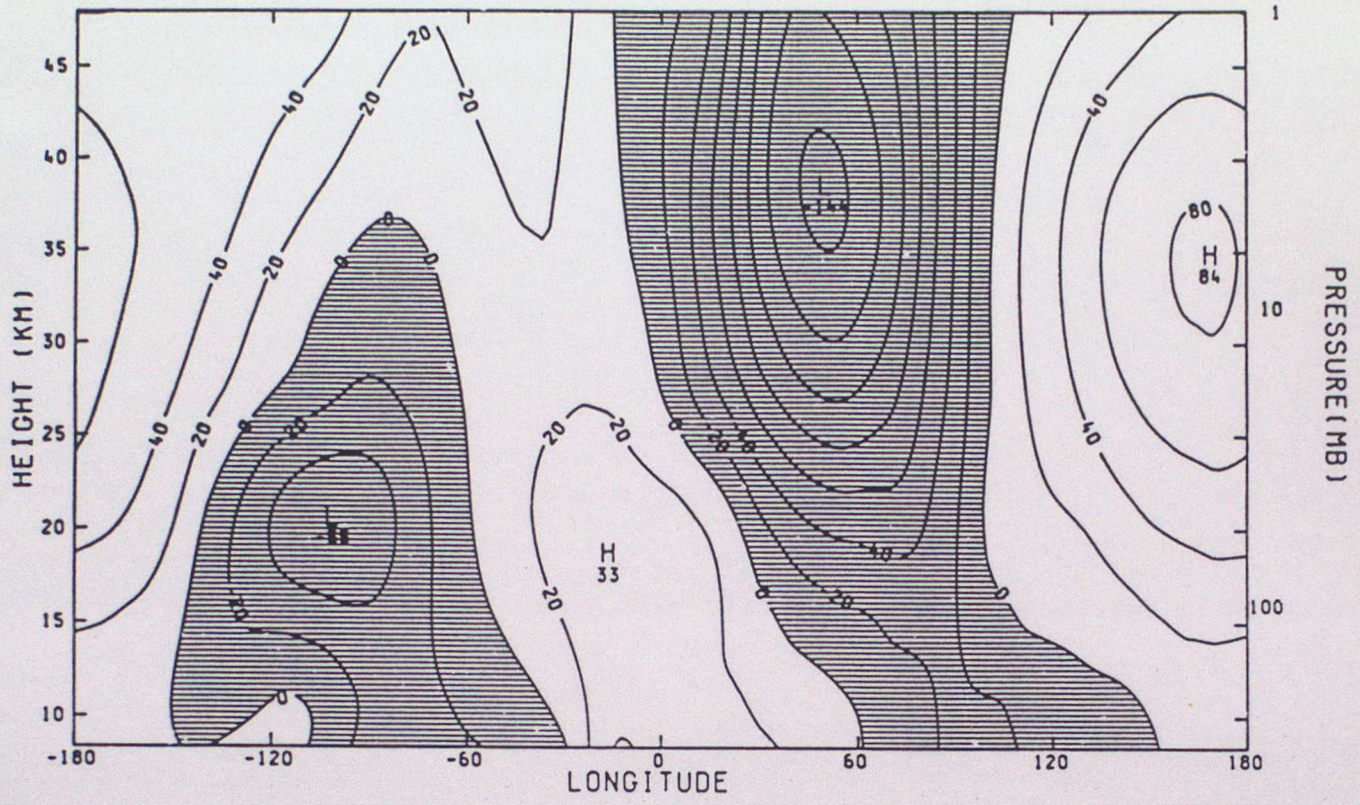
HEIGHT (KM)
PRESSURE(MB)
LONGITUDE
H
33
H
84
-180
-120
-60
0
60
120
180

(d)

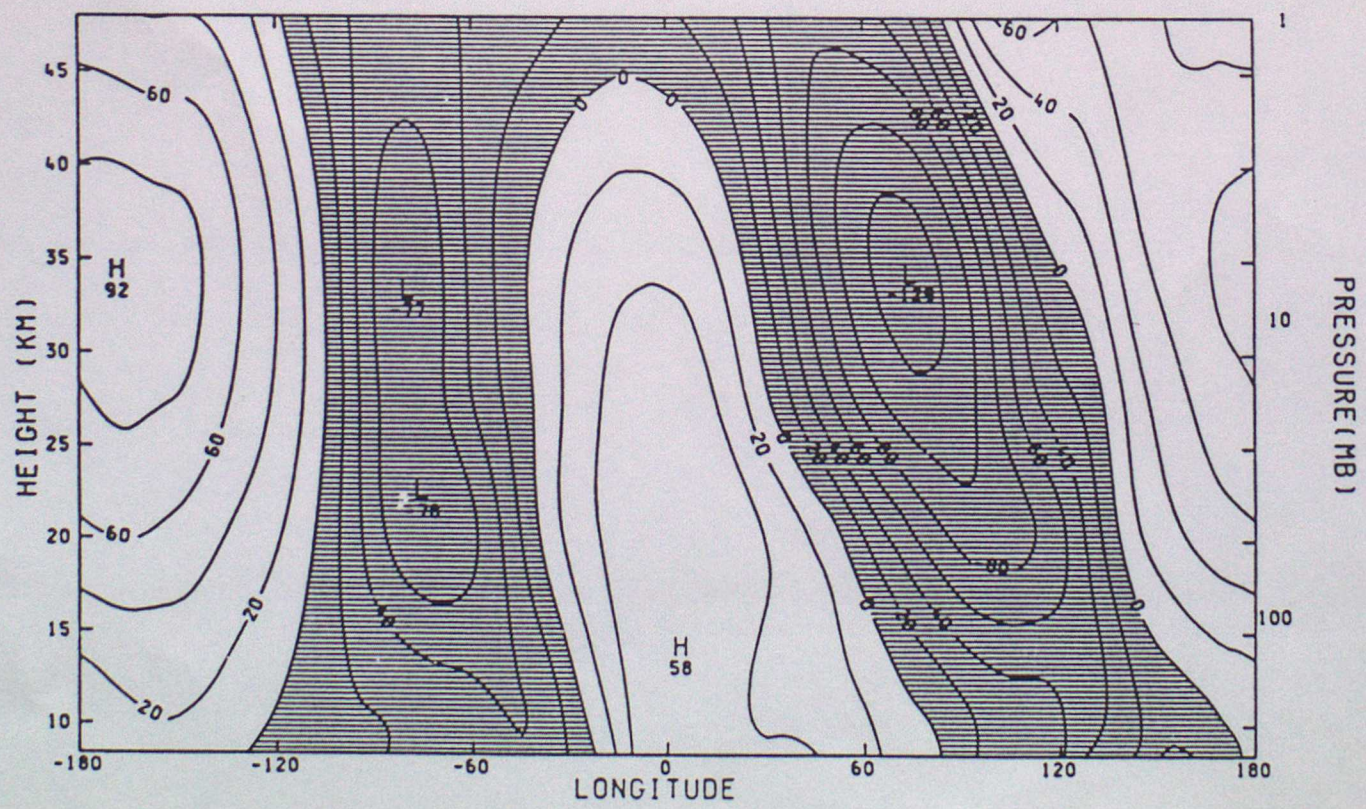
HEIGHT (KM)
PRESSURE(MB)
LONGITUDE
H
92
H
58
-180
-120
-60
0
60
120
180

Fig.13

(a)

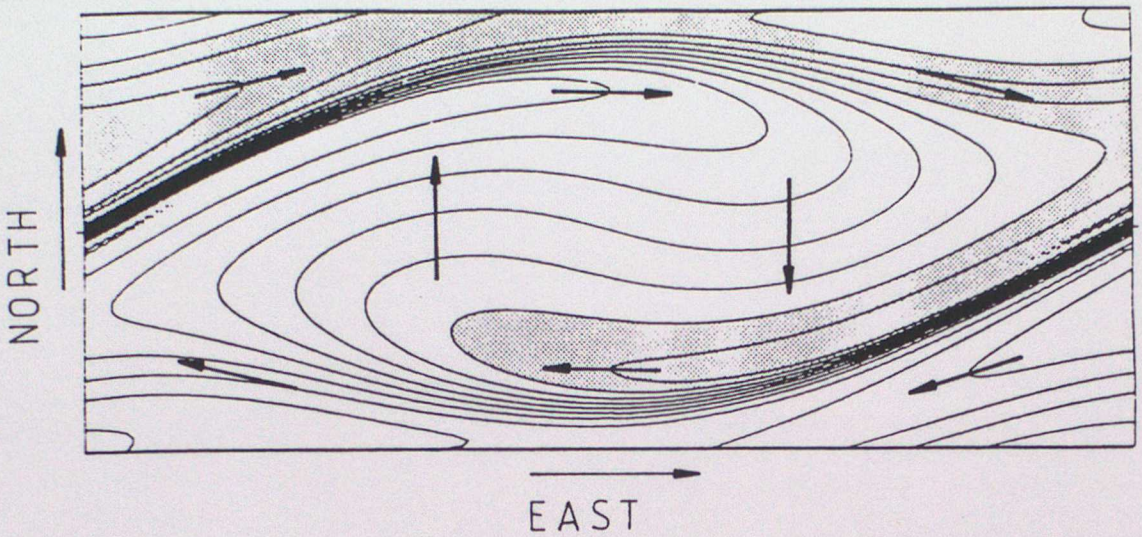

(b)

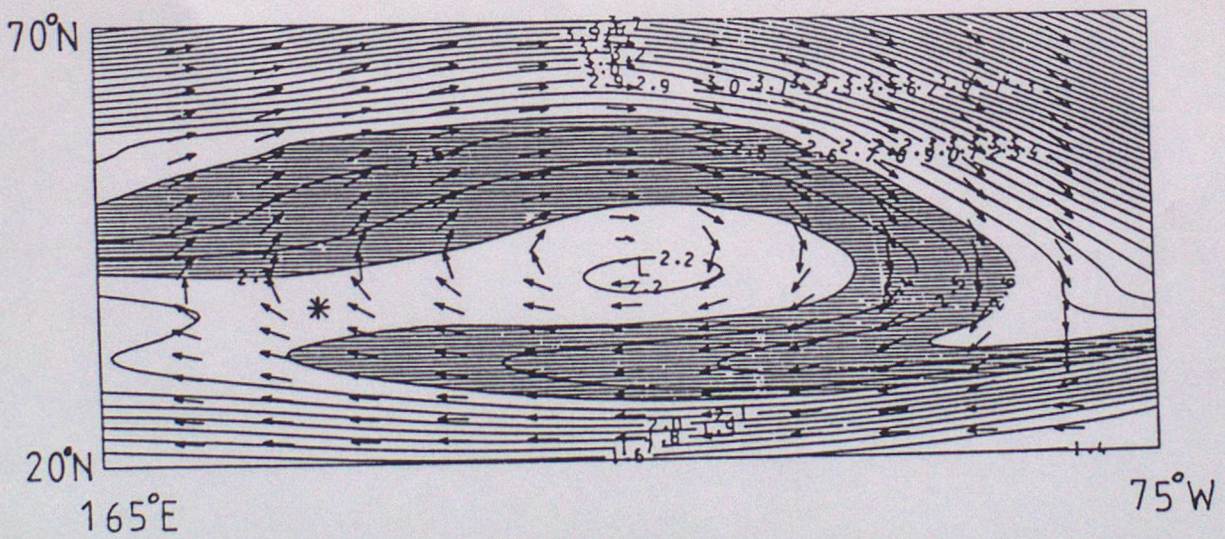

Fig. 14

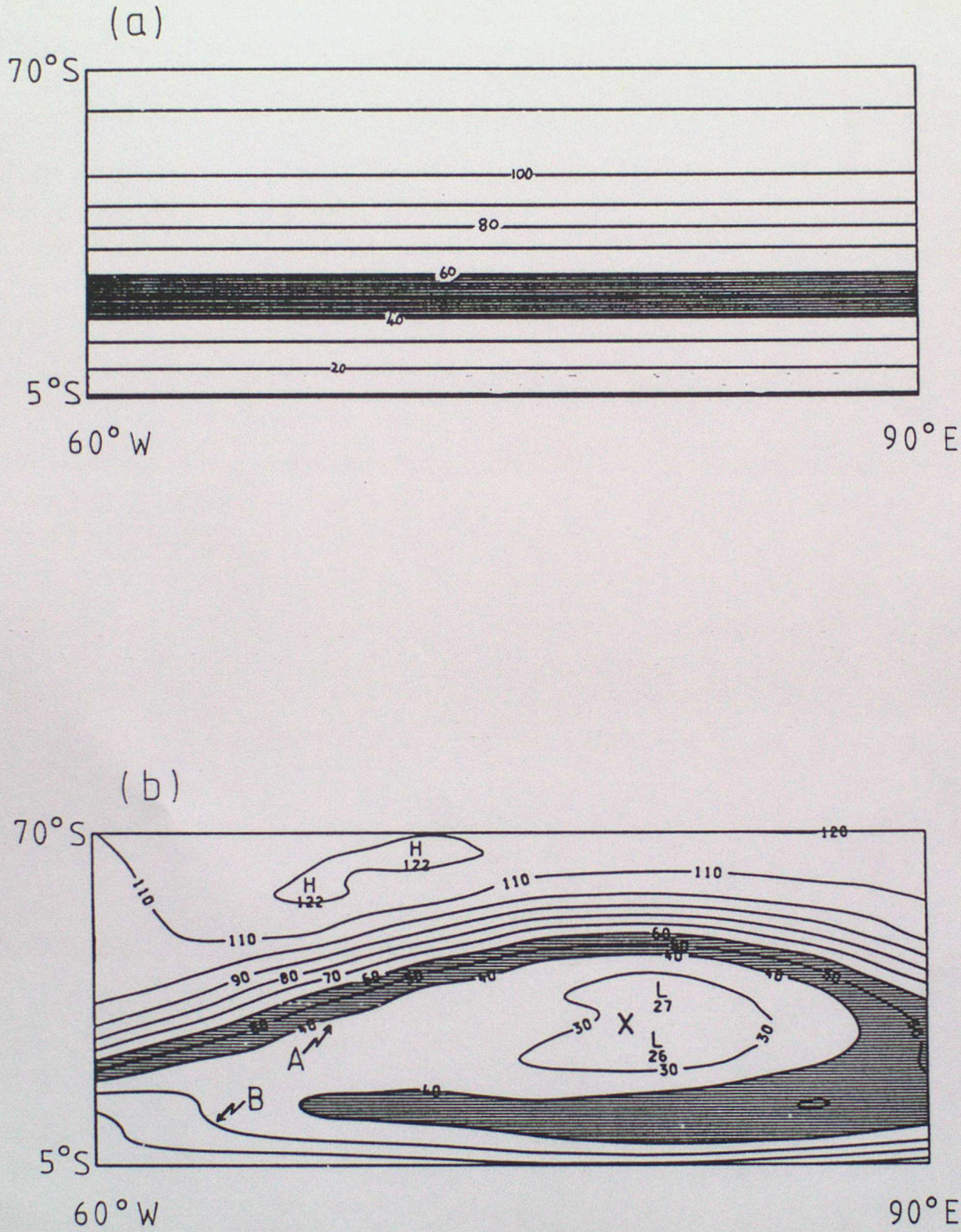
(a)
70°S
5°S
60°W
90°E
100
80
60
40
20
(b)
70°S
5°S
60°W
90°E
H
122
H
122
110
110
110
110
120
90
80
70
60
50
40
60
40
40
30
30
30
30
L
27
L
26
X
A
B
40

Fig. 15

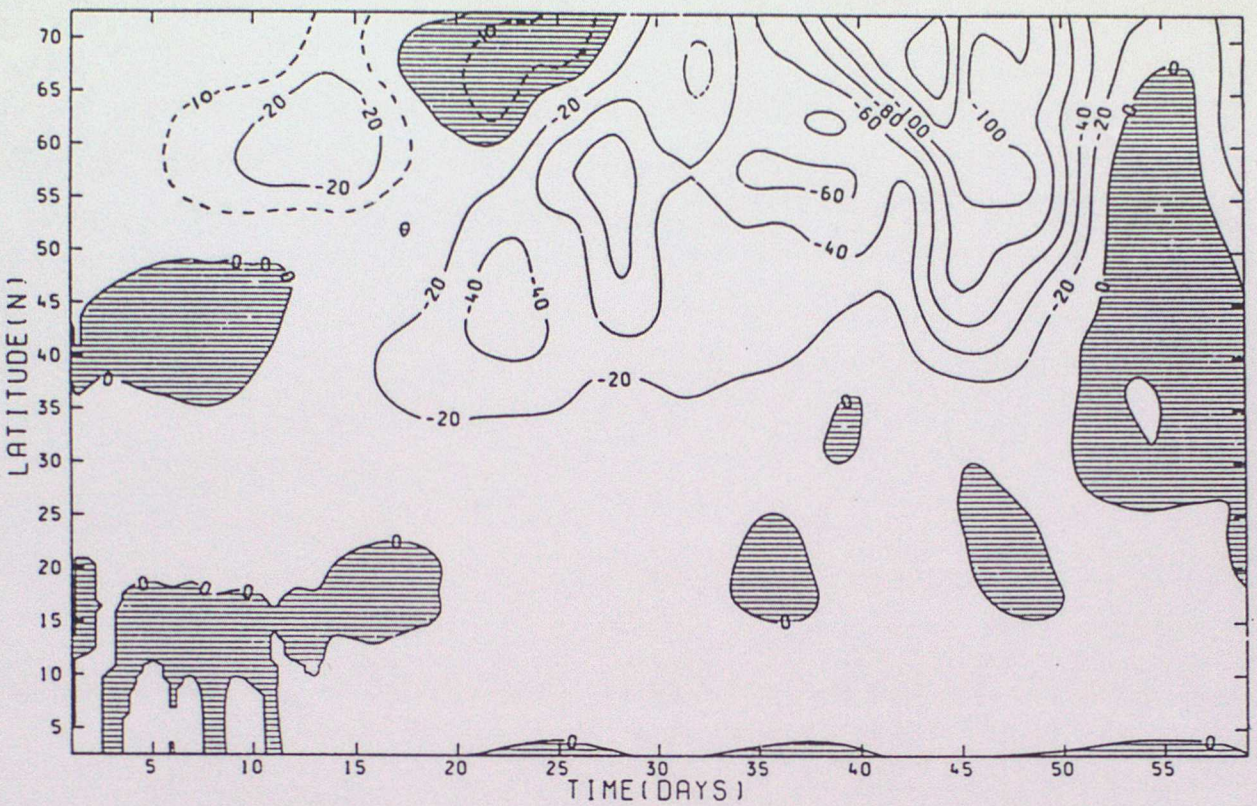
LATITUDE(N)
TIME(DAYS)
70
65
60
55
50
45
40
35
30
25
20
15
10
5
5
10
15
20
25
30
35
40
45
50
55
-10
-20
-40
-60
-80
-100
0

Fig.16

(a)

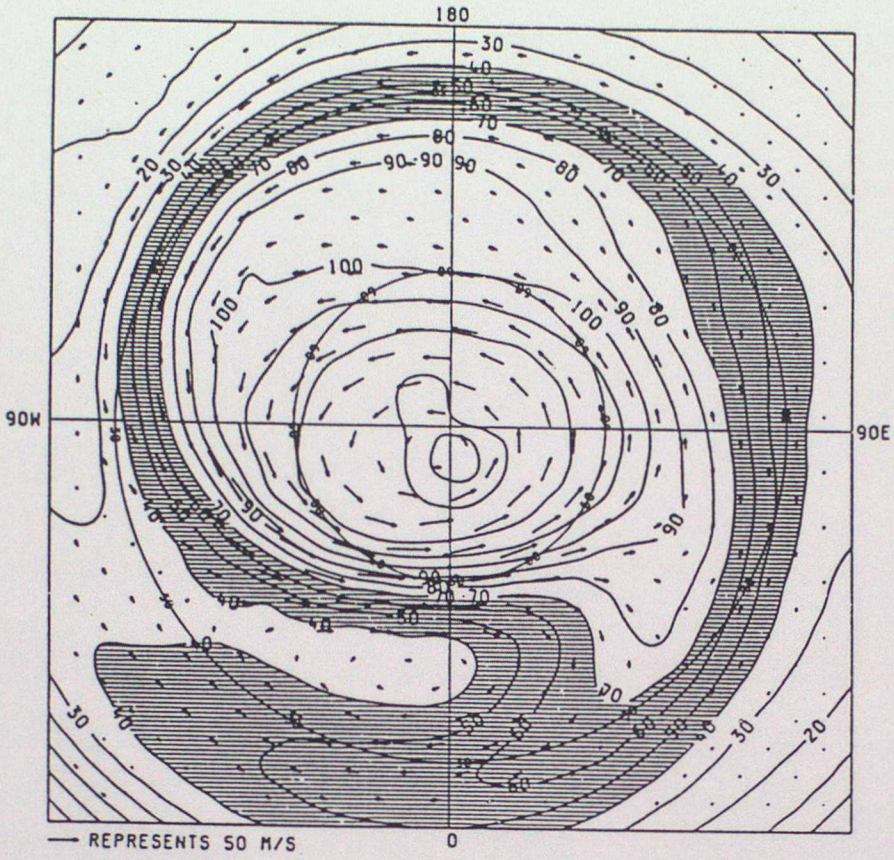
180
90W
90E
0
REPRESENTS 50 M/S

(b)

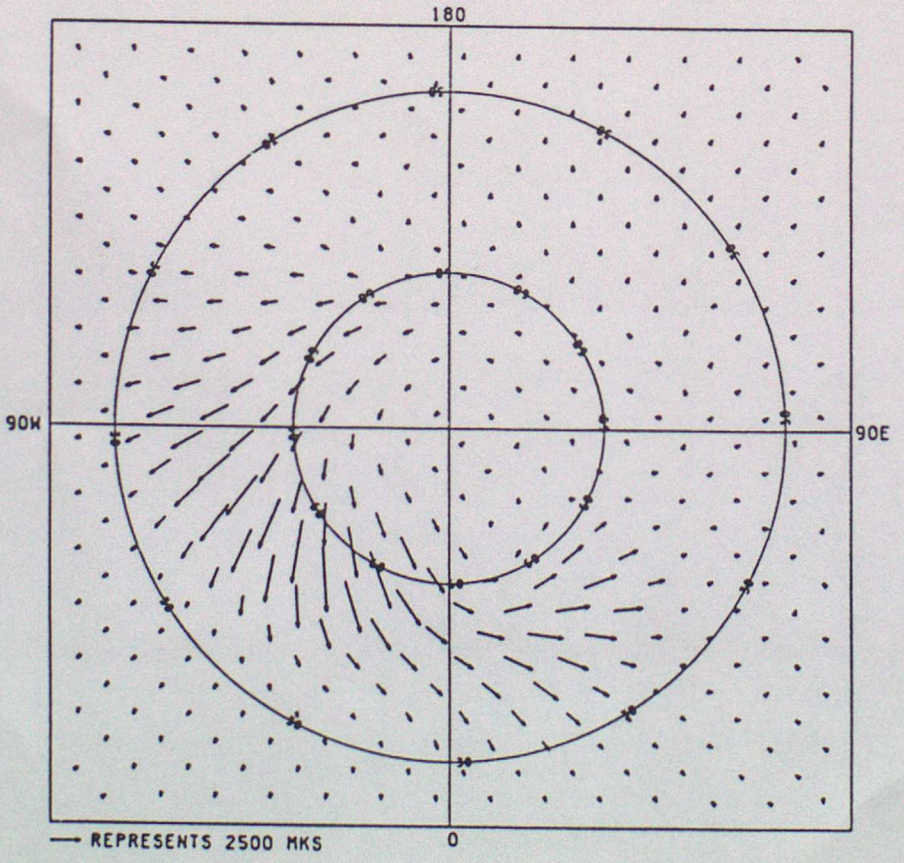
180
90W
90E
0
REPRESENTS 2500 MKS

Fig.17

(c)

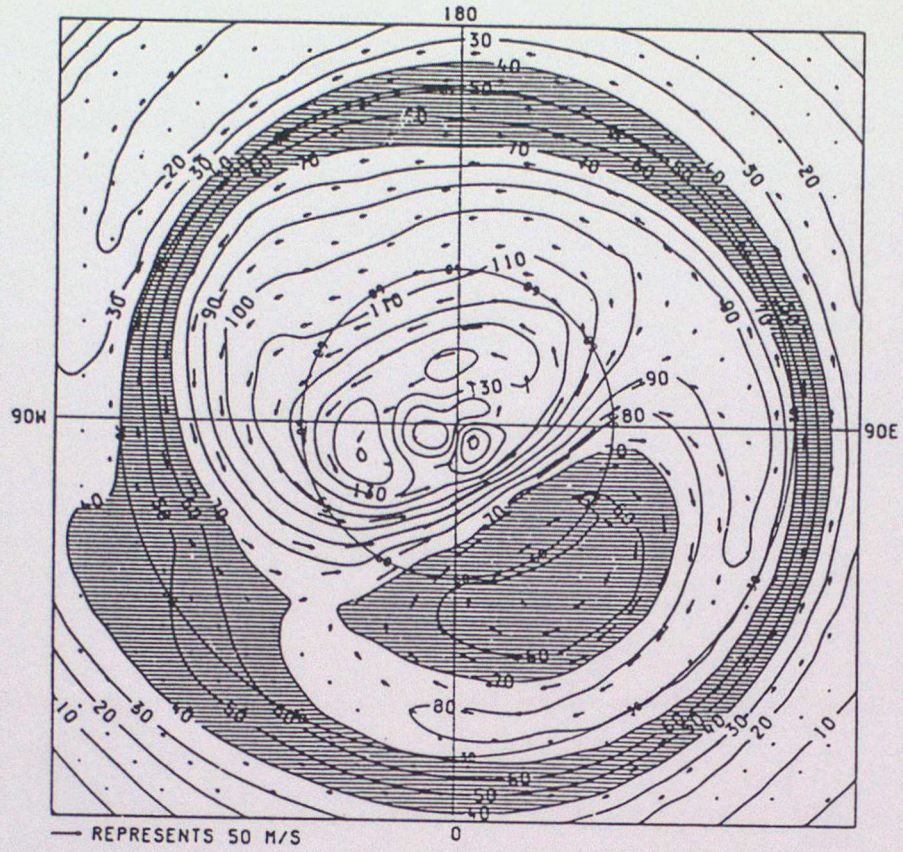
180
90W
90E
0
— REPRESENTS 50 M/S

(d)

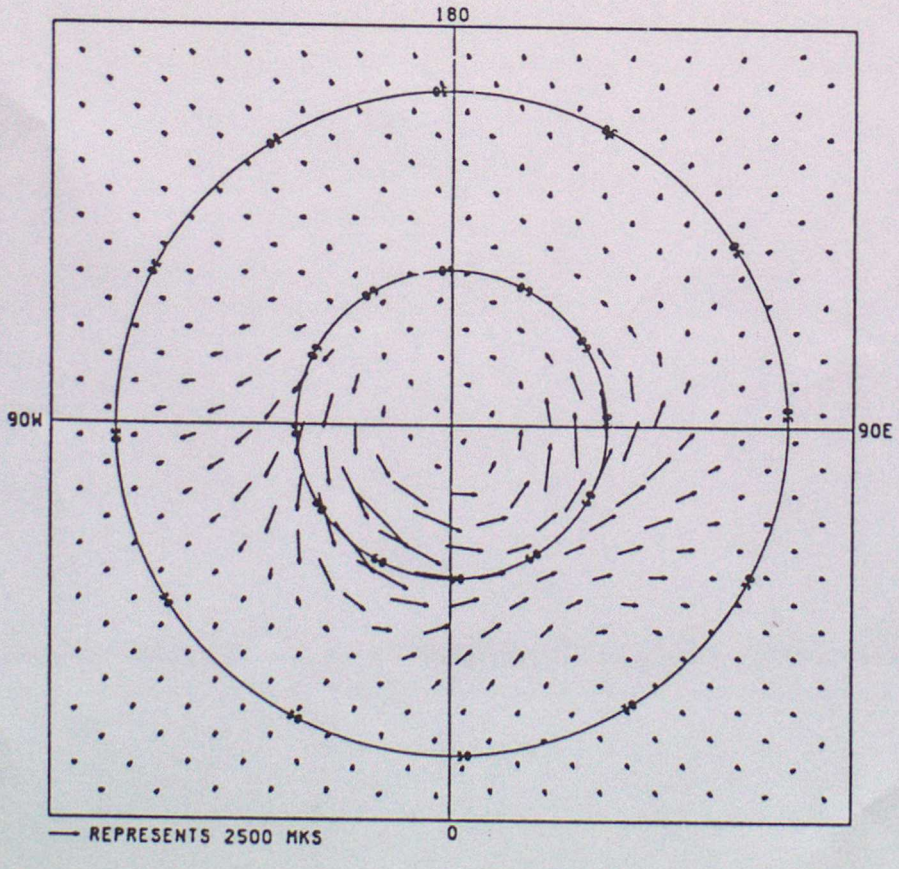
180
90W
90E
0
— REPRESENTS 2500 MKS

Fig. 17

(a)

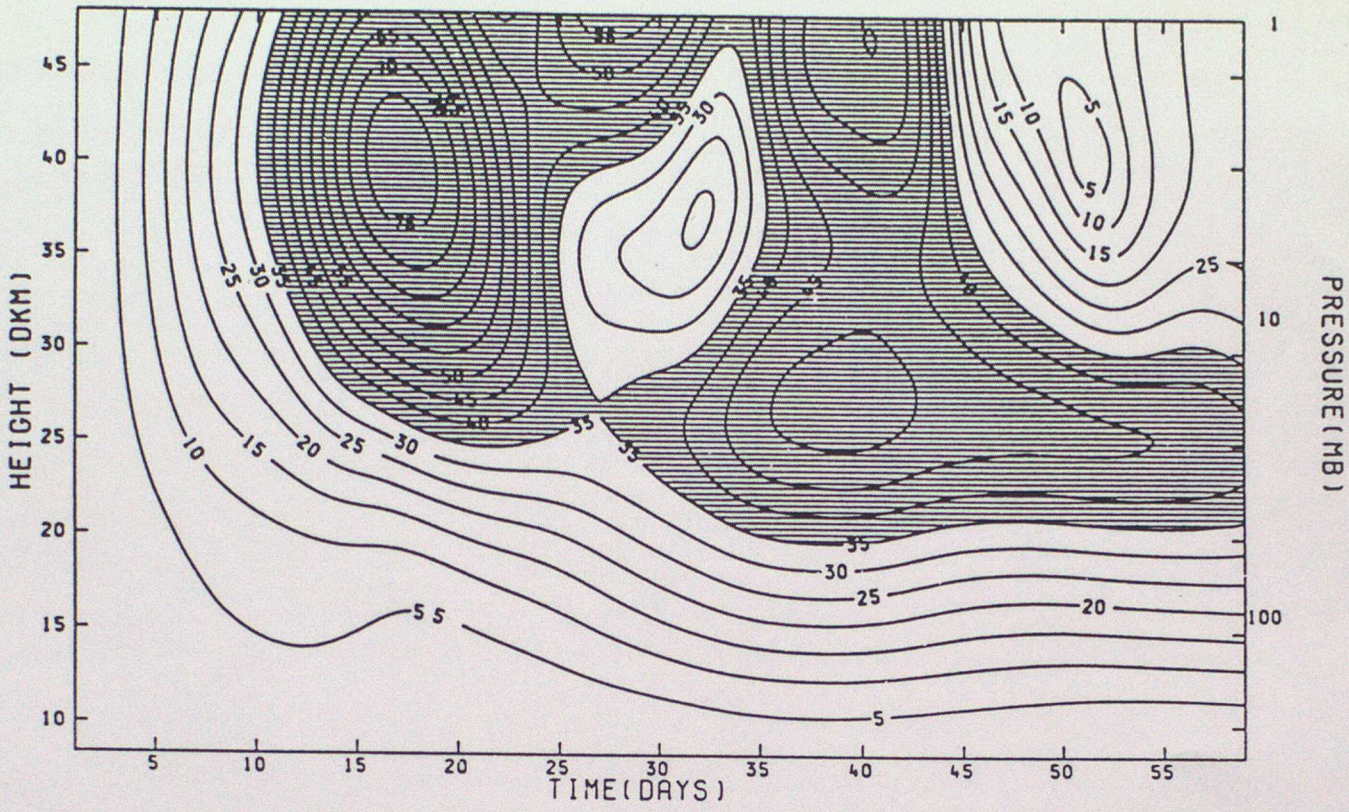
HEIGHT (DKM)
PRESSURE(MB)
TIME(DAYS)

(b)

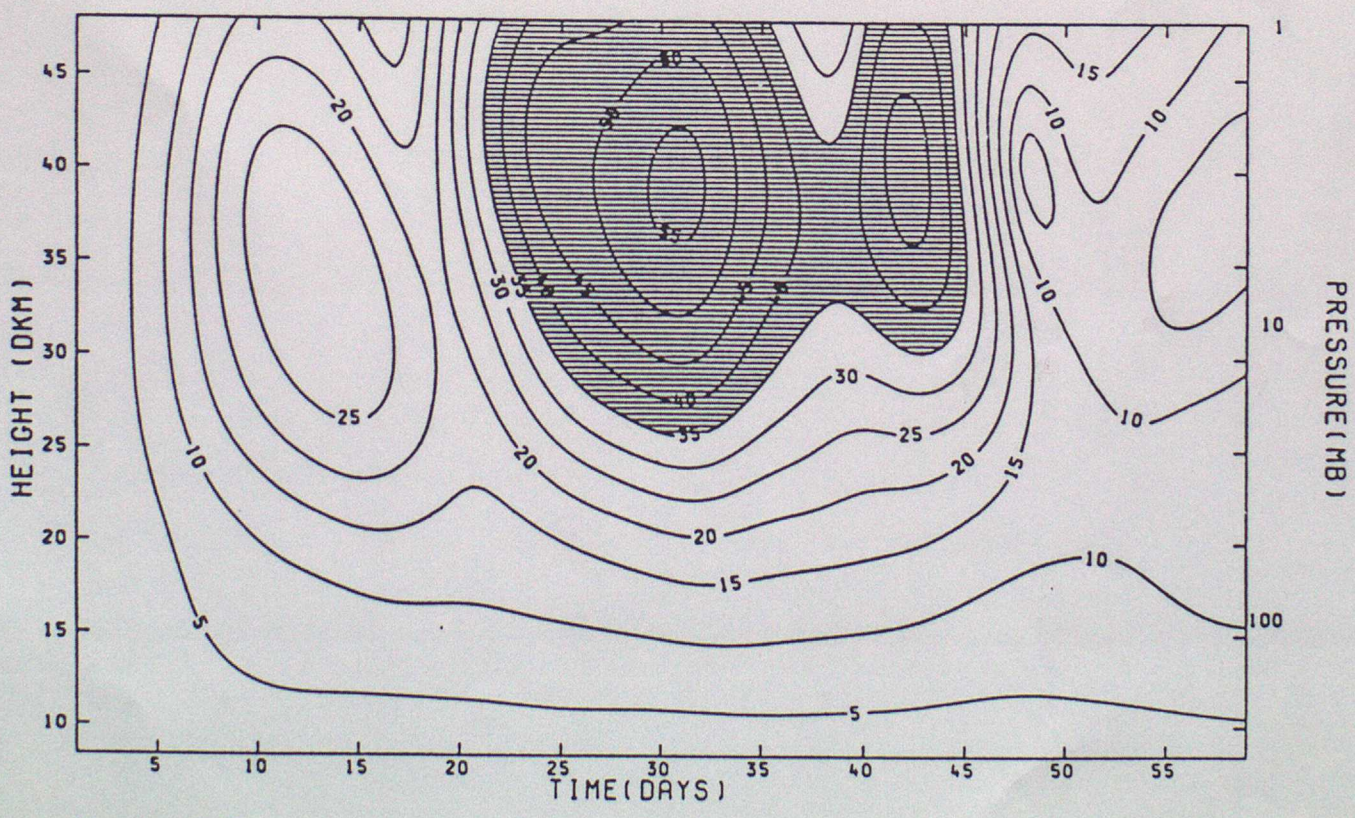
HEIGHT (DKM)
PRESSURE(MB)
TIME(DAYS)

Fig. 18

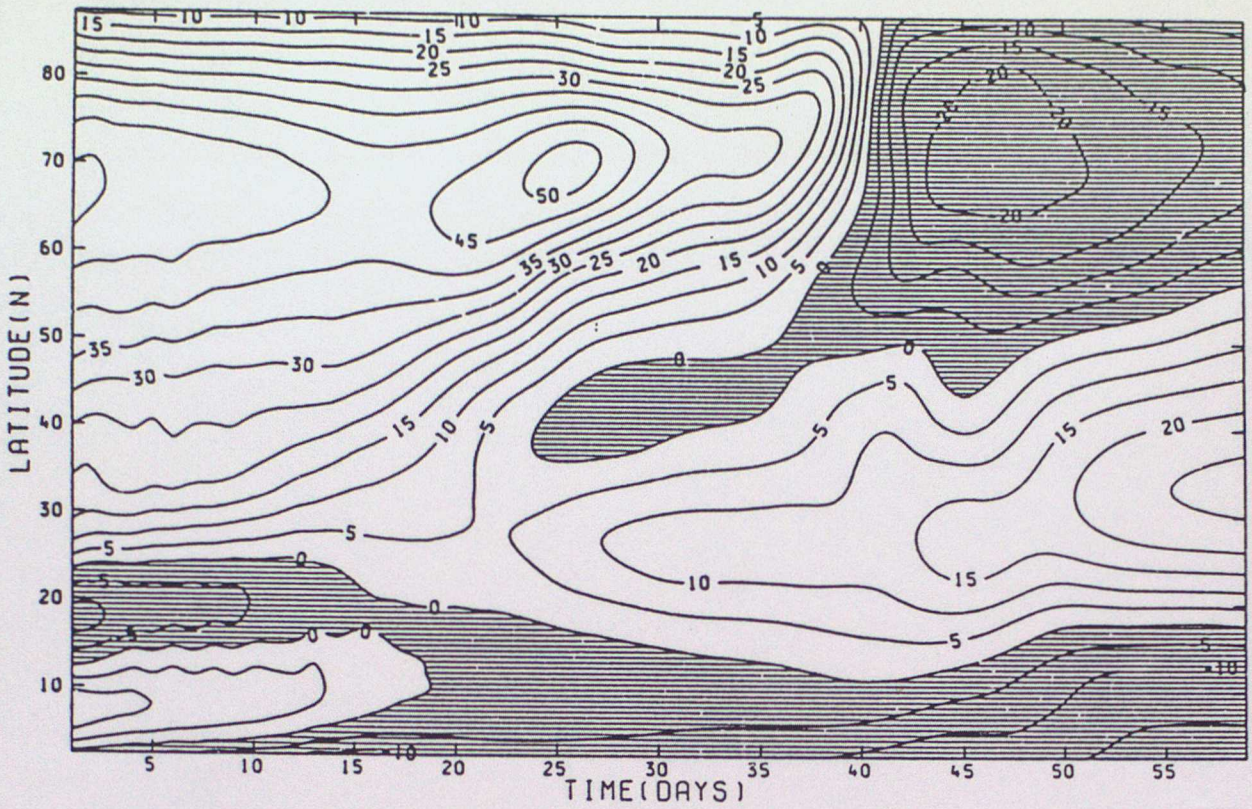

Fig. 19

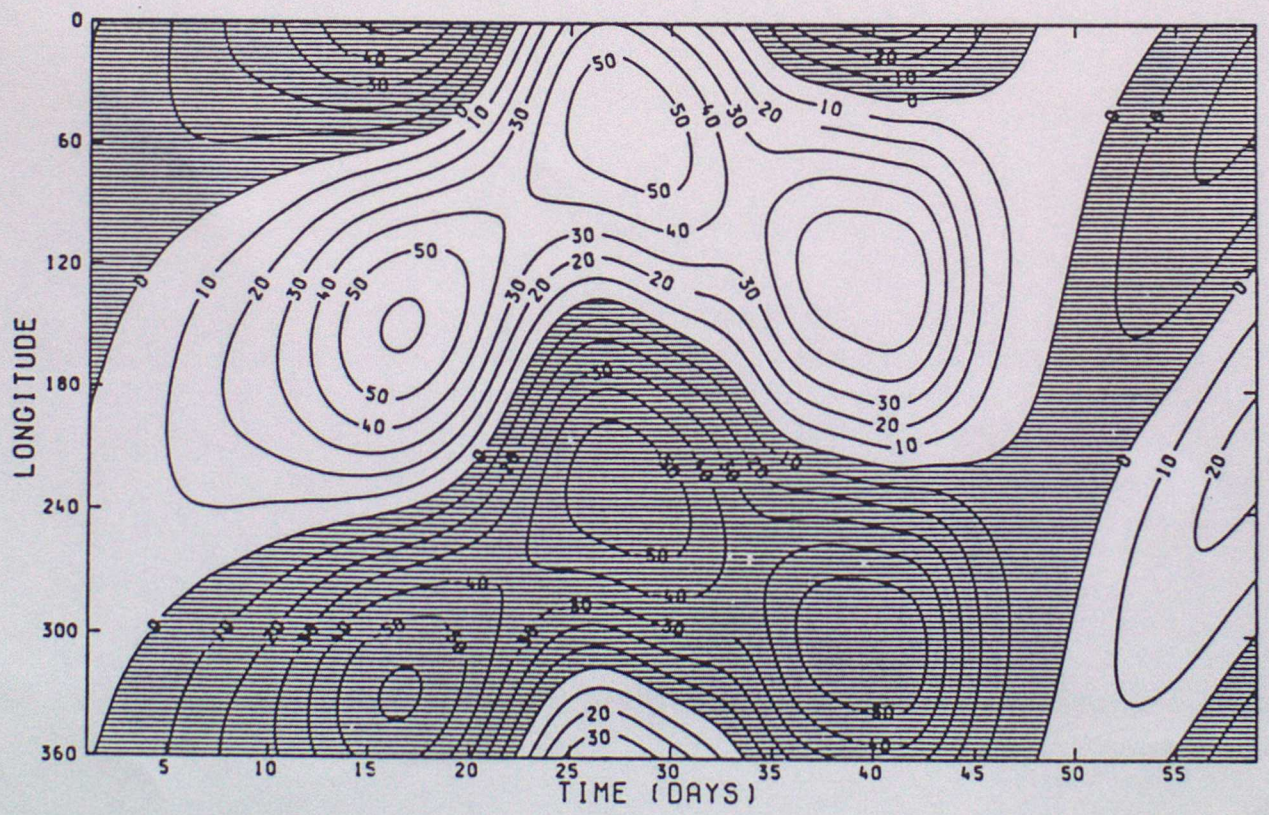

Fig. 20

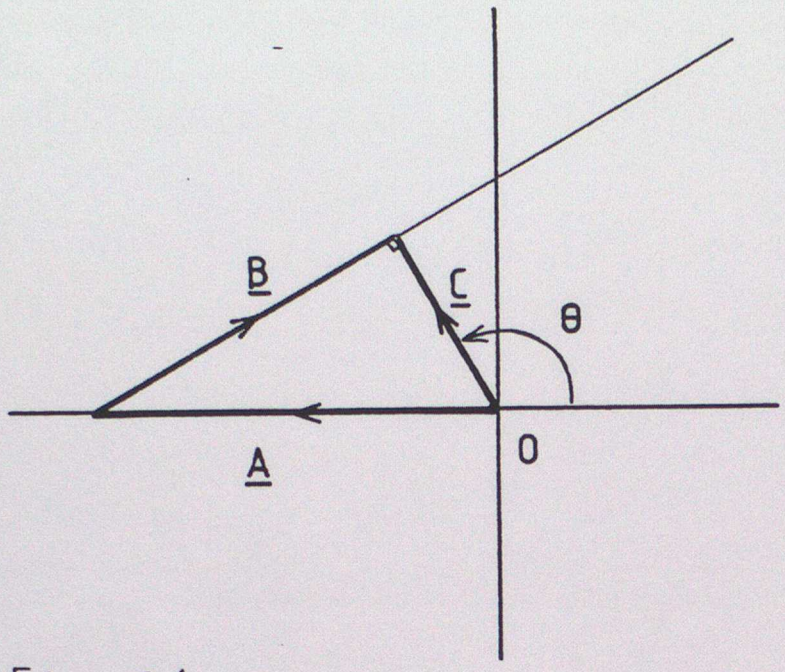
B
C
θ
A
O

Fig. 21

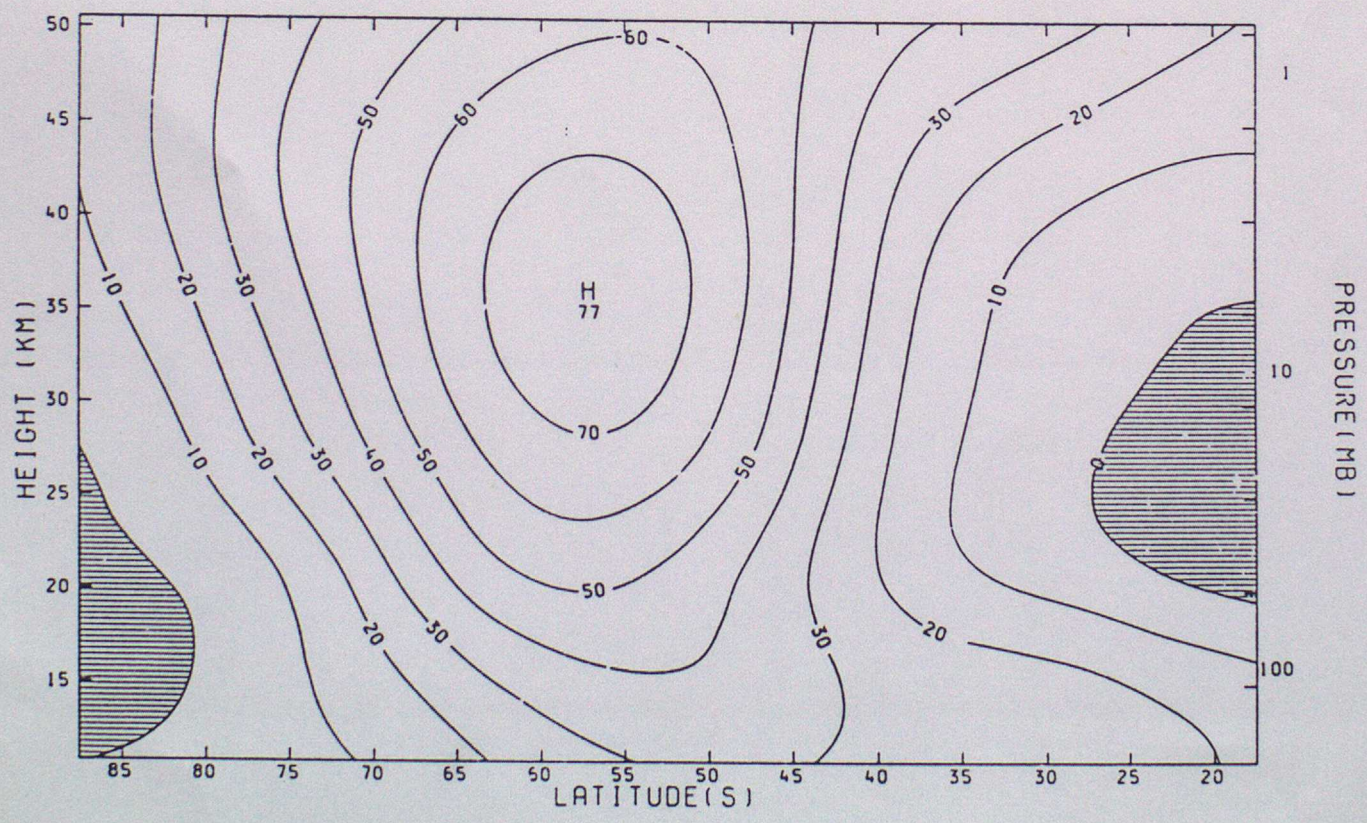
HEIGHT (KM)
LATITUDE(S)
PRESSURE(MB)
H
77
60
50
40
30
20
10
70
0
1
10
100
85
80
75
70
65
60
55
50
45
40
35
30
25
20
15

Fig. 22

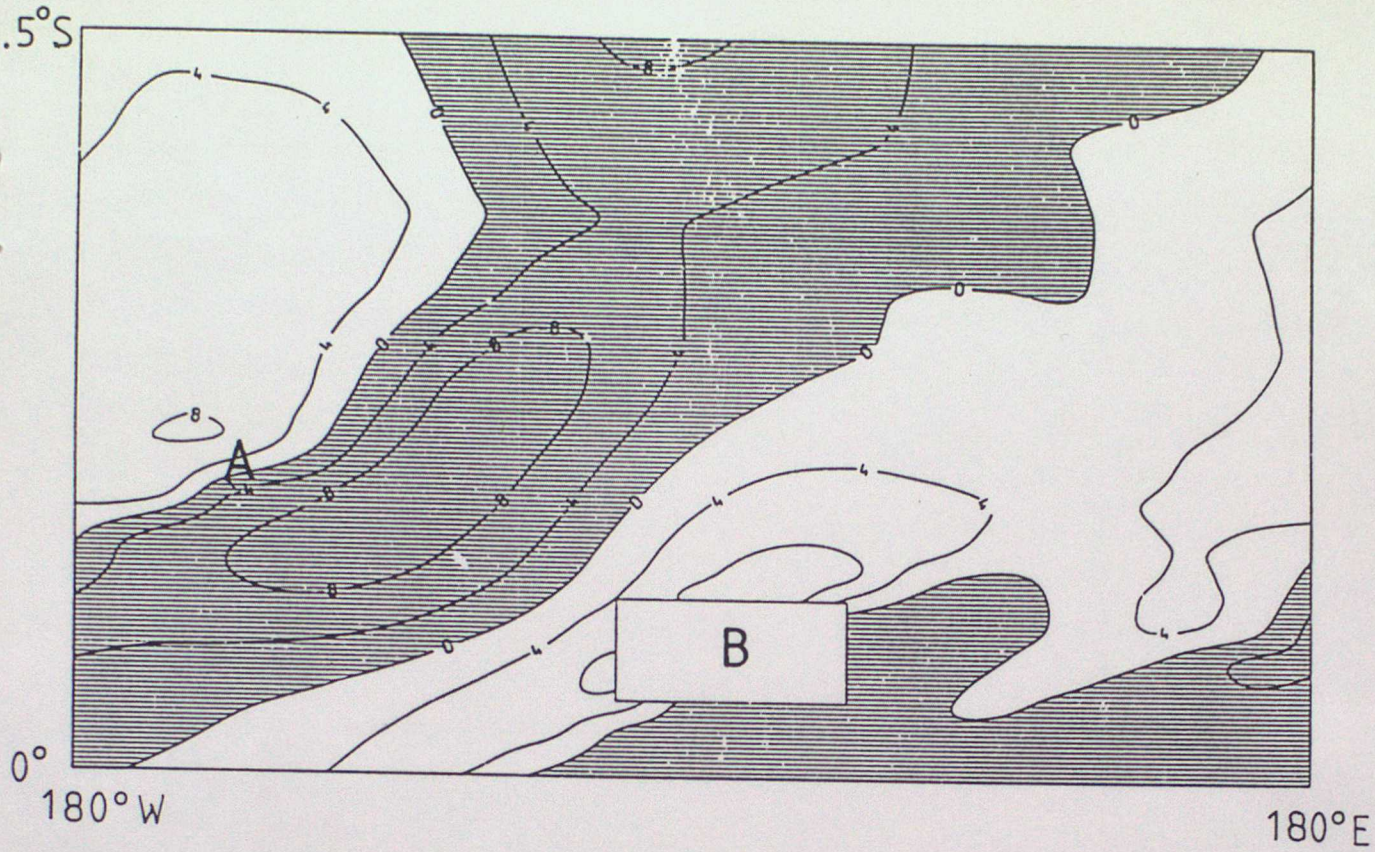

Fig. 23

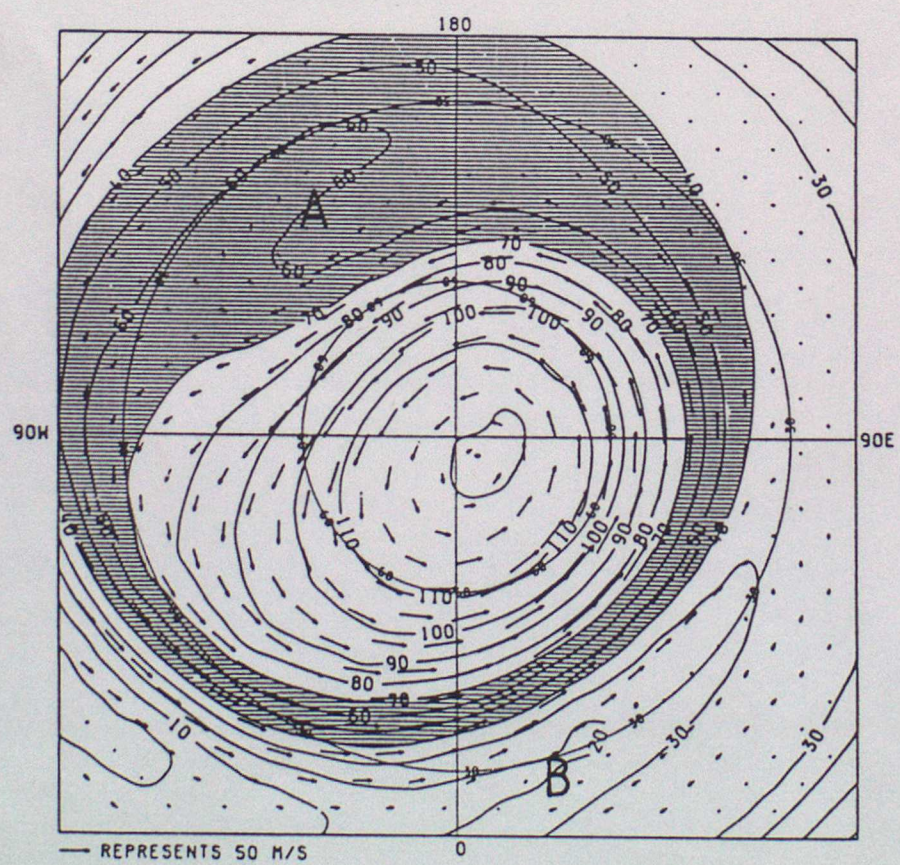

Fig. 24

DYNAMICAL CLIMATOLOGY TECHNICAL NOTES

DCTN 1	June 1984	A scheme for incorporating the thermodynamic sea-ice model into a coupled ocean-atmosphere model. C Gordon and M Bottomley
DCTN 2	Sept 1984	The parametrization of the upper ocean mixed layer in coupled ocean/atmosphere models. C Gordon and M Bottomley
DCTN 3	Sept 1984	The response of a simple thermodynamic sea-ice model to GCM forcing appropriate for perennial sea-ice. M Bottomley
DCTN 4	Sept 1984	Potential vorticity in the stratosphere derived using data from satellites. S A Clough, N S Grahame and A O'Neill
DCTN 5	Sept 1984	Simulation of the seasonal cycle of SST using globally specified climatological data to force simple ocean models. N S Grahame
DCTN 6	Sept 1984	Development of an improved GCM radiation scheme. A Slingo and R C Wilderspin
DCTN 7	Sept 1984	On the specification of surface fluxes in coupled atmosphere/ocean general circulation models. J F B Mitchell, C A Wilson and C M Price
DCTN 8	Sept 1984	A survey of possible repercussions of the Soviet river reversal programme on Arctic sea-ice. H Cattle
DCTN 9	Oct 1984	A study of a strong stratospheric warming during January 1982 T D A Fairlie
DCTN 10	Nov 1984	An intercomparison of the Met O 11 M45 model and the Met O 20 11-level model on the Cyber 205 J F Dyson
DCTN 11	Nov 1984	Simulation of observed time series of temperature and precipitation over eastern England. D M Reed
DCTN 12	Nov 1984	Forecasts and analyses of the onset of the Southwest monsoon. R Kershaw
DCTN 13	Nov 1984	On modelling the effects of CO_2 on climate. J F B Mitchell
DCTN 14	Dec 1984	Development of a revised longwave radiation scheme for an atmospheric general circulation model. A Slingo and R C Wilderspin
DCTN 15	Jan 1985	Rossby wavetrains in the stratosphere forced by localised disturbances in the troposphere. C J Marks (Oxford), A O'Neill and V D Pope

DYNAMICAL CLIMATOLOGY TECHNICAL NOTES

DCTN 16	Jun 1985	Observing system experiments using the Meteorological Office's 15-level model. M A Bromley
DCTN 17	Feb 1985	Atmospheric general circulation simulation of the climate of the Mediterranean region. H Cattle
DCTN 18	Feb 1985	Diurnal variation and cloud in a general circulation model. C A Wilson and J F B Mitchell
DCTN 19	Feb 1985	The sensitivity of the Saharan region in a general circulation model. W M Cunnington and P R Rowntree
DCTN 20	Mar 1985	The impact of aircraft observations on analyses and forecasts from the operational 15-level model. B H Barwell
DCTN 21	Mar 1985	Non-linear effects on heat-induced circulation of the tropical atmosphere. A E Gill and P J Phlips
DCTN 22	Apr 1985	Simulation of cloudiness with the U.K. Meteorological Office 11-layer AGCM. A Slingo and R C Wilderspin
DCTN 23	Apr 1985	An integrated approach to the representation of cloud processes. R N B Smith
DCTN 24	May 1985	Nuclear Winter: Calculations of the shortwave radiative effects of soot aerosols. A Slingo and P Goldsmith
DCTN 25	Jul 1985	Sea ice and the Antarctic winter circulation: a numerical experiment. J F B Mitchell and T S Hills
DCTN 26	Jul 1985	A Budyko-Sellers model for study of ocean-atmosphere interaction. W J Ingram
DCTN 27	Aug 1985	The effect of a shoaling thermocline on equatorially-trapped Kelvin waves. A E Gill and B A King
DCTN 28	Sept 1985	CO_2 climate sensitivity and model dependence of results. J F B Mitchell, C A Wilson and W M Cunnington
DCTN 29	Sept 1985	Handbook of the Meteorological Office 11-layer atmospheric general circulation model. Volume 1 : Model Description Edited by A Slingo
DCTN 30	Sept 1985	Impact of land surface variations on African rainfall in general circulation models. P R Rowntree, M F Wilson and A B Sangster

DYNAMICAL CLIMATOLOGY TECHNICAL NOTES

DCTN 31 Nov 1985 The annual cycle of sea level in the eastern tropical Pacific.
G R Bigg and A E Gill

DCTN 32 Nov 1985 An analytic model of the heat-induced tropical circulation in the presence of a mean wind.
P J Phlips and A E Gill

DCTN 33 Nov 1985 The effect of resolution and diffusion on the simulated climate.
J F Dyson

DCTN 34 Jan 1986 Rossby adjustment over a step.
M K Davey, A E Gill, E R Johnson and P F Linden

DCTN 35 Jan 1986 Issues concerning the evaluation of effective surface roughness of heterogeneous terrain.
D J Carson

DCTN 36 Mar 1986 Climate sensitivity and past climates : evidence from numerical studies
J F B Mitchell

DCTN 37 Mar 1986 Parametrizations of land-surface processes in Meteorological Office numerical weather prediction and climate models
D J Carson

DCTN 38 Apr 1986 Modelling of land-surface processes and their influence on European Climate
D A Warrilow, A B Sangster and A Slingo

DCTN 39 Apr 1986 Simulation of climatic change due to increased CO_2
J F B Mitchell

DCTN 40 May 1986 On the interpretation of the Eliassen-Palm flux divergence.
Part I : Theory
D G Andrews

DCTN 41 June 1986 Experiments on tropical circulation with a simple moist model.
M K Davey and A E Gill

DCTN 42 Jun 1986 Parameter regimes for studying isolated eddies.
P D Killworth and M K Davey

DCTN 43 Jun 1986 A comparison of the impact of an envelope orography and of a parametrization of orographic gravity-wave drag on model simulations.
A Slingo and D W Pearson

DCTN 44 Jul 1986 The effect of a sea-surface temperature anomaly on a prediction of the onset of the south-west monsoon over India.
R Kershaw

DCTN 45 Jul 1986 An introduction to the parametrization of land-surface processes.
D J Carson

DYNAMICAL CLIMATOLOGY TECHNICAL NOTES

DCTN 46 Sept 1986 Lateral boundaries and the heat-induced flow in the tropical atmosphere.
P J Phlips and A E Gill

DCTN 47 Nov 1986 Simulation of the diurnal cycle of outgoing longwave radiation with an atmospheric GCM.
A Slingo, R C Wilderspin and S J Brentnall

DCTN 48 Feb 1987 A 2 x CO_2 climate sensitivity experiment with a global climate model including a simple ocean
C A Wilson and J F B Mitchell

DCTN 49 Feb 1987 Sensitivity of the Met O 20 11-layer model to increased land surface roughness length
C C Heasman

DCTN 50 Feb 1987 The influence of atmospheric waves on the general circulation of the middle atmosphere
D G Andrews

DCTN 51 Feb 1987 Transport mechanisms in the middle atmosphere: an introductory survey
D G Andrews

DCTN 52 Mar 1987 The Met O 20 stratosphere-mesosphere model
M Fisher

DCTN 53 Apr 1987 Simulations of linear and nonlinear disturbances in the stratosphere
A O'Neill and V D Pope